Thermal Sustainability of Low-temperature Geothermal Energy Systems: System Interactions and Environmental Impacts

by

Sima Kouhi Fayegh Dehkordi

A Thesis Submitted in Partial Fulfillment
of the Requirements for the Degree of

Doctor of Philosophy

in

Faculty of Engineering and Applied Science
Mechanical Engineering
University of Ontario Institute of Technology
October 2013

ABSTRACT

In storing heat during summer for use in winter, the ground provides a better source/sink of heat than the outside air in regards to heat pump efficiency, being cooler than the outside air in the summer and warmer in the winter. Due to their good efficiency, the use of geothermal energy is often encouraged; however, two issues arise in the long-term use of ground for thermal purposes: the sustainability and impact of these systems on the environment. Studies show the potential of the geothermal heat exchangers for environmental impacts such as undesirable temperature rises from these systems in temperature-sensitive regions. Furthermore, interference between adjoining installations is being reported, raising issues of sustainability in terms of performance and equitable sharing of natural resources.

The temperature of the soil surrounding the ground heat exchangers (GHEs) and the heat flows in this region are the key factors in determining environmental impacts and their potential thermal interaction. In this study, analytical and numerical models of vertical heat exchangers are presented. First, the effect of system parameters such as borehole spacing on the transient response of two GHEs is described. Second, a numerical finite volume method in a two-dimensional meshed domain is used to evaluate the temperature rise and the heat flows in the soil surrounding borehole systems over the long term. Finally, to examine the effect of temperature rise in the soil surrounding a vertical GHE on the performance of an associated ground heat pump, a reversible heat pump model is coupled to the heat exchanger analytical model via the heat exchanger running fluid temperature. The heat exchanger running fluid temperature, wall temperature and its heat load profile are the main coupling parameters between the three models. The results of the analytical model are compared with ones of a finite volume numerical model.

EXTENDED ABSTRACT

Below a certain depth, the temperature of the ground remains almost unchanged throughout the year. This phenomenon can be exploited by placing a heat exchanger in the ground and coupling it to a heat pump to store heat in the ground during summer for use in winter. The ground provides a better source/sink of heat than the outside air in regards to heat pump efficiency, being cooler than the outside air in the summer and warmer in the winter. Due to their good efficiency, the use of geothermal energy is often encouraged; however, two issues arise in the long-term use of ground for thermal purposes: the sustainability and impact of these systems on the environment. Studies show the potential of the geothermal heat exchangers for environmental impacts such as migration of thermal plumes away from these systems which may cause undesirable temperature rises in temperature-sensitive regions. Furthermore, interference between adjoining installations is being reported, raising issues of sustainability in terms of performance and equitable sharing of natural resources. With increasing interest in installing such systems in the ground and their potential dense population in coming years, regulations need to be implemented to prevent their thermal interaction and their possible negative effects on the design and performance of nearby systems.

The temperature of the soil surrounding the ground heat exchangers (GHEs) and the heat flows in this region are the key factors in determining environmental impacts and their potential thermal interaction. Modeling such systems is important for understanding, designing and optimizing their performances and characteristics. In this study, a number of analytical and numerical models of vertical heat exchangers are presented. Through these models, the temperature of the soil surrounding the GHEs and the heat flows in this region can be determined. Thus, the effect of possible thermal interaction between these systems on their coupling heat pump as well as their environmental impacts can be studied.

First, the two-dimensional transient conduction of heat in the soil around single and multiple GHEs is discussed via numerical and analytical methods. The effect of system parameters such as borehole spacing as well as heat store capacity on the transient response of two GHEs is described. The results of the temperature response of the soil around a borehole, calculated with an analytical line source theory, are compared with the soil temperature rise calculated numerically. In addition, a three-dimensional numerical study is performed to examine the axial heat transfer effects in heat conduction in the soil surrounding a borehole and especially near its top and bottom.

Second, the long-term performance of multiple vertical GHEs is investigated in order to examine their interaction as well as migration of thermal plumes away from these systems which may cause undesirable temperature rises in temperature-sensitive regions. A numerical finite volume method in a two-dimensional meshed domain is used to evaluate the temperature rise in the soil surrounding multiple borehole systems over the long term, for a period of 5 years. A heat flux from the borehole wall is assumed, reflecting the annual variation of heat storage/removal in the ground. By choosing a heat boundary at the borehole wall, it is assumed that the inlet temperature of the circulating fluid running in the U-tube inside the borehole will be adjusted according to the flow rate. The selection of the sinusoidal function is based on the heat pump power consumption and building heating and cooling needs gained via the bin method for a typical building in Belleville, IL.

Next, to account the variation in heating strength along the borehole length due to the temperature variation of the fluid flowing in the U-tube, the finite line source model and the numerical model in a three dimensional domain are both coupled to the model inside the borehole and the results are compared in terms of the soil temperature rise and the borehole wall heat flux. Thus, critical depths at which the maximum heat flow rate occurs, resulting in thermal interaction, can be determined.

Finally, with some improvements to the coupling procedure, the coupled model is used to investigate interacting borehole systems with a periodic heat flow rate in the long term system operation (30 years). To examine the effect of temperature rise in the soil surrounding a vertical GHE on the performance of an associated ground heat pump, a reversible heat pump model is coupled to the model inside the borehole via the running fluid temperature in the U-tube inside the borehole. The running fluid temperature, the borehole wall temperature and the heat load profile are the main coupling parameters between the three models. The results of the analytical model are compared with ones of a finite volume numerical model.

TABLE OF CONTENTS

LIST OF TABLES

LIST OF FIGURES

NOMENCLATURE

a	temperature coefficient
c_p	specific heat at constant pressure, J/kg K
dA	surface element, m^2
d_b	borehole diameter, m
d_e	equivalent diameter, m
d_i	pipe inner diameter, m
d_p	pipe diameter, m
D	uppermost part of the borehole
H	active borehole length, m
h	borehole distance from the coordinate centre, m
h_i	heat transfer coefficient of the circulating fluid, W/m^2K
k	thermal conductivity, W/m K
$\dot{m}$	mass flow rate, kg/s
n	number of time steps
$\dot{Q}$	heat flow rate, W
q'	heat flow rate per unit length of borehole, W/m
q_1'	heat flow rate per unit length of inlet pipe, W/m
q_2'	heat flow rate per unit length of outlet pipe, W/m
q''	heat flux at borehole wall, W/m^2

$\dot{q}_{gen}$ generated heat per unit volume, W/m^3

R thermal resistance, mK/W

R_{11} thermal resistance between the inlet circulating fluid and the borehole wall, mK/W

R_{12} thermal resistance between the inlet and outlet pipes, mK/W

R_{22} thermal resistance between the outlet circulating fluid and the borehole wall, mK/W

R_{b2} thermal resistance between the circulating fluid and the borehole wall based on 2D analysis, mK/W

R_{b3} thermal resistance between the circulating fluid and the borehole wall based on 3D analysis, mK/W

R_p thermal resistance of conduction in the pipe, mK/W

r radial coordinate, m

r_1 distance of point (x,y) in soil around multiple boreholes from Borehole 1, m

r_2 distance of point (x,y) in soil around multiple boreholes from Borehole 2, m

r_b borehole radius, m

r_i pipe inner radius, m

r_p pipe radius, m

T temperature, K

T_f' temperature of the fluid entering the U-tube, K

T_f'' temperature of the fluid exiting the U-tube, K

t time, s

t_s steady-state time, s

Δt time step, s

V volume, m^3

x	x-coordinate (Figure 4-1), m
y	y-coordinate (Figure 4-1), m
z	axial coordinate (Figure 4-1), m
Z	dimensionless depth [Eq. (3-19)]

Greek Letters

α	thermal diffusivity of soil, m^2/s
β	dimensionless parameter [Eq. (3-19)]
β_0	shape factor of the grout resistance [Eq. (3-7)]
β_1	shape factor of the grout resistance [Eq. (3-7)]
ε	heat transfer efficiency of the borehole
Θ	dimensionless temperature [Eq. (3-19)]
θ	temperature difference relative to ground initial temperature, K
$\Delta\xi$	distance between the centroids A and P of two neighbor grids, m
φ	circumferential coordinate, rad
ρ	density, kg/m^3

Subscripts

0	initial
A	centroid A
b	borehole
f	circulating fluid
$f1$	inlet circulating fluid
$f2$	outlet circulating fluid
g	grout
i	ground discretization designation in r direction

nb node number of the adjacent cell

P centroid *P*

p pipe

Superscripts

0 previous time step

n discretization step designation in time

ACKNOWLEDGEMENTS

The author thanks those who helped with the completion of this study.

The author is genuinely thankful to Prof. Marc Rosen for his guidance, advice, support and encouragement during the course of this research. His logic, professional attitude and high standards have been an inspiration to the author to improve her skills during her research at University of Ontario Institute of Technology.

The author thanks Dr. Wey Leong at Ryerson University and Dr. Grant Ferguson at the University of Saskatchewan for their stimulating discussions and correspondence.

The author thanks Denis Tanguay, Ted Kantrowitz and Benjamin Hénault at Canadian Geo-Exchange Coalition for their discussions and/or allowing the author access to their database.

The author is grateful for the technical assistance provided by SimuTech Support on the numerical model of the current study.

The assistance provided by Edward Secnik and Maria Barrase at Clean Energy Research Laboratory at the University of Ontario Institute of Technology is appreciated.

The author kindly acknowledges the financial support provided by the Ontario Ministry of the Environment through its Best in Science program and the Natural Sciences and Engineering Research Council of Canada.

The author thanks her friend, Ali, for his endless encouragements and support throughout this period and his help in troubleshooting errors in computer codes written for this study.

Finally, the author expresses sincere gratitude to her parents for their unconditional love, patience, support and respect for her decisions.

Chapter 1 INTRODUCTION

At the turn of the millennium, one-fifth of the world's population has no access to electricity. Although hundreds of millions of people have attained modern energy sources through energy programs in the last two decades, energy access still remains the main issue to improve the standards of living. To overcome energy issues, the share of renewable energy sources is expected to increase significantly. Furthermore, technologies are needed that can consume the current available electricity more efficiently without compromising living standards. Unfortunately, the share of worldwide renewable electricity generation has not been growing as fast as the global electricity production. To achieve the goal of halving energy related CO_2 emissions by 2050, the current levels of renewable energy need to be doubled by 2020 and technologies that lead to savings in energy consumption need to be promoted. Ground source heat pumps are potential candidates in lowering the electricity use per capita. If they can work sustainably, they can act as very good alternatives to air source heat pumps, reducing the electricity use significantly and, therefore, pushing towards lower CO_2 emissions goals.

Measurements show that, below a certain depth in the ground, the temperature fluctuations observed near the surface of the ground diminish (Figure 1-1), and the temperature remains relatively constant (e.g. at about 6-42°C in various states in the US) throughout the year (Geothermal Heat Pump Consortium 2013). This is due to the high thermal inertia of soil and the time lag between the temperature fluctuations at the surface and their effect deeper in the ground.

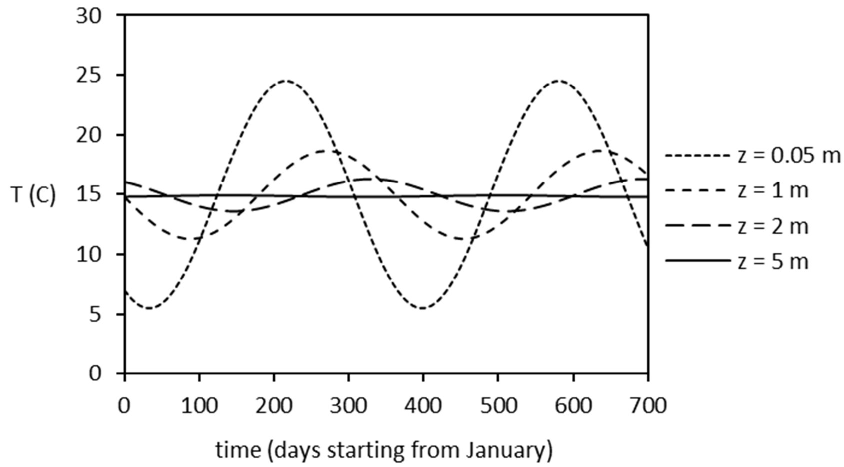

Figure 1-1 Ground temperature fluctuations at various depths [adapted from Hilel (1982)].

Below a certain depth, therefore, the ground generally remains warmer than the outside air in winter and cooler in summer. To exploit the temperature difference between the outside air and the ground, a ground heat exchanger (GHE) can be placed in the ground to preheat a heat carrier in winter and pre-cool it in summer. Also, the relatively cool ground may be used as a sink in summer to store the extracted heat from a conditioned space via a ground heat pump (GHP). In winter, the process may be reversed and the heat pump can extract heat from the relatively warm ground and transport it into the conditioned space. Compared to a conventional air source heat pump (ASHP), which circulates outdoor air to exchange heat, a ground heat pump exchanges heat by circulating a fluid in the ground. The ground has a lower temperature than the outdoor air in the cooling mode and a higher temperature than the outdoor air in the heating mode. Consequently, the temperature lift across a GHP is lower than that of an air source heat pump for both heating and cooling. Thus, the efficiency of the heat pump, which depends directly on the temperature difference between the circulating fluid and the room, is enhanced for a GHP. Therefore, due to concern about greenhouse gas emissions and high energy prices, the placement of heat loops in the ground is an increasingly common practice for heating and cooling residential, commercial, institutional, recreational and industrial structures. Low temperature geothermal energy has the potential to contribute significantly to mitigating both of these problems. Figure 1-2 shows the growth in the ground source heat pump installations from 1996 to 2008 in Canada (Canadian GeoExchange Coalition 2010).

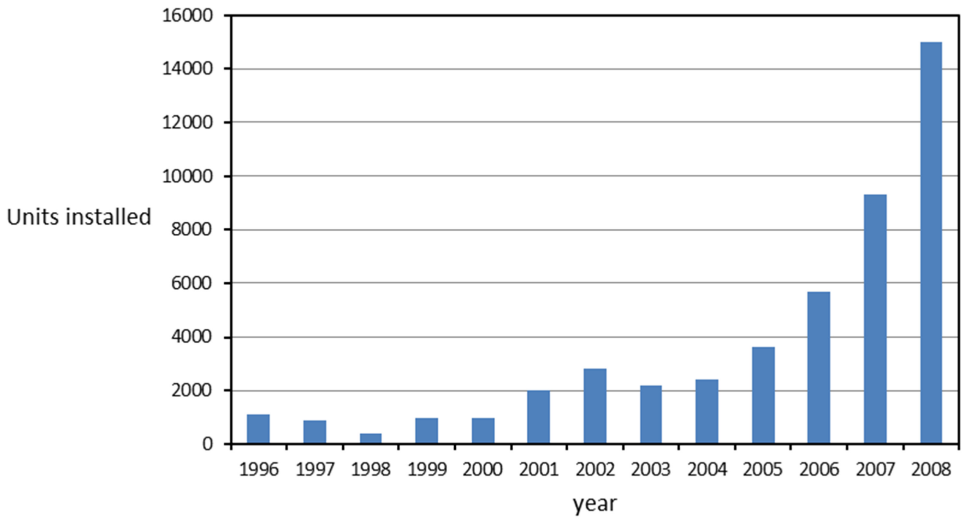

Figure 1-2 Ground source heat pump installation growth from 1996 to 2008 in Canada.

1.1 Motivation

While the use of geothermal systems is widespread, having had a revival in the 1980's and recently, both the sustainability and impact of these systems on the environment are now being questioned. Due to their efficiency, the use of geothermal energy should be encouraged. However, little research is available to guide regulatory agencies and industry towards designs and installations that maximize their sustainability and minimize possible environmental impacts.

1.1.1 Environmental Impacts

Similar to most human activities, studies show the potential of geothermal heat exchangers for causing environmental impacts. While little research has been done regarding the impact of geothermal systems on the local environment, research on the movement of thermal plumes shows the potential for impact. Migration of thermal plumes away from these systems and changes in temperature from either closed or open loop systems or due to changes in ground water flow patterns from open-loop systems may cause undesirable temperature rises in nearby temperature-sensitive ecosystems where small temperature differences are important. For example, temperature disturbances in the ground caused by the operation of geothermal systems may result in disruption to sensitive life stages of aquatic organisms. Similar environmental effects are observed for heat loop and waterline projects (rivers and lakes) (Fisheries and Oceans Canada 2009). Markle and Schincariol (2007) investigate the potential thermal impacts from below-water-table aggregate extraction on a cool-water stream in Southwestern Ontario, Canada which supports Brook trout and cool-water micro-invertebrates. They demonstrate the persistence of thermal plumes (persisting in an aquifer for 11 months and migration up to 250 m down gradient) and the sensitivity of the aquatic environment to very small temperature perturbations. Their results show that there is a surprisingly narrow range for spawning in cold water streams. They need to be cooled in the summer and warmed in the winter by the groundwater flow. Once the ground water temperature is affected due to the performance of GHEs, it can negatively affect the temperature of the cold water streams, making these sites unsuitable for spawning. A study on the effects of thermal fluctuation on the microorganisms in the aquifers of the geothermal well field shows increases in total microbial number in aquifer samples, which correlated with the increase in temperature in the geothermal well field (York et al. 1998). Moreover, counts of cultured bacteria suggested that even when no significant differences in total bacterial number were observed, there may have been changes in the types of microorganisms present in the aquifers of the geothermal well field.

What is unknown at this point is whether the environmental impacts of geothermal systems are acceptable considering the fact that they can reduce fossil fuel consumption and, therefore, lower greenhouse gas emissions and if geothermal systems can be developed in a manner that has reasonably small potential for impacting the environment.

1.1.2 Sustainability

In addition to potential environmental impacts, there are also concerns that continued geothermal system development may result in undesirable effects on ground water resources. The sustainability of geothermal heat pump systems at their design efficiency is now being questioned due to ‘thermal pollution’ from the system itself, adjacent systems, or the urban environment. Studies from Manitoba, where the carbonate rock aquifer beneath Winnipeg has been exploited in thermal applications since 1965, indicate that in many cases these systems are not sustainable or not sustainable at the design efficiency (Ferguson and Woodbury 2005, 2006; Younger 2008). In an area of the Carbonate Rock aquifer beneath Winnipeg in Manitoba, Canada, there are four systems that utilize groundwater for cooling purposes that are closely spaced. Temperatures at the production well have risen as a result of breakthrough of injected water. The results of numerical modeling also indicate that interference effects are present in three of the four systems examined in this study (Ferguson and Woodbury 2006). The influence of these systems on each other implies that these systems have a spacing that is smaller than the optimum for such systems, and indicates that there is a limit to the density of development that can occur in a given aquifer. Cases of thermal breakthrough in the aquifer have occurred in some geothermal systems.

In heating or cooling dominated climates, an annual energy imbalance is placed on the ground loop due to heating, cooling and hot water production. For example, Manitoba has a heating dominated climate and there are concerns regarding the long-term thermal performance of the ground loop. Long-term thermal performance of such ground loop systems with imbalanced energy input and outputs in the ground may result in large temperature rises in the region that the loop is installed as well as the migration of thermal plumes away from these systems which might have stronger environmental impacts. Thermal imbalances could cause significant issues with a heat pump's long-term sustainable performance if not properly considered at the design phase (Andrushuk and Merkel 2009).

1.1.3 Thermal Interaction

Thermal disturbances in the soil associated with GHEs are likely to extend beyond property boundaries and affect adjacent properties. Therefore, with increasing interest in installing such systems in the ground and their potential dense population in coming years, procedures and regulations need to be implemented to prevent disputes between neighbors with potentially interacting systems and their possible negative effects on the design performance of existing nearby systems. As stated by Ferguson (2009), an analogy exists between ground water and heat flow in the ground which allows one to draw on experiences in ground water resource development and source water protection. In many ways, the problem of distributing subsurface energy rights is similar to water rights.

Careful management of geothermal developments to ensure fair access to the subsurface for thermal applications is likely needed. This will require a greater understanding of subsurface heat flow and input from the scientific and technical communities. These concerns have not been well addressed in all cases. Research is needed to allow the investigation of system performance and environmental impact in an integrated manner, so that the best way of utilizing geothermal systems in an environmentally sensitive and sustainable manner can be determined.

1.2 Objectives and Scope

The overall objective of this project is to investigate the sustainability and potential environmental impact of low-temperature geothermal systems[*] that could result from the movement of heat flows in the soil surrounding ground heat exchangers. This information could ultimately provide guidance in regulating the installation of these systems. However, the details of such required regulations on the current system installation procedures are not included in this study.

In particular, a focus is placed on closed-loop systems. Analytical and numerical modelling and simulation of the heat exchange function in these systems will lead to the following:

- Evaluation of the temperature rise in the soil surrounding these systems.
- Examining the migration of thermal plumes away from these systems.
- Examining the existence of thermal interaction among two systems in the long-term system operation.
- Investigating the effect of thermal interaction on heat pump efficiency.
- Investigating parameters associated with potential thermal interaction between two systems.

Modelling the systems include:

- Modelling the soil surrounding the geothermal heat exchangers: In numerical modelling of the soil surrounding the heat exchangers, a large domain of computational cells is used to evaluate the temperature of each element. In the analytical model, the temperature rise in any distance from the borehole wall can be evaluated using the ground heat load of the heat exchanger.
- Modelling the heat exchanger: In the heat exchanger model, the ground heat load is controlled via the inlet and outlet fluid temperatures. A model that is able to

[*] Low-temperature geothermal systems also known as geoexchange systems interact closely with the shallow subsurface and have a near-environment temperature.

estimate the inlet and outlet fluid temperature based on the required transient ground heat load should be developed in order to relate these two temperatures to the soil model.

- Finding a relation between the heat exchanger model and the soil model: The ground heat load of the heat exchanger is needed when determining the temperature rise in the soil surrounding ground heat exchangers. This heat load is associated to the heat exchanger model, heat pump efficiency and the building heating and cooling requirements.
- Finding a relation between the varying parameters in the heat exchanger model and the heat pump efficiency. In order to find a relation between the varying parameters in the heat exchanger model such as the inlet and outlet temperature and the heat pump efficiency, a model representing the heat pump should be developed.

Therefore, in a complete modelling of the system, parameters from the soil model, the heat exchanger model and the heat pump associated to them should be coupled.

The data from modelling the soil surrounding the system will help estimate the temperature rise in the soil further away from the system and the heat flow patterns in the soil surrounding the system with a given ground heat load after a few years of system operation. Specific information regarding negative impacts of this temperature rise and heat flows on nearby eco-systems and surface waters is not investigated in the current study. Furthermore, the current study does not investigate the economics or other impacts on systems' surrounding environment resulting from heat flows from the system.

The data from modelling the heat exchanger and its surrounding soil will help estimate the effect of thermal interaction between two systems, which could be a temperature rise or drop in the vicinity of one system caused by the operation of another, on heat pump efficiency of the systems can be studied. Furthermore, the potential thermal interaction among two or more geothermal systems and key system temperatures such as the temperature of the borehole wall can be determined. Understanding and estimating some of these key temperatures will help model the heat pump and study its performance when thermal interaction occurs. This information will guide proper site characterization, system design, construction and operation so that these systems are sustainable and minimally impact the environment as well as other neighboring systems.

1.3 Overview of the Thesis

In the present report, a summary of the geothermal system types is provided (Chapter 2). Various heat transfer models are reported for GHEs, and several basic analytical and numerical models of vertical heat exchangers, are described and compared (Chapter 3). To evaluate the temperature rise in the soil around borehole heat exchangers, the transient heat conduction equation in the soil is solved via analytical (Chapter 5), two-dimensional and three-dimensional numerical approaches (Chapter 6). First, a two dimensional finite volume numerical solution is applied for the soil region surrounding multiple boreholes using ANSYS FLUENT software (Section B.3). The results of this model can be used in discussing the environmental impacts of geothermal systems resulting from temperature rise in areas further away from the system after a few years of system operation (Section **Error! Reference source not found.**). Furthermore, a three dimensional numerical and an analytical approach is used to examine the existence and the effect of thermal interaction between neighboring borehole systems on their heat pump efficiency (Chapter 6). This is performed by discussing the effect of thermal interaction on the variation in running fluid temperature. The existence of thermal interaction between boreholes and negative environmental impacts is also examined over the life time of the system (Section 7.3).

Chapter 2 GEOTHERMAL SYSTEMS

A geothermal heating and cooling system consists of three main components: a heat pump, an underground heat exchanger and a distribution system such as air ducts. The cost of the system is roughly proportional to the heat exchanger size and, therefore, there is an incentive to evaluate peak monthly and daily loads and average annual loads and to design the heat exchanger as small as possible to meet the required heat transfer for system operation. Heat exchanger performance is influenced by several factors: the structural and geometric configuration of the heat exchanger, the ground temperature distribution, soil moisture content and its thermal properties, groundwater movement and possible freezing in soil. Thus, appropriate and validated tools are needed, with which the thermal behavior of GHEs can be assessed and optimized, considering technical, environmental and economical aspects.

2.1 Ground Heat Exchanger

Ground heat exchangers (GHEs) are commonly classified as open loop [groundwater heat pump (GWHP)] or closed loop [ground coupled heat pump (GCHP)], with a third category for those not belonging to either.

2.1.1 Open Loop

Standing column wells, mine water or tunnel water are examples for this category. In an open loop system, ground water from a water-bearing layer is pumped from an aquifer through one well, passed through the heat pump where heat is added to or extracted from a heat carrier and then discharged either onto the surface or to another well in the aquifer. Because the system water supply and discharge are not connected, the loop is “open” (Geothermal Heat Pump Consortium 2013). In a similar way, open loop systems can be installed to preheat or pre-cool ambient air flowing through tubes buried in the ground. The air is then heated or cooled by a conventional air conditioning unit before entering the building.

2.1.2 Closed Loop

A closed loop system uses continuous underground pipe loops placed horizontally or vertically in the ground with both ends of the pipe system connected to the heat pump.

2.1.2.1 Horizontal Ground Heat Exchanger

In a horizontal ground heat exchanger, a number of plastic pipes are connected either in series or in parallel in a horizontal trench (Figure 2-1). The numbers of pipes and trenches installed vary depending on the system capacity and thermal properties of geological formations. This type of GHE is usually most economic when adequate yard space is available. A horizontal GHE is usually placed at a depth of 1-2 m in the ground and is typically 35-60 m long per kW of heating or cooling capacity (Geothermal Heat Pump Consortium 2013).

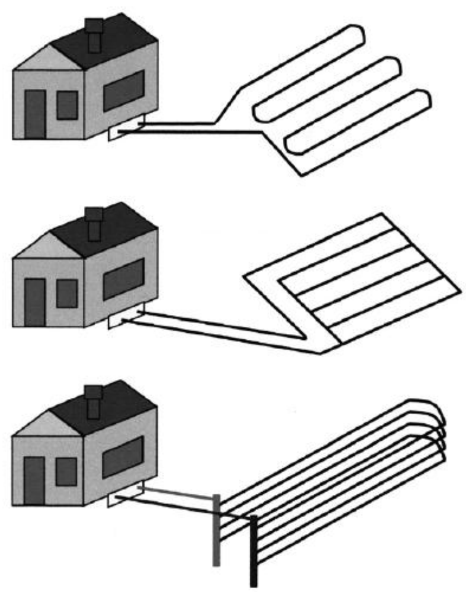

Figure 2-1 Horizontal ground heat exchangers [taken from Florides and Kalogirou (2007)].

2.1.2.2 Vertical Ground Heat Exchanger

In a vertical ground heat exchanger, sometimes called a borehole heat exchanger (BHE), plastic pipes are inserted in either a U-shape or coaxial form (Figure 2-2) into a borehole which is constructed vertically in the ground (Figure 2-3) and is usually filled with grout to enhance thermal contact with the undisturbed ground outside the borehole and also to prevent contamination of aquifers. The grout is often a mixture of Na-bentonite and silica sand which may contain thermally enhanced additives in order to present a significantly higher thermal conductivity than the surrounding soil to facilitate heat transfer from the heat exchanging fluid to the ground and to protect groundwater as required by relevant environmental regulations. The heat carrier fluid is usually water or water mixed with an environmentally benign antifreeze and flows down to the bottom of the borehole along one pipe and back upward in another pipe. A typical borehole heat exchanger is usually 20-300 m deep with a diameter of 10-15 cm (Florides and Kalogirou 2007). For high heating or cooling loads, a borehole system composed of a large number of individual boreholes can be installed. The number of boreholes needed and their depth depend mostly on the size of the building, system demands and the ground temperature. Compared to horizontal heat exchangers, vertical loops are more expensive to install. However, for a given heating and cooling load, they require less piping as the deep ground temperature remains cooler in the summer and warmer in the winter than near-surface ground.

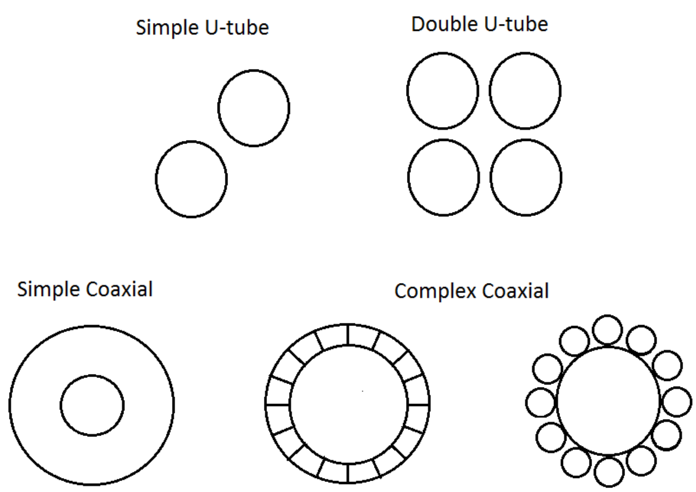

Figure 2-2 Cross section of different types of borehole heat exchangers.

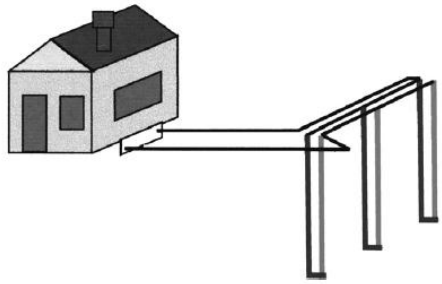

Figure 2-3 Vertical ground heat exchanger [taken from Florides and Kalogirou (2007)].

The distributions of different types of GHEs based on number of installations for some Canadian provinces are shown in Table 2-1. Given the geology and geography, it is seen that the installation of vertical and horizontal ground loop systems vary in different provinces. Overall, closed horizontal loops dominate residential installations in Canada. These systems accounted for 52.5% of residential installations in 2009 while the second largest segment is closed, vertical loops with 34.1% of the installations in the same year (Canadian GeoExchange Coalition 2010).

Table 2-1 Distribution of different heat exchanger types based on number of installations in some Canadian provinces [Adapted from Canadian GeoExchange Coalition (2010)].

Province	Open Loop (% of provincial systems)	Closed Loop (% of provincial systems)		Pond/Lake (% of provincial systems)
		Vertical	Horizontal	
Ontario	12	15	67	6
Quebec	6	85	8	1
British Colombia	15	31	52	2
Alberta	7	72	19	2

2.2 Heat Pump

All heat pumps consist of a condenser, expansion device, evaporator and a compressor (Figure 2-4). In heating mode, the cycle starts as liquid refrigerant at high pressure exits the condenser. The liquid refrigerant passes through an expansion device, which reduces the pressure of the refrigerant. The refrigerant at low pressure passes through a heat exchanger (evaporator) and absorbs heat from the low-temperature source. The refrigerant evaporates into a gas as heat is absorbed. The gaseous refrigerant then passes through a compressor where it is pressurized, raising its temperature. The hot gas then circulates through a condenser where the heat is removed to the heat sink. As the refrigerant rejects heat, it changes phase back to liquid phase and the process begins again.

In general, heat pumps operate between a high-temperature medium (at T_H) and a low-temperature medium (at T_L). In the case of ground heat pumps, when cooling the building (ground heat delivery), the running fluid temperature in the GHE can be considered the high temperature medium and the cooling coil temperature can be considered the low temperature medium in the cooling season. In the heating season (ground heat removal), the heating coil temperature can be considered to be the high temperature while the temperature of the fluid running through the heat exchanger can be considered to be the low temperature. A heat pump, when used in heating mode, extracts energy from a low temperature heat source and transforms it to energy at a desirable temperature level by using a compressor. The compressor requires power input in order to upgrade the energy. The maximum efficiency that may be achieved by a heat pump is defined by the theoretical "Carnot-process" where all the processes are reversible. In an ideal heat pump, the coefficient of performance of the heat pump (COP_{rev}) is only dependent on the high-temperature and the low-temperature. The COP deteriorates by a large temperature difference between the heat sink and the heat source. Therefore, it is important to look for reasonable temperature levels in the heat source and reduce the temperature where heat rejection is to take place.

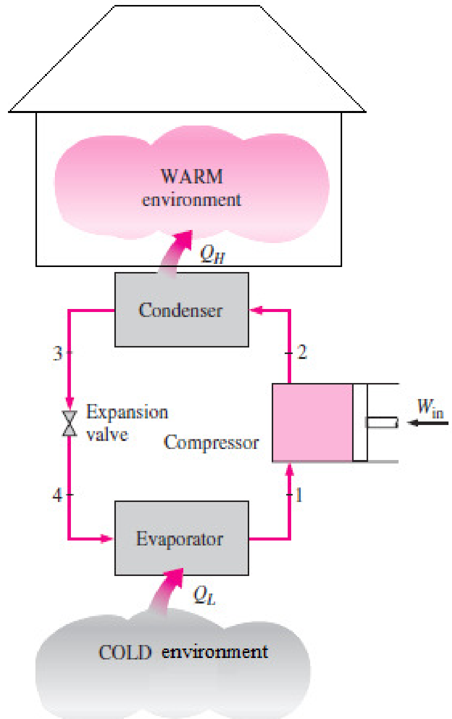

Figure 2-4 Ideal heat pump in the heating season [adapted from Cengel and Boles (2006)].

Chapter 3 LITERATURE REVIEW

Various models have been reported for heat transfer in borehole heat exchangers (BHEs), with three principal applications: design of BHEs (including sizing borehole depth and determining borehole numbers), analysis of in-situ ground thermal conductivity test data, and integration with building system models, i.e. coupling the model with HVAC systems and building heat transfer models to determine performance. Changes in ground temperature and the circulating fluid often must be kept within acceptable limits over the life of the heat exchanger. Based on how heat transfer from the circulating fluid to the surrounding soil is simulated, these methods can be divided into analytical and numerical. Several simulation models for the heat transfer inside and outside the borehole are available, most of which are based on analytical and/or numerical methods. The models vary in the way the problem of heat conduction in the soil is solved, the way the interference between boreholes is treated and the way the methods are accelerated.

3.1 Analytical models

The heat transfer modeling in GHEs via analytical methods is complicated since their study involves transient effects in a time range of months or even years. Because of the complexities of this problem and its long time scale, the heat transfer in GHEs is usually analyzed in two separated regions (Figure 3-1): the region inside the borehole containing the U-tubes and the grout (Zeng et al. 2003a) and the soil region surrounding the borehole. The transient borehole wall temperature is important for engineering applications and system simulation. It can be determined by modeling the region outside the borehole by various methods such as cylindrical heat source theory (Carslaw and Jaeger 1946). Based on the borehole wall temperature, the fluid inlet and outlet temperatures can be evaluated by a heat transfer analysis inside the borehole. In other words, the regions inside and outside borehole are coupled by the temperature of borehole wall. The heat pump model can utilize the fluid inlet and outlet temperatures for the GHE, and accordingly the dynamic simulation and optimization design for a GCHP system can be implemented. This is the basic idea behind the development of the two-region vertical GHE model. Currently, there are many models that combine ground heat conduction outside the borehole and borehole heat exchangers to predict heat extraction/injection rates from/to the ground (Jun et al. 2009). Yang et al. (2010) present a detailed summary of the most typical simulation models of the vertical GHEs currently available including the heat transfer processes outside and inside the boreholes.

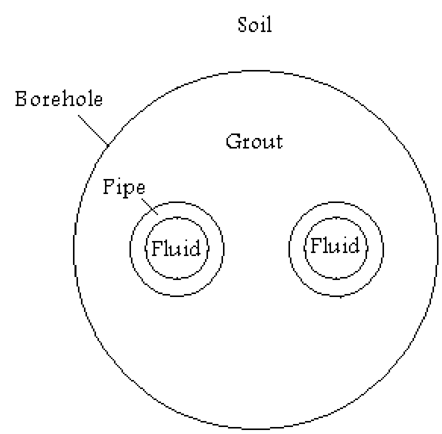

Figure 3-1 Cross-section of vertical ground heat exchanger.

3.1.1 Heat Transfer Inside the Borehole

While most models investigate thermal characteristics of soil outside the borehole, a few models of varying complexity in how they deal with the complicated geometry inside boreholes have been established to describe heat transfer within vertical GHEs. The thermal analysis in the borehole seeks to define the inlet and outlet temperatures of the circulating fluid according to borehole wall temperature, its heat flow and the thermal resistance inside the borehole. The latter quantity is determined by thermal properties of the grouting material, the arrangement of flow channels and the convective heat transfer in the tubes. If the thermal resistance between the borehole wall and inner fluid is determined, the GHE fluid temperature can be calculated. In the absence of natural convection, moisture flow and freezing, the borehole thermal resistance can be calculated assuming steady-state heat conduction in the region between the circulating fluids and a cylinder around the borehole. According to Jun et al. (2009), steady-state heat transfer assumption is made when the running time is greater than the critical time, that is $Fo > 5$, where Fo is the Fourier number, and the impact of thermal capacity of objects inside the borehole can be neglected. Such simplification has been proved approximate and convenient for most engineering practices except for analyses dealing with dynamic responses within a few hours (Yavuzturk 1999).

3.1.1.1 One-dimensional Model

In this model, the axial heat flows in the grout and pipe walls are considered negligible as the borehole dimensional scale is small compared with the infinite extent of the ground beyond the borehole (Bose et al. 1985). As a consequence of the U-tube structure, the heat conduction in the cross section is clearly two-dimensional, which is a little complicated to solve. Therefore, simplified models conceiving the U-tube as a single pipe have been recommended and heat transfer in the borehole is approximated as a steady-state one-dimensional process. The thermal resistance inside the borehole R_b can be defined as the sum of the thermal resistance of the fluid convection, and the thermal resistances of conduction in the pipe R_p and in the grout R_g:

$$R_b = R_p + R_g \tag{3-1}$$

The thermal resistance of the fluid convection and conduction in the pipe is defined as

$$R_p = \frac{1}{2\pi d_i h_i} + \frac{\ln(r_p/r_i)}{2\pi k_p} \tag{3-2}$$

where h_i is determined by the Dittus-Boelter correlation:

$$h_i = \frac{0.023\,\mathrm{Re}^{0.8}\,\mathrm{Pr}^n\,k_f}{d_i} \tag{3-3}$$

The first term on the right side of Eq. (3-2) accounts for the resistance due to fluid convection and the second term accounts for conduction in the pipe. The thermal resistance of the grout can be computed by the equivalent diameter method or the shape factor method. In the first, the two legs of the U-tube are considered as one concentric cylindrical heat source/sink, also referred to as an "equivalent pipe" having identical temperatures inside the borehole, which leads to the following simple expression for the grout thermal resistance:

$$R_g = \frac{1}{2\pi k_b} \ln\left(\frac{d_b}{d_e}\right) \tag{3-4}$$

where d_b is the borehole diameter, d_e is the equivalent diameter and k_b is the thermal conductivity of the grout.

Claesson and Dunand (1983) give the equivalent diameter as

$$d_e = \sqrt{2} d_0 \tag{3-5}$$

while Gu and O'Neal (1998a, 1998b) suggest the following:

$$d_e = \sqrt{2 d_p L_s} \qquad \left(d_p < L_s < d_b\right) \tag{3-6}$$

Note that when the equivalent diameter method is used for computing the thermal resistance inside the borehole, the thermal resistance of fluid convection and conduction in the pipe should remain constant.

In reality, the fluid circulating through different legs of the U-tube exchanges heat with the surrounding ground and is of varying temperature along the tube. Therefore, thermal interference, i.e. thermal "short-circuiting," among U-tube legs, which degrades the effective heat transfer in the GHEs, is inevitable. This oversimplified one-dimensional model is not capable of evaluating this impact or analyzing dynamic responses within a few hours.

Paul (1996) expresses the grout resistance using the concept of the shape factor of conduction as follows:

$$R_g = \left[k_b \beta_0 \left(\frac{r_b}{r_p}\right)^{\beta_1} \right]^{-1} \tag{3-7}$$

where β_0 and β_1 are the shape factors of the grout resistance whose values depend on the relative location of U-tube pipes in the borehole. These factors are obtained by curve fitting of measured effective borehole resistances determined in laboratory measurements. In this approach only a limited number of influencing factors were considered, and all the pipes were assumed to be of identical temperature as a precondition.

3.1.1.2 Two-dimensional Model

Due to the axial convective heat transport and the transverse heat transfer to the ground, the temperature of the fluid varies along a U-tube. In particular, when the flow rate is low, there is a bigger temperature difference between the upward and downward channels which may result in heat exchange between the two channels and a reduced efficiency of the GHE. Hellström (1991) took account of the thermal resistances among pipes in the cross-section perpendicular to the borehole axis and obtained a two-dimensional analytical solution to the heat transfer problem inside the borehole. This model is superior to the oversimplified one-dimensional models in presenting quantitative expressions of the thermal resistance in the cross-section and providing a basis for discussing the impact of the U-tube placement on the heat conduction.

In the two-dimensional model, the temperature of the fluid in the U-tube is defined by superposing two separate temperature responses caused by the heat fluxes per unit length, q_1' and q_2', from the two pipes of the U-tube. The fluid temperatures in the U-tubes (T_{f1} and T_{f2}) can be obtained from the following equations:

$$\begin{aligned} T_{f1} - T_b &= R_{11} q_1' + R_{12} q_2' \\ T_{f2} - T_b &= R_{12} q_1' + R_{22} q_2' \end{aligned} \tag{3-8}$$

where t_b is the temperature on the borehole wall, R_{11} and R_{22} are the thermal resistances between the circulating fluid in each pipe and the borehole wall, and R_{12} is the resistance between the two pipes. Note that the temperature on the borehole wall (T_b) is assumed uniform along the borehole depth and is taken as a reference of the temperature excess. A linear transformation of Eq. (3-8) leads to

$$\begin{aligned} q_1' &= \frac{T_{f1} - T_b}{R_1^{\Delta}} + \frac{T_{f1} - T_{f2}}{R_{12}^{\Delta}} \\ q_2' &= \frac{T_{f2} - T_b}{R_2^{\Delta}} + \frac{T_{f2} - T_{f1}}{R_{12}^{\Delta}} \end{aligned} \tag{3-9}$$

where

$$R_1^{\Delta} = \frac{R_{11}R_{22} - R_{12}^2}{R_{22} - R_{12}}, \quad R_2^{\Delta} = \frac{R_{11}R_{22} - R_{12}^2}{R_{11} - R_{12}}, \quad \text{and} \quad R_{12}^{\Delta} = \frac{R_{11}R_{22} - R_{12}^2}{R_{12}} \tag{3-10}$$

Note that there is no distinction between the entering and exiting pipes since this model does not take into account the heat transfer of the circulating fluid in the axial direction. Eskilson (1987) determines thermal resistance between the fluid and borehole wall as

$$R_{b2} = \frac{R_{11} + R_{12}}{2} \tag{3-11}$$

By assuming identical temperatures and heat fluxes of the pipes in the borehole:

$$T_{f1} = T_{f2} = T_f \quad \text{and} \quad q_1' = q_2' = q_l'/2 \tag{3-12}$$

the borehole resistance is derived for symmetrically placed double U-tubes as

$$R_b = \frac{1}{2\pi k_b}\left[\ln\left(\frac{r_b}{r_p}\right) - \frac{3}{4} + \left(\frac{D}{r_b}\right)^2 - \frac{1}{4}\ln\left(1 - \frac{D^8}{r_b^8}\right) - \frac{1}{2}\ln\left(\frac{\sqrt{2}D}{r_p}\right) - \frac{1}{4}\ln\left(\frac{2D}{r_p}\right)\right] + \frac{R_p}{4} \tag{3-13}$$

The two-dimensional model presents quantitative expressions of the thermal resistance in the cross-section, and provides a basis for discussing the impact of the U-tube disposal on conduction. However, the assumption of identical temperature of all the pipes prevents this model to reveal impact of the thermal interference on GHE performances.

Zeng et al. (2003b) discuss the impact of thermal interference between the U-tube pipes and show that the thermal "short-circuit" phenomena may, reduce heat transfer between the heat carrier fluid and ground, and deteriorate performance of the GHEs.

3.1.1.3 Quasi-three-dimensional Model

A quasi-three-dimensional model was proposed by Zeng et al. (2003a, 2003b) taking into account the fluid axial convective heat transfer and thermal “short-circuiting” among U-tube legs. Being minor in the order, the conductive heat flow in the grout and ground in the axial direction, however, is still neglected to keep the model concise and analytically manageable. The energy balance equations for up-flow and down-flow of the circulating fluid can be written as

$$
\begin{aligned}
-\dot{m}c_p \frac{dT_{f1}}{dz} &= \frac{T_{f1}-T_b}{R_1^{\Delta}} + \frac{T_{f1}-T_{f2}}{R_{12}^{\Delta}} \\
\dot{m}c_p \frac{dT_{f2}}{dz} &= \frac{T_{f2}-T_b}{R_2^{\Delta}} + \frac{T_{f2}-T_{f1}}{R_{12}^{\Delta}}
\end{aligned}
\quad (0 \le z \le H) \tag{3-14}
$$

where z, T_{f1} , T_{f2} and T_b are the temperatures of the fluid running downwards, the fluid running upwards and borehole wall, respectively, z is the direction along the tube and R_1^{Δ} , R_{12}^{Δ} , and R_2^{Δ} are thermal resistances defined in Eq. (3-10).

Here, R_{11} and R_{22} are the thermal resistance between the circulating fluid and the borehole wall, and R_{12} is the resistance between the pipes (Figure 3-2). In most engineering applications, the configuration of the U-tube in the borehole may be assumed symmetric, and when it is assumed that $R_{22}=R_{11}$, the following relations can be derived:

$$
R_1^{\Delta} = R_2^{\Delta} = R_{11} + R_{12}, \quad R_{12}^{\Delta} = \frac{R_{11}^2 - R_{12}^2}{R_{12}} \tag{3-15}
$$

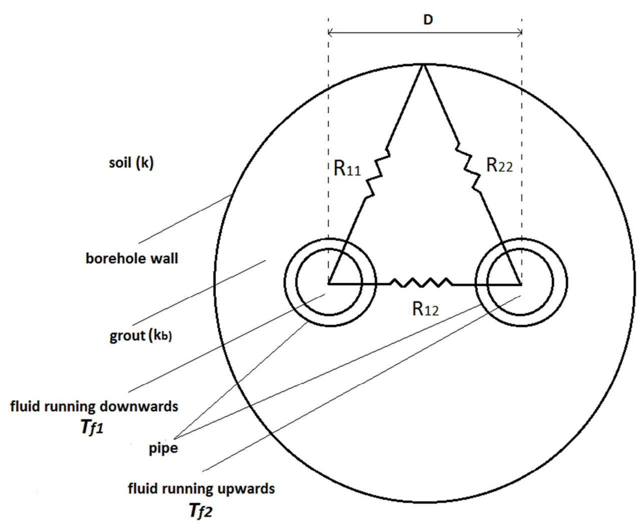

Figure 3-2 Thermal resistances in the borehole.

The steady-state conduction problem in the borehole cross-section was analyzed in detail by Hellström (1991) and Claesson and Hellström (2011) with the line source and Multipole approximations. The line-source assumption results in the following solution:

$$R_{11} = \frac{1}{2\pi k_b}\left[\ln\left(\frac{r_b}{r_p}\right) + \frac{k_b - k}{k_b + k}.\ln\left(\frac{r_b^2}{r_b^2 - D^2}\right)\right] + R_p$$
$$R_{12} = \frac{1}{2\pi k_b}\left[\ln\left(\frac{r_b}{2D}\right) + \frac{k_b - k}{k_b + k}.\ln\left(\frac{r_b^2}{r_b^2 + D^2}\right)\right] \tag{3-16}$$

where r_b, r_p, k_b, k, D and R_p are the radius of the boreholes, radius of the pipe, the grout thermal conductivity, the soil thermal conductivity, the distance between the pipes in the borehole, and the thermal resistance of conduction in the pipe, respectively (Figure 3-2).

The following boundary conditions are applied to the energy equations [Eq. (3-14)]:

$$z = 0, \quad T_{f1} = T'_f$$
$$z = H, \quad T_{f1} = T_{f2} \tag{3-17}$$

where T'_f is the temperature of the fluid entering the U-tube. Using a Laplace transformation, the general solution of Eq. (3-14) is obtained which is complicated in form and can be found elsewhere (Zeng et al. 2003b). At the instance of symmetric disposal of the U-tube inside the borehole, the temperature profiles in the two pipes are reduced as

$$\Theta_1(Z) = \cosh(\beta Z) - \frac{1}{\sqrt{1-P^2}}\left[1 - P\frac{\cosh(\beta) - \sqrt{\frac{1-P}{1+P}}\sinh(\beta Z)}{\cosh(\beta) + \sqrt{\frac{1-P}{1+P}}\sinh(\beta)}\right].\sinh(\beta Z)$$
$$\Theta_2(Z) = \frac{\cosh(\beta) - \sqrt{\frac{1-P}{1+P}}\sinh(\beta)}{\cosh(\beta) + \sqrt{\frac{1-P}{1+P}}\sinh(\beta)}\cosh(\beta Z) + \frac{1}{\sqrt{1-P^2}}\left[\frac{\cosh(\beta) - \sqrt{\frac{1-P}{1+P}}\sinh(\beta)}{\cosh(\beta) + \sqrt{\frac{1-P}{1+P}}\sinh(\beta)} - P\right].\sinh(\beta Z) \tag{3-18}$$

where the dimensionless parameters are defined as

$$\Theta = \frac{T_f(z) - T_b}{T_f' - T_b}, \quad Z = \frac{z}{H}, \quad P = \frac{R_{12}}{R_{11}}$$
$$\beta = \frac{H}{\dot{m} c_p \sqrt{(R_{11} + R_{12})(R_{11} - R_{12})}} \qquad (3\text{-}19)$$

Zeng et al (2003a) illustrate the temperature profiles in the pipes for the symmetric placement of the U-tube inside the borehole. They present a parameter called the heat transfer efficiency of the borehole as

$$\varepsilon = \frac{T_f' - T_f''}{T_f'' - T_b} \qquad (3\text{-}20)$$

which deals with the heat exchanger inside the borehole only, and is independent of time. Here, T_f'' is the temperature of the fluid exiting the U-tube. They obtain the analytical expression of the efficiency of a vertical geothermal heat exchanger for the two-dimensional and quasi-three-dimensional cases and show the fluid temperature differences along the borehole axial direction.

Taking this parameter into account in the temperature profile derived from Eq. (3-14), Diao et al. (2004a) derived the thermal resistance between the fluid inside the U-tube and the borehole wall as

$$R_{b3} = \frac{H}{\dot{m} c_p}\left(\frac{1}{\varepsilon} - \frac{1}{2}\right) \qquad (3\text{-}21)$$

where R_{b3} is the borehole thermal resistance for the three-dimensional analysis. They conceded that the relative error in the borehole resistance between the two-dimensional and quasi-three-dimensional models is figured out to be a function of the single dimensionless parameter, β, only. The value of β is usually less than 0.6, resulting in error of less than 11%.

Zeng et al. (2003b) focus on quasi-three-dimensional heat transfer inside a borehole with double U-tubes, and determine analytical expressions of the thermal resistance of single and double U-tube boreholes for with all possible circuit layouts. Comparisons of the performances of single and double U-tube boreholes show that the double U-tube boreholes are superior to those of the single U-tube, with reductions in borehole resistance of 30-90%. Also, superior performance is observed in double U-tubes in parallel compared to those in series. They also studied a relatively wide range of factors, including geometrical parameters (borehole and pipe sizes and pipe disposal in the borehole), physical parameters (thermal conductivity of the materials, flow rates and fluid properties) and the flow circuit configuration.

Quasi-3-D models reveal drawbacks of 2-D models and are thus preferred for design and analysis of GHEs, as they provide more accurate information for performance simulation and analysis and design. Diao et al. (2004a) discuss and summarize the improvements on the modeling of vertical GHE from the aspect of heat transfer analysis inside the borehole. A summary of the analytical methods for modelling the heat transfer inside the borehole is made in Table 3-1.

Table 3-1 Comparison of various methods in the heat analysis inside the borehole.

	1D (Equivalent diameter)	**1D (Shape factor)**	**2D**	**Quasi 3D**
U-tube disposal	N	Y	Y	Y
Quantitative expressions of the thermal resistance in the cross-section	N	N	Y	Y
Thermal interference	N	N	N	Y
Extinction between the entering and exiting pipes	N	N	N	Y
Axial convection by fluid flow	N	N	N	Y
Axial conduction in grout	N	N	N	N

3.1.2 Heat Transfer Outside the Borehole

Several simulation models for the heat transfer outside the borehole are available, most of which are based on analytical and/or numerical methods. The models vary in the way the problem of heat conduction in the soil is solved, the way the interference between boreholes is treated and the way the methods are accelerated. In the analysis of GHE heat transfer, some complicating factors, such as ground stratification, ground temperature variation with depth, and groundwater movement (Chiasson et al. 2000) usually prove to be of minor importance and are analyzed separately. As a basic problem, the following assumptions are commonly made:

- The ground is homogeneous in its thermal properties and initial temperature.

- Moisture migration is negligible.
- Thermal contact resistance is negligible between the pipe and grout and between the grout and soil.
- The effect of ground surface is negligible.

Unlike the area inside the borehole, heat conduction outside the borehole exhibits transient behavior. The thermal response due to a step-change in the specific heat injection rate $\dot{q}$ given per unit length of the borehole associated with a temperature evolution ($T_b - T_0$) results in a time-dependent ground thermal resistance R_g.

The general heat conduction equation in cylindrical coordinates appears in the following form:

$$\frac{\partial^2 T}{\partial r^2} + \frac{1}{r}\frac{\partial T}{\partial r} + \frac{1}{r^2}\frac{\partial^2 T}{\partial \varphi^2} + \frac{\partial^2 T}{\partial z^2} + \frac{\dot{q}_{gen}}{k} = \frac{1}{\alpha}\frac{\partial T}{\partial t} \tag{3-22}$$

where t is the time from the start of operation, α is the thermal diffusivity of soil, and T is the temperature of the ground. The first two terms on the left side of Eq. (3-22) are the heat flux components in the radial (r) direction, the third and the fourth terms are related to the circumferential (φ) and axial (z) directions, respectively, and the fifth term relates to the heat generated in the control volume. The right side of Eq. (3-22) represents the transient effects of heat conduction.

The heat conduction in the radial direction is dominant when there is no ground water flow and the effect of the ground surface can be neglected for the initial 5-10 years (depending on the borehole depth). Therefore, the heat transfer is usually modeled with a one-dimensional line-source (Eskilson 1987) or cylindrical-source theory (Carslaw and Jaeger 1946). To gain more accuracy, some authors have considered the axial heat flow in the ground for longer durations (greater than 5-10 years).

3.1.2.1 Line-source Model

The earliest approach to calculating the heat transfer in the soil surrounding a GHE is Kelvin's line-source model, i.e. the infinite line-source (Hellsrom 1991; Ingersoll et al. 1954) which uses Fourier's law of heat conduction. In the line-source theory, the borehole is assumed as an infinite line-source in the ground which is regarded as an infinite medium with an initial uniform temperature. Due to its minor order, heat transfer in the axial direction along the borehole, which accounts for the heat flux across the ground surface and down to the bottom of the borehole, is considered negligible. This assumption is valid for a length of the borehole distant enough from the borehole top and bottom. Therefore, heat conduction in the ground is assumed as an unsteady radial heat conduction problem, i.e. $T(r,t)$ and the following simplified heat conduction equation can be derived:

$$\frac{\partial^2 T}{\partial r^2}+\frac{1}{r}\frac{\partial T}{\partial r}=\frac{1}{a}\frac{\partial T}{\partial t} \tag{3-23}$$

The following assumptions are made for the line-source model in GHEs:

- Thermal properties of the soil are isotropic and uniform.
- Moisture migration is negligible.
- Impact of ground water advection is negligible.
- Thermal contact resistance is negligible between the pipe and grout and between the grout and soil.
- The effect of ground surface is negligible.

The boundary conditions for a line source of heat are introduced as

$$\begin{aligned} &-2\pi r_b k\frac{\partial T}{\partial r}=q' && r\to 0\\ &T-T_0\to 0 && r\to\infty\\ &T-T_0=0 && t=0 \end{aligned} \tag{3-24}$$

where T_0 is the initial temperature of the ground (t = 0), q' is the heating rate per unit length of the line source, and k is the soil conductivity. The first boundary condition in Eq. (3-24) is related to the heat flow rate per unit length at the borehole wall conducted in the soil which is derived from the Fourier's law of heat conduction (Eskilson 1987). At larger distances ($r\to\infty$) the temperature of the soil is not affected by the line source of heat and remains equal to the initial condition. The last condition relates to the initial temperature of the soil at $t=0$. The temperature response in the ground due to a constant heat flow rate per unit length of the line source (q') is given by

$$T(r,t) - T_0 = \frac{q'}{4\pi k}\int_{\frac{r^2}{4at}}^{\infty} \frac{e^{-u}}{u} du \qquad (3\text{-}25)$$

The left side of Eq. (3-25) gives the temperature excess of the soil around a single borehole at radial distance r and at time t when heat flow rate per unit length of the borehole (q') is transferred through the soil. The exponential integral on the right side of Eq. (3-25) can be calculated numerically. It is seen that a higher rate of heat flow (q') on the borehole wall results in a higher temperature rise around the borehole.

The line heat source model is a simple model requiring little computation time and therefore is the most widely used theory in design methods to analyze GHE heat transfer. However, due to its assumption of the infinite line-source, temperatures computed from this theory at a short distance from the center and after a short time exceed the maximum possible fluid temperature computed from an energy balance. Ingersoll and Plass (1948) estimate that using this method may cause a noticeable error when $\alpha t / r_b^2 < 20$, where r_b is the borehole radius, t is the time from the start of system operation and α is the thermal diffusivity of the soil around the borehole. Therefore, this method can only be applied to small pipes for short-term operation of GHP systems, i.e., from a few hours to months. To make the analytical results obtained by this method more accurate and comparable to numerical ones, several studies have focused on improvements, among which the results of Hart and Couvillion (1986) are some of the most accurate. They propose an equation for the ground temperature around a line source in terms of a power series of the ratio of radial distance and farfield distance. The definition of farfield distance depends on the radius of the borehole. Lamarche and Beauchamp (2007) develop alternative forms for the finite line source solution with shorter computation times.

3.1.2.2 Cylindrical-source Model

Another analytical model based on Fourier's law of heat conduction was first developed by Carslaw and Jaeger (1946). In this model, the borehole is assumed to be a cylindrical pipe with infinite length buried in the ground which is considered a homogeneous infinite medium with constant properties. During the transient stage of heat storage in the soil, the thermal capacities of the fluid and immediate region next to the core are neglected in the early time results of the cylindrical source theory. In addition, it is assumed that heat transfer between the borehole and soil with perfect contact is pure heat conduction. Therefore, using the same assumptions presented for the line source theory in the previous section, the governing equation of the transient heat conduction in cylindrical coordinates can be simplified as

$$\frac{\partial^2 T}{\partial r^2}+\frac{1}{r}\frac{\partial T}{\partial r}=\frac{1}{a}\frac{\partial T}{\partial t} \quad r_b < r < \infty \tag{3-26}$$

with the following boundary conditions:

$$\begin{aligned} &-2\pi r_b k\frac{\partial T}{\partial r}=q' && r=r_b.\tau>0 \\ &T-T_0=0 && \tau=0, r>r_b \end{aligned} \tag{3-27}$$

where r_b is the borehole radius and t_0 is the initial temperature of the soil. The governing equation for this model can be solved analytically for either a constant pipe surface temperature or a constant heat transfer rate from the pipe to the ground. The analytical solution of Eq. (3-26) given by Carslaw and Jaeger (1946) is

$$T-T_0=\frac{q'}{k}\mathrm{G}\left(\frac{at}{r_b},\frac{r}{r_b}\right) \tag{3-28}$$

and $G(z,p)$ is a function of time (t) and distance from the borehole center (r), and involves integrations from zero to infinity of a complicated function, including Bessel functions (Bandyopadhyay et al. 2008):

$$T(r,t)-T_0=\frac{q'}{\pi^2 k}\int_0^\infty \frac{e^{-\frac{u\alpha t}{r^2}}-1}{J_1^2(u)+Y_1^2(u)}\left[J_0(u)Y_1(u)-J_1(u)Y_0(u)\right]\frac{du}{u^2} \tag{3-29}$$

To obtain the temperature on the borehole wall ($r/r_b=1$), which is the representative temperature in the design of GHEs, some graphical results and tabulated values for the $\mathrm{G}(\alpha t/r_b, r/r_b)$ function at $r/r_b=1$ (the borehole wall) can be found in related references (Ingersoll et al. 1954).

Similar to the line-source model, cylindrical source solutions have limitations at the early stage of transient heat conduction flux build up after a step heat input is applied to the system fluid. The cylindrical source solution assumes a steady flux across a hollow cylindrical surface (borehole boundary) and omits the grout and fluid from the problem domain. Yet during the transient flux build up, the thermal capacities of the fluid and immediate region next to the core are neglected in the early time results of the cylindrical source theory.

Kavanaugh (1992) moved the reference cylindrical surface from the borehole boundary to an intermediate surface inside the borehole nearer to the core to improve the accuracy of the cylindrical source solution. This modification allows the reference surface to reach a near-steady-flux condition earlier than with the borehole boundary as the reference surface. However, the effect of neglecting the thermal capacity of the fluid remains a shortcoming of the cylindrical source theory.

Hellström (1991) applies a numerical inversion technique to solve the inverse Laplace transform of the governing differential equation for the one-dimensional transient heat conduction equation in polar coordinates and develops an alternative form for the cylindrical source solution.

Hikari et al. (2004) derive simplified forms for the cylindrical source solution at the borehole surface depending on the Fourier number.

3.2 Semi-analytical Methods

In both analytical models of Kelvin's theory and the cylindrical source model, the borehole depth is considered infinite and the axial heat flow along the borehole depth is assumed negligible. Furthermore, when time tends to infinity, the temperature rise of the Kelvin's theory for an infinite line source tends to infinity, making the infinite model weak for describing heat transfer mechanism in long time steps. On the other hand, the temperature from the finite line-source model approaches steady state corresponding to the actual heat transfer mechanism. Therefore, they can only be used for short time range of operations of GHP systems. To take into account axial temperature changes for boreholes with finite lengths and in long durations, a number of approaches for ground loop heat exchangers have been devised that combine numerical and analytical methods.

Eskilson's approach to the problem of determining the temperature distribution around a borehole is based on a hybrid model combining analytical and numerical solution techniques. Eskilson (1987) applies a numerical finite-difference method to the transient radial-axial heat conduction equation for a single borehole:

$$\frac{\partial^2 T}{\partial r^2}+\frac{1}{r}\frac{\partial T}{\partial r}+\frac{\partial^2 T}{\partial z^2}=\frac{1}{a}\frac{\partial T}{\partial t} \tag{3-30}$$

assuming no temperature change on the ground surface (by superimposing an identical mirror borehole above the ground surface with negative strength). Note that, compared to Eq. (3-26), the third term on the left side of Eq. (3-30) accounts for the axial heat flow along the borehole depth. Assuming the ground to be homogeneous with constant initial and boundary temperatures, the boundary conditions are presented as

$$\begin{aligned} T(r,0,\tau) &= T_0 \\ T(r,z,0) &= T_0 \\ q'(t) &= \frac{1}{H}\int_D^{D+H} 2\pi r k \frac{\partial t}{\partial r}\Big|_{r=r_b} dz \end{aligned} \tag{3-31}$$

where H is the active borehole length and D is the uppermost part of the borehole. The thermal capacitance of the individual borehole elements such as the tube wall and the grout are neglected. The temperature fields from a single borehole are superposed in space to obtain the response from the whole borefield. The temperature response of the borefield is converted to a set of non-dimensional temperature response factors, called g-functions. The g-function allows the calculation of the temperature change at the borehole wall in response to a step heat input for a time step. Once the response of the borefield to a single step heat pulse is represented with a g-function, the response to any arbitrary heat rejection/extraction function can be determined by devolving the heat rejection/extraction into a series of step functions, and superimposing the response to each step function. Therefore, the temperature distribution at the wall of a single borehole with finite length to a unit step heat pulse is defined as

$$T_b - T_0 = -\frac{q'}{2\pi k} g\left(t/t_s, r_b/H\right) \tag{3-32}$$

where $t_s = H^2/9\alpha$ is the steady-state time and the g-function is the non-dimensional temperature distribution at the borehole wall, which is computed numerically. The g-function curves are developed based on selected borefield configurations.

For the temperature responses of multiple boreholes, using a superimposition method in space to determine the overall temperature response of the GHE, g-functions of the GHEs with different configurations (i.e. any heat rejection/extraction at any time) have to be pre-computed and stored in the program as a large database with one of the parameters fixed. Therefore, an interpolation function is applied in using the database causing some computing errors. The model is intended to provide the response of the ground to heat rejection/extraction over longer periods of time (up to 25 years). Since the numerical model that provides the g-functions does not account for the local borehole geometry, it cannot accurately provide the shorter term response.

Modifying Kelvin's line-source model, Zeng et al. (2002, 2003a) and Diao et al. (2004a) present an analytical solution to the transient finite line-source problem considering the effects of the finite borehole length and the ground surface as a boundary. Their study is based on the following assumptions: the temperature of the ground surface t_0 remains constant and equal to its initial value over the time period concerned and the heating rate per length of the source (q') is constant. With these assumptions, the non-dimensional solution of the temperature excess is

$$\theta\left(\overline{R}, Z, Fo\right) = \frac{q'}{4k\pi}\int_0^1 \left\{ \frac{erfc\left(\dfrac{\sqrt{\overline{R}^2 + \left(Z-\overline{H}\right)^2}}{2\sqrt{Fo}}\right)}{\sqrt{\overline{R}^2 + \left(Z-\overline{H}\right)^2}} - \frac{erfc\left(\dfrac{\sqrt{\overline{R}^2 + \left(Z+\overline{H}\right)^2}}{2\sqrt{Fo}}\right)}{\sqrt{\overline{R}^2 + \left(Z+\overline{H}\right)^2}} \right\} d\overline{H} \tag{3-33}$$

where the dimensionless parameters are defined as

$$\theta = T - T_0, \quad Z = \frac{z}{H}, \quad \overline{H} = \frac{h_z}{H}, \quad \overline{R} = \frac{r}{H}, \quad Fo = \frac{\alpha t}{H^2} \tag{3-34}$$

and the integral can be computed numerically. A comparison of the analytical results and the numerical data from Eskilson's solution show satisfactory agreement, especially when $at/r_b^2 \geq 5$. With respect to long durations, the explicit solution of a finite line-source model better describes the temperature responses of the borehole for long time steps.

Furthermore, in both Eskilson's model and the finite line-source model, the radial dimension of the borehole and, therefore, the thermal capacity of the borehole, including the U-tubes, the circulating fluid and the grout, are neglected. Eskilson estimates that the results for temperature responses on the borehole wall due to this assumption are only valid for a time greater than $5r_b^2/\alpha$, where the terms are as defined earlier.

It can be seen from Eq. (3-33) that the temperature of the medium varies with time, the radial distance from the borehole and the borehole depth. A representative temperature for the borehole wall is often chosen which represents the mean borehole wall temperature along the borehole depth and is used in the heat transfer analysis inside the borehole. To choose a representative temperature for the borehole wall ($r=r_b$) along the borehole depth, one can either choose the temperature at the middle of the borehole depth ($z=0.5H$) or the integral mean temperature along the borehole depth, which may be determined by numerical integration of Eq. (3-33). The difference between the two is analyzed and found to be insignificant (Zeng et al. 2002).

Yang et al. (2009) propose and develop an updated two-region vertical U-tube GHE analytical model. It divides the heat transfer region of the GHE into two parts at the boundary of borehole wall, and the two regions are coupled by the temperature of borehole wall. They use both steady and transient heat transfer methods to analyze the heat transfer process inside and outside the borehole, respectively. To model the region outside the borehole, they use cylindrical source theory and for the region inside the borehole a quasi-three-dimensional model. Both models are coupled by the transient temperature of the borehole wall. The experimental validation of the model indicates that the calculated fluid outlet temperatures of the GHE agree well with the corresponding test data and the relative error is less than 6%.

Cui et al. (2006) establish a transient three-dimensional heat conduction model to describe the temperature response in the ground caused by a single inclined line source. Heat transfer in the GHEs with multiple boreholes is then studied by superimposition of the temperature excesses resulted from individual boreholes. The thermal interference between inclined boreholes is compared with that between vertical ones. The analyses can provide a basic and useful tool for the design and thermal simulation of the GHEs with inclined boreholes.

To deal with loads varying with time, the method of load aggregation can be employed (Bernier et al. 2004). The load profile is divided into various constant load steps starting at particular time instants. The overall performance is the summation of effects from each load step. Bernier et al. (2004) suggest a multiple load aggregation algorithm to calculate the performance of a single borehole at variable load based on the cylindrical source model.

Hellström (1991) proposes a simulation model for vertical ground heat stores, which are densely-packed ground loop heat exchangers used for seasonal thermal energy storage. This type of system may or may not incorporate heat pumps to heat buildings. This model divides the medium with multiple boreholes into two regions: 'local' which is the region surrounding a single borehole and 'global' which is the farfield beyond the bulk volume of the multiple boreholes. He calculates the store performance based on a steady flux solution and solutions for the local and global regions. The numerical model used for the global region is a two-dimensional explicit finite-difference scheme in the radial-axial coordinate system.

Kavanaugh (1995) proposes an equation for calculating the required total borehole length by including various terms into the steady state heat transfer equation to account for load cycle effect, and thermal interference from adjacent boreholes and within tubes inside a borehole. These methods estimate the performance of the entire borefield.

Bandyopadhyay et al. (2008) developed a three-dimensional model to simulate BHEs. They obtain a semi-analytical solution for the U-tube geometry in grouted boreholes using a Laplace transform and subsequent numerical inversion of the Laplace domain solution. The solution results are found to agree with the results from the finite element method.

In the analytical models presented above, a number of assumptions are employed in order to simplify the complicated governing equations. Therefore, the accuracy of the analytical solutions is reduced. The assumptions include treating the two pipes as one pipe coaxial with the borehole or simplifying the pipe and the borehole as an infinitely long line source and not taking into account the thermal capacity inside the borehole. Therefore, regarding time varying heat transfer rates and the influence of surrounding boreholes on both long and short time scales, analytical methods are not as suitable as numerical methods, which are discussed in the next section. However, due to their much shorter computation times, they are still used widely in designing GHEs.

3.3 Numerical Models

System simulation models require the ability to operate at short time scales, often less than one minute. Therefore, the dynamic response of the grout material inside the borehole should be considered. Mei and Baxter (1986) consider the two-dimensional model of the radial and longitudinal heat transfer, which is solved with a finite difference scheme. Yavuzturk (1999) and Yavuzturk et al. (1999) present a fully implicit finite-volume numerical model based on a two-dimensional radial-axial coordinate system for the simulation of transient heat transfer in vertical ground loop heat exchangers. Their model is essentially an extension of Eskilson's g-function model to take into account the short-time behavior of the thermal response, for periods of one hour and less. Using an automated parametric grid generation algorithm, numerical grids are generated for various pipe diameters, shank spacing and borehole diameters. Furthermore, the numerical method and grid-generation techniques are validated with a comparable analytical model. Because the short time-step g-function represented the response of the entire GHE, it necessarily utilized a fixed convective resistance. The authors later found it necessary (Yavuzturk and Spitler 2001) to modify the model to include variable convective resistance, but this was done at the expense of modeling the thermal mass of the fluid in the borehole.

Xu and Spitler (2006) describe the development of a new short time-step model for vertical ground loop heat exchangers. Like the Yavuzturk and Spitler (1999) model, it is an extension to the original long time-step Eskilson model (Eskilson 1987). However, whereas that model used a short time-step g-function to account for short time-step effects, their model replaces the response function approach at short time-steps with a one-dimensional numerical model, which explicitly accounts for the thermal mass of the fluid and the convective resistance as a function of flow rate, fluid mixture, and fluid temperature. This is integrated with Eskilson's long time-step model. By careful control of the one-dimensional model parameters, the model is able to give acceptably accurate short-term response, without the computational time that would be required to run such a model continuously throughout the simulation.

Muraya (1995) uses a transient two-dimensional finite-element model of the heat transfer around a vertical U-tube heat exchanger for a GHP system to study the thermal interference between the U-tube legs. He develops two finite element codes: one for pure heat conduction and another for coupled heat conduction and moisture diffusion. The finite element heat model is coded to approximate solutions to the partial differential heat diffusion equation where no analytical solutions are available. The heat exchanger effectiveness is defined in the model based on soil and grout properties, shank spacing, farfield and loop temperatures, and heat dissipation rates to account for the interference between the U-tube legs. Heat exchanger effectiveness is found to be independent of a dimensionless temperature based on temperatures of the tubes and soil, and varies only with separation distance at steady state. The model is validated by two analytical cylindrical source models under constant-temperature and constant-heat flux conditions.

Kavanaugh (1985) uses a two-dimensional finite-difference method to study the performance of a borehole with a concentric tube. Rottmayer et al. (1997) uses a two-dimensional finite-difference formulation on a polar grid to calculate the lateral heat transfer along 3-m vertical lengths of a borehole. Although axial conduction is neglected, each length section of the model is coupled via the boundary conditions to a model of flow along the U-tube. This quasi-three-dimensional model accounts for the variations in temperature of the circulating fluid in the axial direction.

Lee and Lam (2008) simulate the performance of borehole GHEs using a three-dimensional finite-difference method in rectangular coordinates. They evaluate the heat transfer inside the borehole using a finite-difference method based on quasi-steady state conditions, allowing variable temperature and loading along the borehole. Their results show that neither the temperature nor the loading is constant along the borehole, and that the maximum temperature occurs near the top part of the borehole while borehole loading reaches a minimum near the bottom of the borehole. The ground temperature profile changes with distance from the borehole, where the depth of maximum temperature shifts to the mid-level of the borehole at large distances. This implies that using the result obtained from a single borehole with superposition is not sufficient to predict precisely the performance of a borefield. A better approach would be to discretize the entire borefield and to simulate all boreholes simultaneously. Finally, the authors compare their results with a line source solution with superposition and determine that the deviation of their results from the analytical ones increases with the scale of borefield.

Li and Zheng (2009) propose a three-dimensional unstructured finite-volume numerical model of a vertical U-tube GHE. They use the Delaunay triangulation method to mesh the cross-section domain of the borefield. The mesh includes both the exterior of the borehole as well as its interior. Thus, the transient effect in the borehole in a short time scale is simulated. To further improve computational accuracy, they divide the soil into several layers in the axial direction, which accounts for the effect of the axial change in temperature. The numerical results of this model show good agreement with experimental data. This model may be used for simulation of a GHE under any time step size, although its use in transient analysis based on a short time step (an hour or less) is preferred.

In a GSHP system, the heat pump and the circulating pumps switch on and off during a given hour; therefore, the effect of thermal mass of the circulating fluid and the dynamics of fluid transport through the loop need to be taken into account. To address this issue, He et al. (2009) developed a three-dimensional numerical model, which simulates fluid transport along a pipe loop as well as heat transfer with the ground. The authors carry out the simulation of the GSHP system in EnergyPlus with 10 min time steps for one year and use the GLHEPro tool to simulate the borehole heat exchanger. They validate the model by reference to analytical models of borehole thermal resistance and also fluid transport inside the pipe, and compare the predicted outlet temperature with those of a similar two-dimensional model and an implementation of a short time step g-function model. The results show that the delayed response associated with the transit of fluid around the pipe loop is of some significance in moderating swings in temperature during the short period when the heat pump starts to operate. Their BHE model exhibits a lower heat transfer rate over longer periods of operation compared to two-dimensional models. This is due to the mean temperature differences between the fluid and the ground being lower in the three-dimensional model. Fang et al. (2002) consider the variation in load and on-off cycling of the GHE by superimposition of a series of heating pulses. The temperature on the borehole wall can then be determined for any instant based on specified operational conditions.

3.4 Other Modeling Aspects

In solving the governing equations in both analytical and numerical approaches, parameters such as moisture migration and groundwater flow might exist. In the solutions presented in the previous section, it is assumed that these parameters are not present. However, neglecting them can result in errors in the solution in some cases.

3.4.1 Ground Surface Boundary Condition

Energy and moisture balances at the ground surface can be performed following the model used by Tarnawski (1982), which involves very complex processes, taking into account solar radiation, cloud cover, surface albedo, ambient air temperature and relative humidity, rainfall, snow cover, wind speed, and evapotranspiration. Such details provide a proper account of the renewable energy resource. The energy balance on the ground surface can be written as

$$q_n + q_{adv} + q_{sn} + q_h - q_{lo} - q_e = 0 \tag{3-35}$$

where q_n, q_{adv}, q_{sn}, q_h, q_{lo} and q_e are heat flux by conduction from underground, advective energy (rain), net incoming short wave radiation, convective heat transfer, net outgoing longwave radiation, and latent heat flux by evaporation, evapotranspiration, melting snow or sublimation, respectively. Of all these fluxes, the radiation exchange is the most important while the convective heat transfer and heat flow by evaporation are of secondary importance.

However, due to the complexity of adding all the above heat fluxes in the numerical model, some studies assume the ground surface temperature variation at the ground surface to take the form of a sine-wave or Fourier series (Salah El-Din 1999; Mihalakakou and Lewis 1996; Mihalakakou 2002; Jacovides et al. 1996) while some assume the ground surface boundary to have a constant temperature equal to periodic air temperature or isothermal to the soil temperature deep in the ground. Moreover, some studies simplify the problem further and assume an adiabatic boundary condition at the ground surface.

3.4.2 Moisture Migration in the Soil

When neglecting the existence of moisture in the soil, the heat flux is described in terms of conduction, latent heat transport and sensible heat flow. The coupled heat and moisture flow in a soil system is described with a thermal energy balance coupled with a mass balance. This adds to the complication of the problem since the complete model contains a set of transient simultaneous partial differential equations with many soil parameters that are not readily available. Research shows that the effects of moisture migration are not significant to the operation of a vertical GHE, it is expected that these effects are more pronounced with a horizontal ground heat exchanger (HGHE). This is because natural variations of temperature and moisture near the ground surface and operation of the HGHE may create a potentially greater moisture movement. During the cooling season, migration of soil moisture away from the GHE may lead to a drastic drop in soil thermal conductivity and consequently a significantly reduced heat transfer, which has a devastating effect on GHE performance. Therefore, although moisture migration effects can be neglected in early stages of design or conceptual development, not considering them in long-term operation of GCHP systems makes it impossible to assess the performance and potential failure of these systems (Leong and Tarnawski 2010).

Mei (1986) proposed a GHE model based on an energy balance between the circulating fluid inside the coil and the surrounding soil. The thermal interaction between the circulating fluid and soil is calculated taking into account heat flow with or without moisture transfer in the soil.

To reduce the computational time, Piechowski (1999) solved heat and moisture diffusion equations at the locations with the largest temperature and moisture gradients, i.e. within a distance of 0.15 m from the pipe-soil interface. For the remaining soil region, the heat diffusion equation was applied only. Although the approach offers considerable reduction in simulation time, it is still time demanding, as small simulation time steps, on the order of minutes, are required. Therefore, this modeling approach is not suitable for simulating the long-term performance of large GCHP systems.

Leong and Tarnawski (2010) evaluate the effects of simultaneous heat and moisture transfer on the performance of a solar-assisted ground source heat pump system with vertical ground heat exchangers by using a computer simulation package called Vertical Ground Heat Exchanger Analysis, Design and Simulation (VGHEADS). Two modeling approaches are compared: pure heat conduction vs. simultaneous heat and moisture transfer. By disregarding moisture migration in the soil, they find a 2%

difference in the annual heat rejection to the ground with respect to the case of simultaneous heat and moisture transfer.

3.4.3 Groundwater Movement

A further complication in the design of ground-coupled heat pump systems is the presence of groundwater. Due to the difficulties encountered both in modeling and computing the convective heat transfer and in learning about the actual groundwater flow in engineering practice, each of the methods presented in the previous sections is based on Fourier's law of heat conduction and neglect the effects of groundwater flow in carrying away heat. Where groundwater is present, flow will occur in response to hydraulic gradients, and the physical process affecting heat transfer in the ground is inherently a coupled one of heat diffusion (conduction) and heat advection by moving groundwater.

Underground water occurs in two zones: the unsaturated zone and the saturated zone. The term "groundwater" refers to the water in the saturated zone. The surface separating the saturated zone from the unsaturated zone is known as "water table." At the water table, water in soil or rock pore spaces is at atmospheric pressure. In the saturated zone (below the water table), pores are fully saturated and water exists at pressures greater than atmospheric. In the unsaturated zone, pores are only partially saturated and the water exists under tension at pressures less than atmospheric. Groundwater is present nearly everywhere, but it is only when the local geology results in the formation of aquifers that significant flows of groundwater can be expected.

Aquifers are described as being either confined or unconfined. Confined aquifers are bounded between two or more layers of rock (or clay soils) of low permeability. Unconfined aquifers are bounded at their upper surface by the water table. In practice, the boreholes of ground loop heat exchangers may partially penetrate unconfined aquifers and/or at greater depths penetrate into confined aquifers. A summary on the current knowledge of aquitard science with emphasis on aspects on ground water resources use and management, investigations of aquitard integrity, and specific technical methodologies, categories of data collection, and synthesis is given by Awwa Research Foundation (2006a, 2006b).

In general, for material with high hydraulic conductivity and thus high discharge rates, steadily flowing groundwater is expected to be beneficial to the thermal performance of closed-loop GHEs. According to the conduction model, the required ground-loop heat exchanger lengths are significantly greater than the required lengths if the annual load were balanced so as to adequately dissipate the imbalanced annual loads. On the other hand, a moderate groundwater advection is expected to make notable difference in alleviating the possible heat buildup around the borehole over time. As a result, it is desirable to account for the groundwater flow in the heat transfer model to avoid over-sizing of the GHEs. Therefore, it is essential to have tools that allow for the evaluation not only of technical aspects of GSHP systems but also the effects of groundwater flow on the system efficiency and, further, the temperature changes in the aquifer exerted by the energy extraction or injection rates.

Chiasson et al. (2000) analyze the effect of groundwater using a two-dimensional finite-element scheme by discretizing a 4x4 borefield and including the interior of boreholes in the discretization. A simple but useful method of assessing the relative importance of heat conduction in the ground versus heat advection by moving groundwater is demonstrated through the use of the dimensionless Peclet number. They used a finite element numerical groundwater flow and heat transfer model to simulate the effects of groundwater flow on a single closed-loop heat exchanger in various geologic materials. Their simulations show that the advection of heat by groundwater flow significantly enhances heat transfer in geologic materials with high hydraulic conductivity, such as sands, gravels, and rocks exhibiting fractures and solution channels.

Gehlin and Hellström (2003) investigate the ground water effect on thermal response test of an infinite borehole using a two-dimensional finite difference method with regular square meshes. The borehole is represented by four squares.

Diao et al. (2004b) study the combined heat transfer of conduction and advection in the vertical borehole heat exchangers by an analytical approach. Similar to Chiasson et al. (2000), they use a two-dimensional model of a borehole in an infinite porous medium with uniform water advection. They solve the model analytically by approximating the borehole by a line heat source and derive an explicit expression of the temperature response describing correlation among various factors, which have impacts on this process. Compared with the conventional Kelvin's line-source model, which makes no account of the water advection, this solution indicates that the impact of moderate groundwater flow on the heat transfer process may be prominent. The actual magnitude of the impact, however, depends mainly on the flow rate, which can be characterized by the non-dimensional parameter. This explicit and concise expression can provide an appropriate footing for qualitative and quantitative analysis of this impact for vertical GHEs in GCHP systems. In their results, it is noticeable that the ratio of the temperature rises at certain locations of the same distance from the source is independent of time.

Nam et al. (2008) use a numerical model that combines a heat transport model with groundwater flow to develop a heat exchanger model with an exact shape. The simulation code, FEFLOW, is used to calculate heat exchange rate between GHE and the surrounding ground and to estimate the distribution of the subterranean temperature. The authors validate their numerical simulation technique by comparing the results with available experimental data, and find good agreement between the two.

MT3DMS is a widely used program for simulation of solute transport in porous media. Owing to the mathematical similarities between the governing equations for solute transport and heat transport, this program appears also applicable to simulation of thermal transport phenomena in saturated aquifers. Hecht-Mendez et al. (2010) evaluate simulations of a single borehole ground source heat pump (GSHP) system in three scenarios: a pure conduction situation, an intermediate case, and a convection-dominated case. Two evaluation approaches are employed: first, MT3DMS heat transport results are compared with analytical solutions. Second, finite difference simulations by MT3DMS are compared with those by the finite element code FEFLOW and the finite difference code SEAWAT. The results suggest that MT3DMS can be successfully applied to simulate GSHP systems, and likely other systems with similar temperature ranges and gradients in saturated porous media.

3.5 Modelling Horizontal Ground Heat Exchangers

A number of studies have been conducted by various researches in the design, simulation and testing of horizontal GHEs.

Mei (1986) propose an approach for calculating soil thermal resistance surrounding a horizontal GHE. His approach is based on the energy balance between the circulating fluid in the pipe and the surrounding soil. In this approach, soil thermal resistance results from the soil thermal properties and the GHE geometry, and also from the operating strategy of the system. No initial estimation of the soil resistance to heat flow is required. Furthermore, the heat transfer interaction between the circulating fluid and the soil is not assumed, but calculated, based on the inlet water temperature to the GHE, and the mass flow rate. Another important difference is that the soil temperature distribution can be directly calculated, which allows for a more accurate prediction of the water temperature profile in the pipe.

A mathematical model of a horizontal type GHE is developed by Piechowski (1999). This model uses elements of the model proposed by Mei (1986). However, some major modifications are made in order to include heat and mass transfer in the soil as well as to enhance the accuracy of the model, and at the same time, to increase the speed of calculations. This is done by concentrating computational effort in the vicinity of the pipe where the most important heat and mass transfer phenomena are taking place. The proposed model calculates the temperature and moisture gradients at the pipe-soil interface.

Esen et al. (2007a) develop a numerical model of heat transfer in the ground for determining the temperature distribution in the vicinity of the horizontal ground heat exchanger (HGHE). In their experimental study, they present the COP_{sys} of the GCHP system and the temperature distributions measured in the ground in 2002–2003 heating season. An analytical solution of the transient temperature response has been derived in a semi-infinite medium with a line source of finite length.

Leong et al. (2006) study the use of a horizontal GHE and the impact of heat deposition and extraction in the ground are studied. They design an optimum GCHP system for an existing dwelling in Ontario using a computer model, called GHEADS There are many factors to be considered when one wants to optimize the design of a GHE. The optimum design of the GHE in their study may only be applicable to the studied dwelling, because it is specific to the site characteristics (such as soil type and climatic conditions) and system operating parameters (such as magnitude and frequency of heating and/or cooling operation). The optimum GCHP system designed for the existing dwelling appears to have both economic and environmental benefits.

Various studies of the horizontal GHEs have been performed experimentally with some including numerical validations (Esen et al. 2007b; Coskun et al. 2008; Pulat et al. 2009; Inalli and Esen 2004).

3.6 Summary and Conclusions

In this chapter, various vertical heat exchanger models are reviewed, ranging from primarily one-dimensional ones to two- and three-dimensional models which have been devised in the recent years.

Various analytical models that are currently being used to calculate heat transfer characteristics of these heat exchangers are examined. The following conclusions are drawn: the solutions inside the borehole are mostly steady state, whereas transient effects must be taken into account outside the borehole; most analytical models for the region outside the borehole do not take into account the thermal capacity of the borehole and assume infinite borehole length (but they are still used widely in designing GHEs because of their much shorter computation times); the analytical models available mostly focus on a constant ground heat load and further studies are needed to improve these models for use in transient periodic ground heat load; the analytical models are able to give a solution to the area inside the borehole or outside the borehole depending on their objective. In cases where a full system is being studied, such as in the current study, the literature lacks studies where these analytical models are coupled. Conducting a review of the numerical models, it is also concluded that the numerical methods are less often applied due to their computational time and the large solution domain.

Although a number of studies have focused on the development and application of ground heat pump systems, further investigation is needed, particularly in the area of estimating the heat delivery/removal strength when the soil surrounding them experiences thermal interaction, i.e. a temperature rise or drop. In order to account for the sustainability of the system and heat pump efficiency when thermal interaction among boreholes occur, it is important to develop and utilize models that account for the drop in heat delivery strength when the borehole wall temperature increases during the operation time or by another nearby operating system.

Effects such as moisture migration and groundwater flow are studied to learn about their importance in modeling vertical ground heat exchangers as well as to estimate the degree of complexity of the problem once they are included in the model. It is concluded that moisture migration does not have a large impact on temperature and the heat flows in the soil surrounding vertical heat exchangers. The ground water flow, when present, is found to have an impact on the heat flows in the soil surrounding a vertical ground heat exchanger. However, this impact could be negligible for low rates of groundwater flow.

Furthermore, it is found that using a model that is able to simulate the heat exchange processes within the system and surrounding environment through local scale assessment, simulation of migration of thermal plumes into the hydrogeological environment through intermediate and regional scale assessment will help gain an estimation of ecological impacts.

Chapter 4   MODEL DEVELOPEMENT

To examine the effects of borehole systems on nearby eco systems, the transient conduction of heat in the soil surrounding these systems needs to be modeled in order to evaluate the temperature rise and the heat flows in the soil surrounding the boreholes. The existence of thermal interaction among multiple boreholes and their possible negative effects on the design performance of the existing nearby boreholes can be examined by improving the model to account for changes in the heat pump coefficient of performance (COP).

The governing equations are presented in two sections here. In the numerical solution, the integral forms of the governing equations are presented with all the terms. In the analytical section, the models that can be used for modeling the temperature rise in the domain are mentioned. Coupling these models is a contributive key to the analytical modeling in this study and is presented in Chapter 5 .

4.1 Physical Domain

A domain consisting of two vertical borehole heat exchangers having a distance of D_b from each other is considered [Figure 4-1 (a) and (b)]. The circulating fluid runs through a U-tube [Figure 4-1 (c)] and delivers or removes heat to its surrounding which is grout in the borehole and the soil surrounding the borehole.

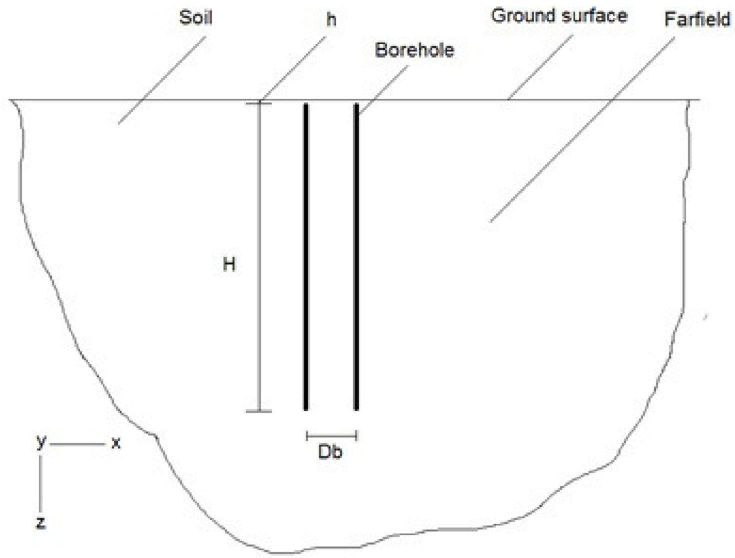

(a)

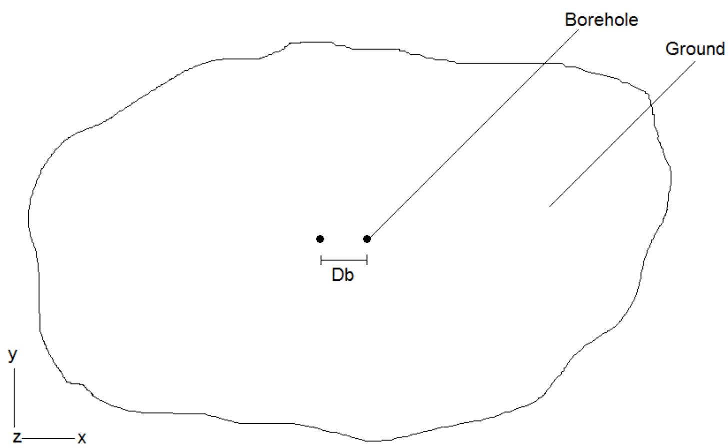

(b)

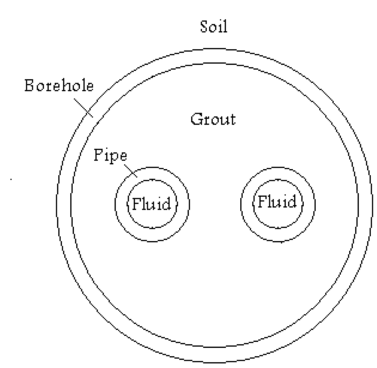

(c)

Figure 4-1 Schematic of (a) *xz* cross section of two boreholes installed at a certain borehole distance (D_b), (b) *xy* cross section of two boreholes installed at a certain borehole distance, and (c) cross section of inside a borehole.

4.2 Assumptions

Modeling a borehole heat exchanger completely by accounting for all the varying parameters affecting the borehole heat exchange operation is challenging. In the current study, various models are presented according to the two objectives of the study. They are all developed based on a set of simplifying assumptions. Some of the simplifying assumptions are due to a lack of experimentally evaluated physical parameters or due to the ability of the modeling tools available while others are due to negligible effects of a parameter in the current model. Therefore, the following assumptions are made in two groups here.

The flowing assumptions are made due to lack of experimentally evaluated physical parameters or inability of modeling tools that are available which could affect simulation results of the current study

- Thermal properties of the soil, grout and the running fluid are isotropic and uniform.
- Impact of ground water advection is negligible.

The thermal properties in the ground such as thermal conductivity, specific heat and its density change with different soil types. Along the length of a typical vertical ground heat exchanger, the soil around the boreholes could be of different layers with variable thicknesses and, therefore, will be of different properties. However, in the current study, it is assumed that the thermal properties of the soil are constant in order to simplify the model.

When groundwater flow is present, the heat flow rate in the soil surrounding the borehole could increase towards the direction of the flow. However, in the current study it is assumed that groundwater flow is not present to simplify the model.

The flowing assumptions are made which are expected to have minor impact on the validity of simulation results of the current study

- Moisture migration is negligible.
- The dominant mode of heat transfer in the soil and the grout is conduction.
- The dominant mode of heat transfer in the circulating fluid region is convection.
- There is no thermal energy generation in any of the regions.

- The circulating fluid is incompressible and the pressure variation is neglected.
- The ground surface is assumed to be isothermal and steady during system operation.
- Thermal resistance of the borehole wall and the pipe is neglected.
- Contact resistance between the borehole wall and the soil and the borehole wall and the grout is neglected.

Assumptions specific to the various models are mentioned where the model is presented.

4.3 Numerical Approach

In the current problem, the general form of continuity, momentum and energy equation for an incompressible fluid appear as

$$\nabla \cdot \vec{v} = 0 \tag{4-1}$$

$$\rho\left(\frac{\partial \vec{v}}{\partial t} + \nabla \vec{v} \cdot \vec{v}\right) = -\nabla p + \mu \nabla^2 \vec{v} + F \tag{4-2}$$

$$\rho c_p\left(\frac{\partial T}{\partial t} + \nabla T \cdot \vec{v}\right) = k \nabla^2 T + \mu \phi \tag{4-3}$$

where $\vec{v}$, T, p, ρ, μ, k, and ϕ are the flow velocity vector, temperature, static pressure, density, molecular viscosity, conductivity, and viscous dissipation, respectively. The three terms on the right-hand side of Eq. (4-3) represent energy transfer due to conduction and viscous dissipation, respectively, and the terms on the left-hand side of this equation represent energy change and energy transfer due to convection.

Heat transfer in the soil and the grout is in the form of conduction while the dominant mode of heat transfer in the running fluid region is convection. Therefore, the soil, grout and the running fluid region are presented separately.

4.3.1 Circulating Fluid Region

The dominant mode of heat transfer in the circulating fluid region is convection. All governing equations that are given above are applied in this region to evaluate the running fluid temperature, T_f.

An initial temperature (equal to the undisturbed ground temperature), T_0, is assumed:

$$T_f = T_0 \quad \text{at} \quad t = 0 \tag{4-4}$$

The circulating fluid model, takes the inlet fluid temperature as its boundary to evaluate the temperature of the running fluid along the borehole as well as its outlet temperature:

$$T_f\big|_{z=0} = T_f'(t) \tag{4-5}$$

where T_f' is the running fluid inlet temperature that varied with time. At the inlet of the U-tube, the momentum equation takes the following boundary:

$$\vec{v}\big|_{z=0} = -v_0\hat{k} \tag{4-6}$$

where v_0 is the inlet velocity of the running fluid.

It is assumed that for a certain length (h) at the top of the U-tube, the tube wall has an adiabatic condition. Therefore,

$$\frac{\partial T_f}{\partial r^*} = 0 \qquad 0 \le z \le h \tag{4-7}$$

where r^* is the direction perpendicular to the U-tube surface.

4.3.2 Grout Region

Based on the assumptions presented in Section 4.2, heat transfer in the grout region is in the form of conduction and the energy equation for this region [Eq. (4-3)] reduces to

$$\frac{1}{\alpha}\frac{\partial T_g}{\partial t} = \nabla^2 T_g \tag{4-8}$$

An initial temperature (equal to the undisturbed ground temperature), T_0, is assumed:

$$T_g = T_0 \quad \text{at} \quad t = 0 \tag{4-9}$$

The model for the grout area simply relates the temperature of the running fluid (T_f) to the borehole wall temperature (T_b). The temperature of the grout at the U-tube can be used as a coupled boundary condition to the temperature of the running fluid. Therfore,

$$T_g\Big|_{at\ the\ tube\ wall} = T_f\Big|_{at\ the\ tube\ wall} \qquad z \geq h \tag{4-10}$$

where T_f can be calculated via the model for the running fluid described in Section 4.3.1. The grout model takes a uniform temperature (equal to the undisturbed ground temperature) at the ground surface. Therefore,

$$T_g\Big|_{z=0} = T_0 \tag{4-11}$$

where T_0 is the undisturbed ground temperature.

4.3.3 Soil Region

Based on the assumptions presented in Section 4.2, heat transfer in the soil region is in the form of conduction and the energy equation [Eq. (4-3)] reduces to

$$\frac{1}{\alpha}\frac{\partial T_s}{\partial t} = \nabla^2 T_s \tag{4-12}$$

An initial temperature (equal to the undisturbed ground temperature), T_0, is assumed:

$$T_s = T_0 \quad \text{at} \quad t = 0 \tag{4-13}$$

The soil model takes a uniform temperature (equal to the undisturbed ground temperature) at the ground surface and at the farfield:

$$T_s\big|_{z=0} = T_0 \tag{4-14}$$

$$T_s\big|_{at\ farfield} = T_0 \tag{4-15}$$

Note that the farfield temperature boundary condition is only used for numerical simulation of the system. This temperature is assumed to be equal to ground initial temperature and completes the model. However, it is not supposed to affect the temperature of the soil surrounding the borehole that is calculated during the simulation. Therefore, this boundary could be switched with an adiabatic boundary.

The soil at the bottom of the borehole takes the same temperature as the grout at the bottom of the borehole:

$$T_s\big|_{z=H+h} = T_g\big|_{z=H+h} \qquad 0 \le r^{**} \le r_b \tag{4-16}$$

where r^{**} is radial distance from the borehole axis and r_b is the borehole radius. In a similar manner, at the borehole wall, when coupling this boundary to the model inside the borehole, the temperature of the borehole wall calculated from the grout model can be used in order to evaluate the temperature of the soil surrounding the borehole. Therefore,

$$T_s\big|_{r^{**}=r_b} = T_g\big|_{r^{**}=r_b} \qquad h \le z \le H + h \tag{4-17}$$

Note that when only the heat flows in the soil are the focus of discussion, the grout and the running fluid regions are not included in the problem set up and the boundary condition in Eq. (4-17) is modified to a heat boundary condition from the borehole wall to the soil:

$$-k\frac{\partial T_s}{\partial r}\bigg|_{r^{**}=r_b} = q''(t) \tag{4-18}$$

A summary of the boundary conditions that are applied to the numerical model and are given in Sections 4.3.1, 4.3.2, and 4.3.3 are shown in Figure 4-2.

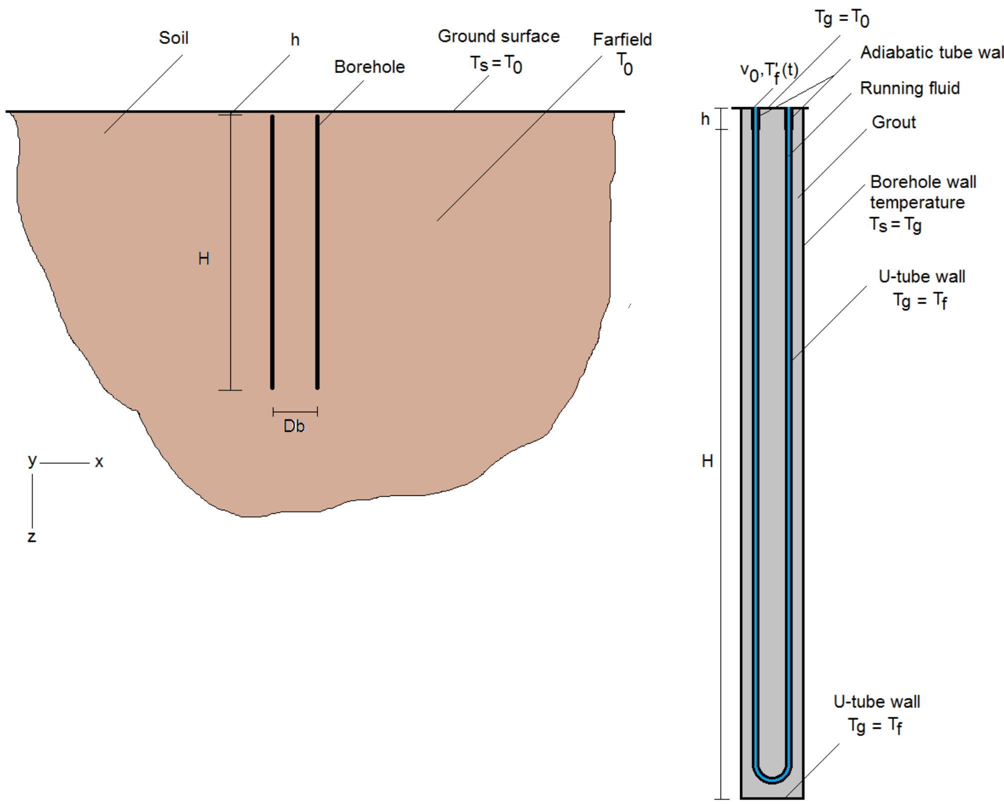

Figure 4-2 Boundary conditions assumed on two boreholes of distance D_b.

4.4 Analytical Approach

The governing equations for inside the borehole (grout and the running fluid), and outside the borehole (soil), are presented separately in this section.

4.4.1 Heat Transfer Inside the Borehole

A quasi-three-dimensional model was proposed by Zeng et al. (2003a, 2003b) taking into account the fluid axial convective heat transfer and thermal "short-circuiting" among U-tube legs can be used (Section 3.1.1.3). Being minor in order, the conductive heat flow in the grout and ground in the axial direction, however, is still neglected to keep the model concise and analytically manageable.

4.4.2 Heat Transfer Outside the Borehole

The dominant mode of heat transfer in the soil is conduction. The general heat conduction equation in cylindrical coordinates, assuming no heat generation in the soil, appears in the following form:

$$\frac{\partial^2 T}{\partial r^2}+\frac{1}{r}\frac{\partial T}{\partial r}+\frac{1}{r^2}\frac{\partial^2 T}{\partial \varphi^2}+\frac{\partial^2 T}{\partial z^2}=\frac{1}{\alpha}\frac{\partial T}{\partial t} \qquad (4\text{-}19)$$

where t is the time from the start of operation, α is the thermal diffusivity of soil, and T is the temperature of the ground. The first two terms on the left side of Eq. (4-19) are the heat flux components in the radial (r) direction, the third and the fourth terms are related to the circumferential (φ) and axial (z) directions, respectively. The right side of Eq. (4-19) represents the transient effects of heat conduction.

In the analytical approach, the model presented by Zeng et al. (2002, 2003a) (Section 3.2) can be used for the modeling and simulation of vertical boreholes installed in the ground.

4.5 Heat Pump Efficiency

In general, heat pumps operate between a high-temperature medium (at T_H) and a low-temperature medium (at T_L). In the case of ground heat pumps, when cooling the building (ground heat delivery), the running fluid temperature can be considered the high temperature medium and the cooling coil temperature can be considered the low temperature medium in the cooling season. In the heating season (ground heat removal), the heating coil temperature can be considered to be the high temperature while the temperature of the fluid running through the heat exchanger can be considered to be the low temperature. In an ideal heat pump where all the processes are reversible, the coefficient of performance of the heat pump ($\mathrm{COP_{rev}}$) is only dependent on the high-temperature and the low-temperature:

$$\mathrm{COP_{rev}}=\frac{1}{1-\dfrac{T_L}{T_H}} \qquad (4\text{-}20)$$

The high and low temperature in the above equation can be evaluated from the running fluid temperature model.

4.6 Physical Parameters and Geometrical Specifications

The model input parameters and properties described in this section are taken from various books and studies available in the open literature (Incropera and DeWitt, 2000; Gao et al. 2008; Hepbasli et al. 2003; Shonder and Beck 1999). Note that some of these values are presented in ranges since these values are sometimes modified in the various models presented in the current study. The specific thermal properties and system specifications of each model is included in Appendix B where the models are presented in more detail.

Table 4-1 Physical properties and system specifications [Adapted from (Incropera and DeWitt, 2000; Gao et al. 2008; Hepbasli et al. 2003; Shonder and Beck 1999)].

Soil	
Undisturbed ground temperature	9-10 C (282-283 K)
Soil thermal conductivity	1.0-1.5 W/mK
Soil specific heat capacity	1200-1550 J/kgK
Soil density	1200-1950 kg/m^3
Grout	
Grout thermal conductivity	1.7-2.6 W/mK
Grout specific heat capacity	1250 J/kgK
Grout density	1600 kg/m^3
Running fluid	
Running fluid thermal conductivity	0.0242 W/mK
Running fluid specific heat capacity	4182 J/kgK
Running fluid density	998.2 kg/m^3
Running fluid mass flow rate	0.225 kg/s
Borehole geometry	
Total borehole length, H	50-200 m
Borehole radius, r_b	0.050 m
U-tube radius, r_p	0.010-0.016 m
U-tube centre-to-centre half distance, $2D$	0.026 m

4.7 Summary

In this chapter a three dimensional mathematical model of multiple borehole heat exchangers is developed. The models that are presented account for all heat transfer occurring within a GHE. The partial differential equations describing heat transfer in all models are summarized as follows:

Running fluid:

Continuity: $\nabla \cdot \vec{v} = 0$

Momentum: $\rho\left(\frac{\partial \vec{v}}{\partial t} + \nabla \vec{v} \cdot \vec{v}\right) = -\nabla p + \mu \nabla^2 \vec{v} + F$

Energy: $\rho c_p \left(\frac{\partial T}{\partial t} + \nabla T_f \cdot \vec{v} \right) = k \nabla^2 T_f + \mu \phi$

Grout:

Energy: $\frac{1}{\alpha} \frac{\partial T_g}{\partial t} = \nabla^2 T_g$

Soil:

Energy: $\frac{1}{\alpha} \frac{\partial T_s}{\partial t} = \nabla^2 T_s$

The boundary and initial conditions to be applied in the above equations are included in this chapter. The thermal properties of the system as well as its geometrical characteristics can be found in Table 4-1Table 4-1 Physical properties and system specifications [Adapted from (Incropera and DeWitt, 2000; Gao et al. 2008; Hepbasli et al. 2003; Shonder and Beck 1999)].

Chapter 5 ANALYTICAL APPROACH

In this chapter two analytical approaches are used to calculate the temperature profiles in the soil surrounding boreholes as well as inside the borehole. To model the heat transfer inside the borehole the model presented by Zeng et al. (2003a) (Section 3.1.1.3) can be used to formulate the temperature profiles of the fluids flowing in the U-pipes in the boreholes. The heat transfer outside the borehole is modeled by modifying the semi-analytical model presented by Zeng et al. (2002, 2003a) (Section 3.2), that evaluates the temperature in the soil surrounding a borehole, by using a temporal superposition method that is able to estimate these temperatures when the ground heat load is transient. A coupling procedure is presented in this chapter that uses both models inside the borehole and outside the borehole in order to relate the temperature variations in the soil surrounding the borehole to their corresponding temperature variations in the running fluid inside the borehole. The coupling procedure used to couple the two models is also presented in this chapter.

5.1 Heat Flow Rate Variation along the Borehole

The model presented by Zeng et al. (2002, 2003a) derives an analytical relation for the temperature excess of the soil assuming a constant heat flow rate on the borehole wall (here, the line source). Modifying this model slightly to account for the variation of heat flow rate along the line source [$q'(\overline{H})$], the temperature profile in the soil around the boreholes is calculated as

$$\theta(\overline{R},Z,Fo)=\frac{1}{4k\pi}\int_0^1 q'(\overline{H})\left[\frac{erfc\left(\frac{\sqrt{\overline{R}^2+(Z-\overline{H})^2}}{2\sqrt{Fo}}\right)}{\sqrt{\overline{R}^2+(Z-\overline{H})^2}}-\frac{erfc\left(\frac{\sqrt{\overline{R}^2+(Z+\overline{H})^2}}{2\sqrt{Fo}}\right)}{\sqrt{\overline{R}^2+(Z+\overline{H})^2}}\right]d\overline{H} \tag{5-1}$$

where the dimensionless parameters are defined as

$$\theta=T-T_0,\quad Z=\frac{z}{H},\quad \overline{H}=\frac{h_z}{H},\quad \overline{R}=\frac{r}{H},\quad Fo=\frac{\alpha t}{H^2} \tag{5-2}$$

Also, $q'(\overline{H})$ denotes the heating strength per unit length, t the time from the start of operation, α the thermal diffusivity of soil, z the axis along the borehole length, r the radial axis, H the borehole heating length, h_z the depth at which borehole heating starts, T_0 ground initial temperature and T the temperature of the ground.

This solution [Eq. (5-1)] is used as the basis for more complicated cases such as having a system of n boreholes or in time varying heat transfer rates.

5.1.1 Multiple Boreholes

Since the conduction equation is linear, the temperature response in the soil surrounding multiple boreholes can be calculated by supersposing the temperature rise in the soil caused by each single borehole. The validity of superposition method in thermal response in the soil surrounding multiple boreholes by is examined in Section 7.1.1. It is shown that the results of the two methods agree well and the effect of the temperature rise due to one borehole on the thermal performance of other boreholes can be neglected. Therefore, the temperature response in the soil surrounding a borehole system of n boreholes can be calculated by superposing the temperature response evaluated by each borehole from Eq. (5-1):

$$\theta(R,Z,Fo)=\sum_1^n\int_0^1\frac{q_i'(\overline{H})}{4k\pi}\left[\frac{erfc\left(\frac{\sqrt{\overline{R}_i^2+(Z_i-\overline{H})^2}}{2\sqrt{Fo}}\right)}{\sqrt{\overline{R}_i^2+(Z_i-\overline{H})^2}}-\frac{erfc\left(\frac{\sqrt{\overline{R}_i^2+(Z_i+\overline{H})^2}}{2\sqrt{Fo}}\right)}{\sqrt{\overline{R}_i^2+(Z_i+\overline{H})^2}}\right]d\overline{H} \tag{5-3}$$

where q_i' is the heat flow rate per unit length of Borehole i (Figure 5-1) and

$$\overline{R}_i = \frac{\sqrt{(x-l_i)^2+(y-w_i)^2}}{H} \tag{5-4}$$

where l_i and w_i refer to the position of borehole i in x and y coordinates, respectively (Figure 5-1). For the two boreholes that are shown in Figure 5-2, Eq. (5-3) can be simplified to

$$\theta(\overline{R},Z,Fo)=\theta_1(\overline{R}_1,Z,Fo)+\theta_2(\overline{R}_2,Z,Fo)=$$

$$\int_0^1 \frac{q'(\overline{H})}{4k\pi}\left[\frac{erfc\left(\frac{\sqrt{\overline{R}_1^2+(Z-\overline{H})^2}}{2\sqrt{Fo}}\right)}{\sqrt{\overline{R}_1^2+(Z-\overline{H})^2}}-\frac{erfc\left(\frac{\sqrt{\overline{R}_1^2+(Z+\overline{H})^2}}{2\sqrt{Fo}}\right)}{\sqrt{\overline{R}_1^2+(Z+\overline{H})^2}}\right]d\overline{H}$$
$$+\int_0^1 \frac{q'(\overline{H})}{4k\pi}\left[\frac{erfc\left(\frac{\sqrt{\overline{R}_2^2+(Z-\overline{H})^2}}{2\sqrt{Fo}}\right)}{\sqrt{\overline{R}_2^2+(Z-\overline{H})^2}}-\frac{erfc\left(\frac{\sqrt{\overline{R}_2^2+(Z+\overline{H})^2}}{2\sqrt{Fo}}\right)}{\sqrt{\overline{R}_2^2+(Z+\overline{H})^2}}\right]d\overline{H} \tag{5-5}$$

where, as seen in Figure 5-2, $\overline{R}_1$ and $\overline{R}_2$ are dimensionless distances of Borehole 1 and 2 from coordinate center (0,0).

$$\overline{R}_1=\frac{R_1}{H}=\frac{\sqrt{(x+h)^2+y^2}}{H} \quad and \quad \overline{R}_2=\frac{R_2}{H}=\frac{\sqrt{(x-h)^2+y^2}}{H} \tag{5-6}$$

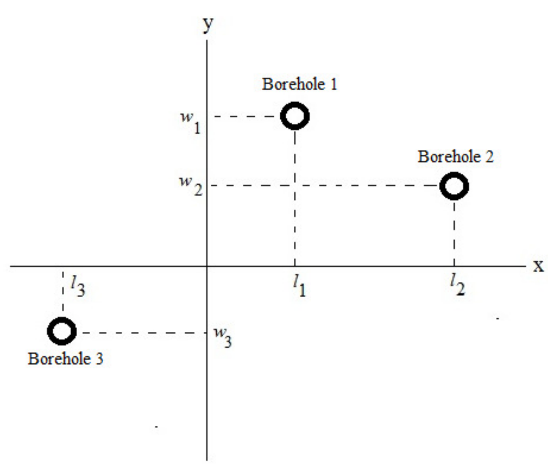

Figure 5-1 Clarification of l_i and w_i in a system of three boreholes.

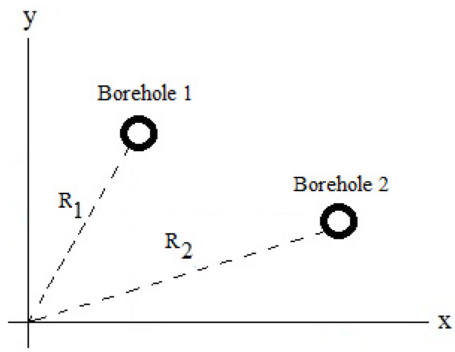

Figure 5-2 System geometric parameters for two boreholes at distances R_1 and R_2 from a fixed point in the surrounding soil.

Note that in using the line source theory in the case of multiple boreholes, the effect of the boreholes on thermal performance of each other is neglected. Eskilson (1987) calculated the error involved in the temperature difference calculated via this method and found it to be negligible.

5.2 Time Varying Heat Transfer Rates

In time varying heat transfer rates, the problem of heat conduction from the borehole wall to the soil becomes subject to a time-dependant boundary condition $q'(\overline{H},\tau)$. The variations of heat injection/removal on the borehole can be approximated by a sequence of constant heat fluxes $q_i'(\overline{H})$ where the *i*th heat flux is applied at $t=\tau_i$ and lasts for a time span Δt_i. Assuming that the governing equations and boundary conditions for the problem are linear, we can obtain the temperature distribution in the body by applying the principle of superposition and obtain the temperature distribution in the body corresponding to the arbitrary continuous boundary condition which we can express as a sequence of, say, *n* small steps. Therefore, if the temperature rise distribution in the soil corresponding to a constant boundary condition $q'(\overline{H})$ is

$$\theta(\overline{R},Z,Fo)= \int_0^1 q'(\overline{H})I(r,z,t)d\overline{H} \tag{5-7}$$

where

$$I(\overline{R},Z,Fo)=\frac{1}{4k\pi}\left[\frac{erfc\left(\frac{\sqrt{\overline{R}^2+(Z-\overline{H})^2}}{2\sqrt{Fo}}\right)}{\sqrt{\overline{R}^2+(Z-\overline{H})^2}}-\frac{erfc\left(\frac{\sqrt{\overline{R}^2+(Z+\overline{H})^2}}{2\sqrt{Fo}}\right)}{\sqrt{\overline{R}^2+(Z+\overline{H})^2}}\right] \tag{5-8}$$

The temperature distribution in the soil corresponding to the varied $q_i'(\overline{H})=q'(\overline{H},\tau_i)$ at time t is

$$\begin{aligned}\theta(\overline{R},Z,Fo)= & \int_0^1 q_1'(\overline{H})\,I(\overline{R},Z,Fo_{t-\tau_1})\,d\overline{H}\\ & +\int_0^1\left[q_2'(\overline{H})-q_1'(\overline{H})\right]I(\overline{R},Z,Fo_{t-\tau_2})\,d\overline{H}\\ & +\int_0^1\left[q_3'(\overline{H})-q_2'(\overline{H})\right]I(\overline{R},Z,Fo_{t-\tau_3})\,d\overline{H}\\ & +\ldots+\\ & +\int_0^1\left[q_n'(\overline{H})-q_{n-1}'(\overline{H})\right]I(\overline{R},Z,Fo_{t-\tau_n})\,d\overline{H}\end{aligned} \tag{5-9}$$

Here,

$$Fo_{t-\tau_i}=\frac{\alpha(t-\tau_i)}{H^2} \tag{5-10}$$

and q_i' is the heat flow rate on the line source (here, the borehole) at time τ_i to τ_{i+1}. The concept presented in Eq. (5-9) is shown in Figure 5-3. To evaluate the integrations in Eq. (5-9) in the current study, a computer code in Fortran is used (Appendix D).

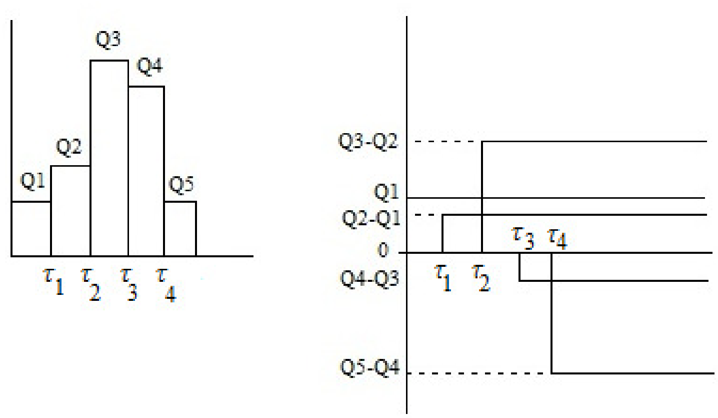

Figure 5-3 Time varying heat transfer rates.

5.3 Model Coupling

One of the main strengths of the current analytical method is its ability to present a relation between the temperature variations in the soil surrounding the borehole and the resulting temperature variations in the running fluid temperature. This data is specifically useful since the objective of the current study is to find the relation between a temperature rise or drop in the soil surrounding a borehole that is caused by a neighbor system (thermal interaction) on the temperature of the running fluid which is in direct contact with the heat pump cycle. This information is also helpful since it can help determine heat delivery/removal strength of the circulating fluid inside the borehole. In order to determine heat delivery/removal strength of the circulating fluid inside the borehole, the borehole wall temperature must be defined by coupling the heat transfer model inside the borehole to the one outside the borehole via the borehole wall temperature or the heat flow rate per unit length of the borehole. How the two models are coupled and what parameters are kept constant vary depending on the objective of the study.

5.3.1 Model Coupling via the Heat Flow Rate

The heat transferred to the soil from each of the pipes in the borehole can be obtained as

$$q'(z) = \frac{T_{f1}(z) - T_b}{R_1^\Delta} + \frac{T_{f2}(z) - T_b}{R_2^\Delta} \tag{5-11}$$

where $R_1^\Delta = R_2^\Delta$ for a symmetric U-tube configuration. Using the dimensionless parameters introduced in Eq. (3-19), Eq. (5-11) can be rewritten in terms of the dimensionless parameters:

$$q'(z) = \left(T_f' - T_b\right)\left[\frac{\Theta_1(Z)}{R_1^\Delta} + \frac{\Theta_2(Z)}{R_2^\Delta}\right] \tag{5-12}$$

This is the spatial distribution of the heating strength along the rod. In contrast to past studies, this heating strength varies along the rod and is not constant (Figure 5-4). In order to compare the results gained by constant heat flux model with the results gained by the VHS model, an equivalent inlet temperature (T_f') for the VHS model, resulting in the same total heat conduction in the soil, can be assumed. The total heat flow rate is calculated by integrating the heat flow rate along the borehole:

$$\frac{Q}{H} = \int_0^1 q'(Z)dZ = \int_0^1 \left(T'_f - T_b\right)\left[\frac{\Theta_1(Z)}{R_1^\Delta} + \frac{\Theta_2(Z)}{R_2^\Delta}\right]dZ \tag{5-13}$$

Assuming a constant borehole wall temperature and inlet fluid temperature, Eq. (5-13) can be used to calculate the equivalent inlet fluid temperature in VHS model that results in the same heat delivery/removal to the surrounding soil.

$$T'_f = T_b + \frac{\frac{Q}{H}}{\int_0^1 \left[\frac{\Theta_1(Z)}{R_1^\Delta} + \frac{\Theta_2(Z)}{R_2^\Delta}\right]dZ} \tag{5-14}$$

Note that the integration in the denominator of Eq. (5-14) has a constant value depending on the geometric specifications of the borehole and thermal characteristics of the grout.

In ground heat delivery, the heating strength of the variable heat source declines along the borehole as the running fluid temperature decreases by losing heat to the grout and then the soil. In ground heat removal, the heat removal strength of the variable heat source declines along the borehole as the running fluid temperature increases by gaining heat from the grout and then the soil. This heat flow rate [Eq. (5-12)] can be used in the model outside the borehole [Eq. (5-1)] to model the temperature variations in the soil due to a variable heat source (VHS).

The relations derived in this section are able to show the existence of a variable heating strength due to the variable temperature of the running fluid along the borehole wall and the results are discussed in Section 7.1.2. In the variable heat source model, certain simplifying assumptions such as constant ground temperature are made. When calculating the heat input to the ground, it becomes clear that it varies with the borehole wall temperature. This assumption ignores the drop in heat injection strength when the borehole wall temperature increases and, therefore, underestimates the inlet temperature of the circulating fluid that is required to meet the heat injection needs of the system. In the fewer cases of multiple boreholes, superimposition of the temperature excesses resulted from individual boreholes seems to be the most popular solution in analytical approaches. In numerical approaches, the boundary condition that plays the role of heat delivery/removal is a heat flow rate per unit length boundary type that, regardless of being constant or variable based on the building needs, does not reflect the drop in the heat injection/removal strength when temperature of the soil around the borehole increases/decreases by its own performance or another nearby system's performance. This assumption forces the system to deliver a desired amount of heat to the ground regardless of the ground temperature. In reality, the amount of heat delivered to the ground is driven by the temperature difference between the circulating fluid and the ground temperature. In some cases, the assumption of constant borehole wall temperature is acceptable considering how the conduction problem is simplified. However, when determining how thermal interaction between two operating GHEs can affect their performance, the effect of the transient borehole wall temperature on their heat delivery strength and inlet fluid temperature becomes a very important factor. Therefore, the current solution is only valid for low temperature variations in the soil surrounding the boreholes which is only achieved by assuming lower heat flux values on the borehole wall. Modifying the current model to one with typical industrial values for ground heat pump systems will need the soil temperature to be assumed variable. This will complicate the coupling procedure and will increase the computation time for evaluating the running fluid temperature as well as borehole wall temperature.

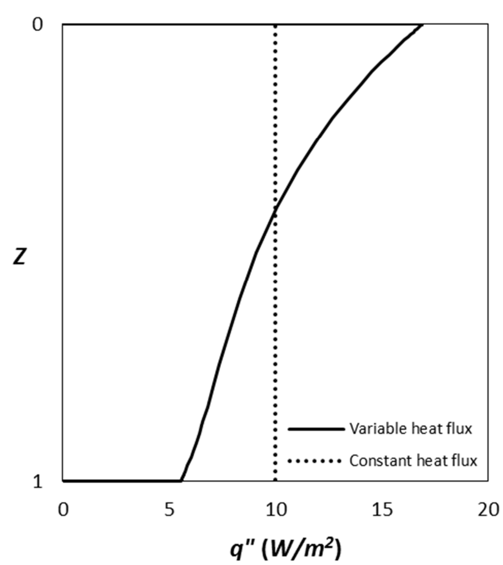

Figure 5-4 Distribution of heat flux along the borehole length.

5.3.2 Model Coupling via the Borehole Wall Temperature

To study the effect of the temperature increase in the soil surrounding the borehole on the operation of the heat pump for a given heat flow rate, the outlet temperature of the running fluid is the most important parameter and it can be calculated by coupling the two models for inside and outside the borehole. In this case, in order to maintain the required heat flow rate, as the temperature of the borehole wall increases/decreases over time, the inlet temperature of the running fluid is updated to an increased/decreased value in order to deliver/remove the required heat to/from the ground. With the increasing/decreasing inlet fluid temperature, outlet temperature of the running fluid is modified accordingly. Monitoring the outlet temperature of the running fluid is advantageous since it is the coupling parameter between the model inside the borehole and the heat pump. In addition, this temperature is often the key parameter in the system to examine if the heat pump will operate under the soil temperature conditions.

In order to formulate the process, the solution to the model inside the borehole [Eq. (3-18)] at *Z*=0 is used to calculate the running fluid outlet temperature.

$$T_{f,out} = T_{f2}(0) = T_b + \left(T_f' - T_b\right)\Theta_2(0) \tag{5-15}$$

where $\Theta_2(0)$ varies with system parameters that are known to the system designer or simulator [Eq. (3-18)].

$$\Theta_2(0) = \frac{\cosh(\beta) - \sqrt{\dfrac{1-P}{1+P}}\sinh(\beta)}{\cosh(\beta) + \sqrt{\dfrac{1-P}{1+P}}\sinh(\beta)} \tag{5-16}$$

It is seen in Eq. (5-15) that the outlet temperature of the running fluid varies with the borehole wall temperature (T_b) and the inlet running fluid temperature (T_f'). Another correlation between the outlet fluid temperature and the inlet running fluid temperature can be written as

$$T_{f,out} = T'_f - \frac{q'_{ave} H}{\dot{m} c_p} \tag{5-17}$$

where q'_{ave} is the average heat flow rate per unit length of the borehole. Note that $q'_{ave}H$ in Eq. (5-17) is the total amount of heat that is delivered to/removed from the ground. Using Eqs. (5-15) and (5-17), one can determine the inlet and outlet temperature of the running fluid that is needed to deliver/remove a required amount of heat to/from the soil at a given borehole wall temperature. Thus,

$$\begin{aligned} T'_f &= T_b - \frac{q'_{ave} H}{\dot{m} c_p \left[1 - \Theta_2(0)\right]} \\ T_{f,out} &= T_b - \frac{q'_{ave} H \, \Theta_2(0)}{\dot{m} c_p \left[1 - \Theta_2(0)\right]} \end{aligned} \tag{5-18}$$

As mentioned previously, the borehole wall temperature and the borehole heat flow rate are the coupling parameters between the model inside the borehole and the model outside the borehole. The borehole heat flow rate can be substituted in the model outside the borehole [Eq. (5-1)], or its modified versions [Eqs. (5-3) and (5-9)], and the borehole wall temperature can be evaluated accordingly. In order to use the solution to the line source theory in evaluation of the borehole wall temperature, Eq. (5-1) is used for $\overline{R} = r_b/H$. This may cause a small error in the calculated value for the borehole wall temperature since using the line source model outside the borehole at $\overline{R} = r_b/H$ assumes thermal properties of the soil for regions smaller than ($\overline{R} < r_b/H$) whereas, in reality, the grout and running fluid with different thermal properties are present in $\overline{R} < r_b/H$ instead of soil.

The temperature of the borehole wall varies along the borehole length in Eq. (5-1). However, in derivation of the solution to the model for inside the borehole [Eq. (3-18)], a constant borehole wall temperature along the borehole length is assumed. Thus, Eq. (5-18) is only valid for cases where the borehole wall temperature is assumed constant or its average is used. In Eq. (5-1), the variation of the borehole wall temperature along the borehole length is so small that the value of the borehole wall temperature at Z=0.5 can be used as a good estimate of the average borehole wall temperature. Integrating this value along the borehole length is another alternative that is not preferred due to its computation time. A comparison of the two options (Figure

5-5) confirms the accuracy of using the borehole wall temperature in mid-length of the borehole as a good estimate of average borehole wall temperature.

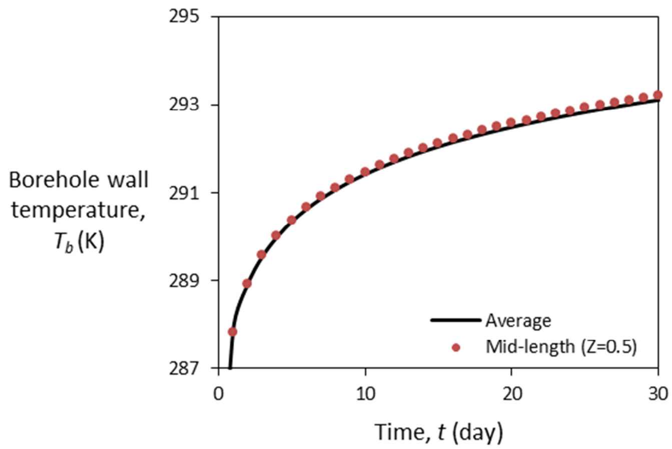

Figure 5-5 Comparison between average borehole wall temperature along borehole length and borehole wall temperature at borehole mid-length (Z=0.5).

Thus, the borehole wall temperature is calculated for any time after the start of system operation as below:

$$T_b(Fo) = T_0 + \frac{1}{4k\pi}\int_0^H q'(\overline{H})\left\{\frac{erfc\left(\frac{\sqrt{\overline{R}_b^2+(0.5-\overline{H})^2}}{2\sqrt{Fo}}\right)}{\sqrt{\overline{R}_b^2+(0.5-\overline{H})^2}} - \frac{erfc\left(\frac{\sqrt{\overline{R}_b^2+(0.5+\overline{H})^2}}{2\sqrt{Fo}}\right)}{\sqrt{\overline{R}_b^2+(0.5-\overline{H})^2}}\right\}d\overline{H} \tag{5-19}$$

In time-varying heat transfer rates, the borehole wall temperature can be calculated from Eq. (5-9) by substituting borehole radius (R_b) and Z=0.5. Hence,

$$\begin{aligned} T_b(Fo) = T_0 + & \int_0^1 q_1'(\overline{H})\, I(\overline{R}_b, 0.5, Fo_{t-\tau_1})\, d\overline{H} \\ & + \int_0^1 \left[q_2'(\overline{H}) - q_1'(\overline{H})\right] I(\overline{R}_b, 0.5, Fo_{t-\tau_2})\, d\overline{H} \\ & + \int_0^1 \left[q_3'(\overline{H}) - q_2'(\overline{H})\right] I(\overline{R}_b, 0.5, Fo_{t-\tau_3})\, d\overline{H} \\ & + \ldots + \\ & + \int_0^1 \left[q_n'(\overline{H}) - q_{n-1}'(\overline{H})\right] I(\overline{R}_b, 0.5, Fo_{t-\tau_n})\, d\overline{H} \end{aligned} \tag{5-20}$$

The accuracy of the solution can be improved by increasing the number of the time steps. Here, the variations in the ground heat load profile are assumed to be known according to the building needs and the heat pump operation. The borehole wall temperature can be updated at every time step [Eq. (5-20)] in order to estimate the inlet and outlet running fluid temperatures [Eq. (5-18)]. However, evaluating the borehole wall temperature in time varying heat flow rates [Eq. (5-20)] becomes computationally intensive and requires efficient algorithms that lower the number of time steps (Marcotte and Pasquier 2008; Bernier et al. 2004; Yavuzturk and Spitler 1999).

5.4 Relation between Thermal Interaction and Heat Pump Efficiency

In ground heat pumps, when cooling the building (ground heat delivery), the running fluid temperature can be considered the high temperature medium and the cooling coil temperature can be considered the low temperature medium in the cooling season. In the heating season (ground heat removal), the heating coil temperature can be considered to be the high temperature while the temperature of the fluid running through the heat exchanger can be considered to be the low temperature. In an ideal ground heat pump where all the processes are reversible, the coefficient of performance of the heat pump can be written as

$$\mathrm{COP}_{\mathrm{cooling}} = \frac{1}{1 - \dfrac{T_{cooling\ coil}}{T_f}} \tag{5-21}$$

$$\mathrm{COP}_{\mathrm{heatling}} = \frac{1}{1 - \dfrac{T_f}{T_{heating\ coil}}} \tag{5-22}$$

where T_{coil} is the coil temperature and is assumed to be constant and within a standard range here. Note that the coefficient of performance in Eqs. (5-21) and (5-22) can only be used for a reversible heat pump. Since the objective of this study is to rather estimate the effect of thermal interaction on the performance of the heat pump than to evaluate its COP, the heat pump $\mathrm{COP}_{\mathrm{rev}}$ is used as an estimate of how much the heat pump efficiency can vary with a temperature rise of a certain degree in the soil surrounding the borehole. In presence of specific heat pump data, case specific results for the heat pump coefficient of performance can be achieved using the same procedure that is used in this study.

In the cooling season (ground heat delivery), the thermal interaction in the soil from a neighboring system can appear in the form of an unwanted temperature rise in the soil surrounding the borehole affecting the running fluid temperature and thus COP. In the heating season (ground heat removal), when the heat is being extracted from the ground, thermal interaction can appear in the form of the escape of heat stored in the ground towards a neighboring operating system that has created a low temperature region surrounding it by extracting heat from the ground. This may result in lower running fluid temperature and lower COP.

5.5 Summary

In this chapter, the model available for outside the borehole is used as a basis for calculating the borehole wall temperature. The procedure for coupling this temperature with the model available for inside the borehole to calculate the inlet and outlet running fluid temperature according to the variable borehole wall temperature, which is one of the key contributions of the analytical solution presented in the current study, is also presented in this chapter. Figure 5-6 shows a summary of the coupling procedure.

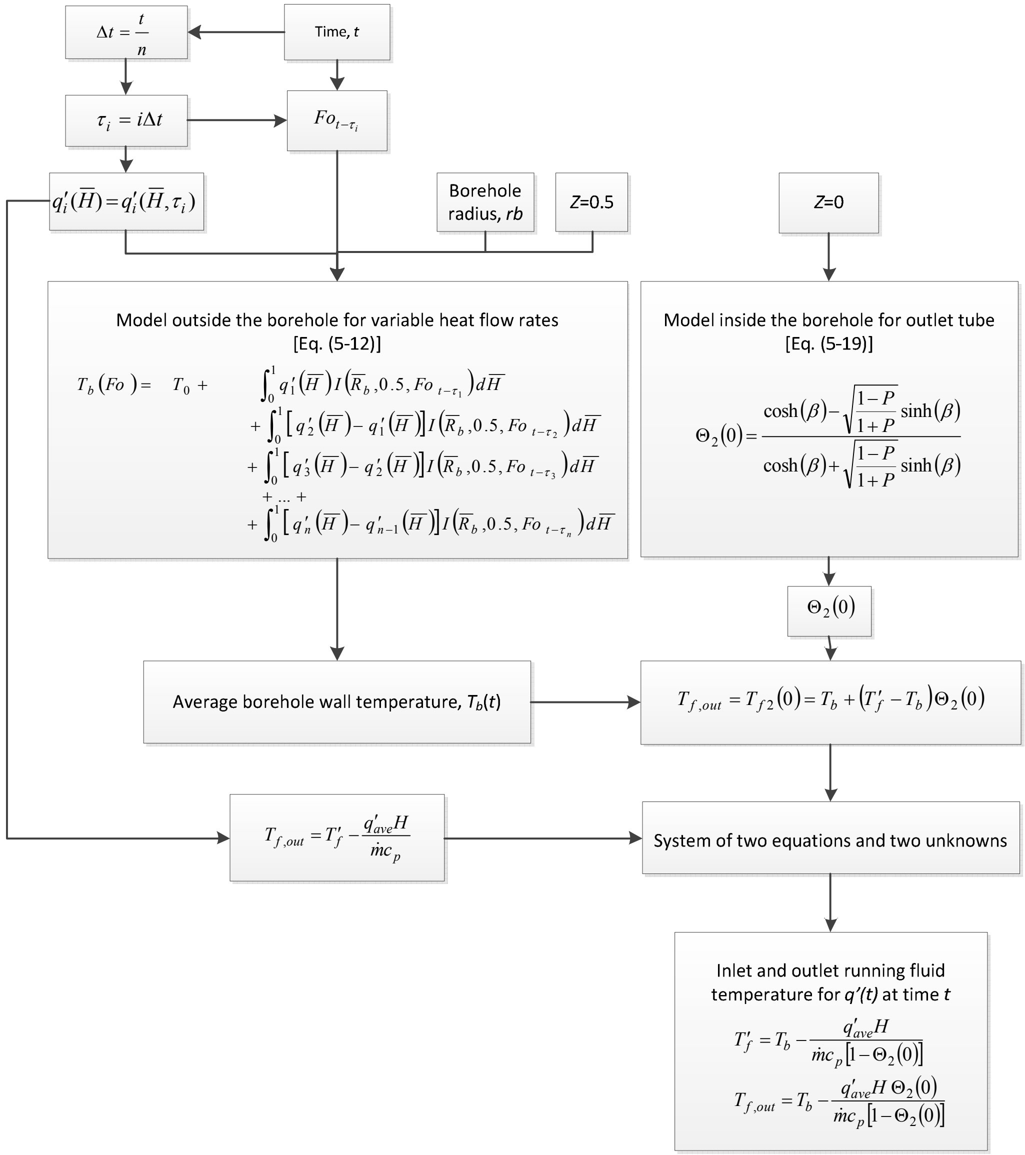

Figure 5-6 Coupling procedure for borehole wall temperature and the model for inside the borehole to calculate the inlet and outlet running fluid temperature according to the variable borehole wall temperature.

Chapter 6 NUMERICAL APPROACH

In this chapter a numerical approach is used to calculate the temperature profiles in the soil surrounding boreholes in a two and three dimensional domain as well as in the borehole. For both single and multiple borehole cases, the transient governing integral equations for the conservation of energy is solved with a control volume method in ANSYS FLUENT. In comparison to superposing one-dimensional solutions in the analytical solution to account for circumferential heat transfer effects, the two-dimensional heat conduction equation is solved taking into account the circumferential heat transfer effects as well as the radial ones. However, similar to the analytical solution, the two-dimensional numerical solution does not account for the temperature gradients in the direction adjacent to the borehole length corresponding to the axial heat transfer effects in the soil. Unlike many of the studies on the heat transfer around multiple boreholes, the transient governing equations for a three dimensional domain including soil, grout and running fluid are also solved via the numerical method.

Many of the numerical algorithms currently used in simulating heat transfer and fluid mechanics problems are available in ANSYS FLUENT. In some cases an algorithm used in one type of problem is not considered a wise selection in another problem. Incorrect selection of some numerical algorithms when setting up a model in ANSYS FLUENT can result in longer computation times; in some cases, a solution may not converge. This is especially important in modeling larger solution domains or ones containing transient boundary conditions such as the current problem. Therefore, when using ANSYS FLUENT as a solver to the specific conditions of each problem, the user must know the details of each of the algorithms that are selected and decide which one best suits the problem. In the current chapter, the methods selected for simulating the current problem are presented.

In the current study various models examined; some to justify the final models used or to examine the effect of certain parameters on the results and some towards the objective of the current study: long-term heat flows in the soil surrounding the system and system thermal interaction. Since all numerical models that are used in this study use a similar pressure based solver in ANSYS FLUENT, only one of them is presented in this chapter to present the numerical model. Thus, although the full numerical model presented in this chapter solves the governing equations in soil, grout and running fluid in a three dimensional domain (Figure 6-1), it is not used in gaining all the results presented in the next chapter. For some of the results presented in the next chapter, some simplified versions of this model are used. The rest of the simulations and geometries can be found in Appendix B.

6.1 Grid Formation

To start the solution, a control-volume-based technique is used that divides the domain into discrete control volumes using computational grids. Structured curvilinear grids have proven to be quite difficult to find viable mapping when geometry becomes complex. In these cases, it is often advantageous to be able to sub-divide the flow domain into several different sub-regions or blocks, each of which is meshed separately and joined up correctly with its neighbors. For more complex geometries, more blocks are used up to the point where each individual mesh is treated as a block, resulting in the so-called unstructured grid. This gives unlimited geometric flexibility and allows the most efficient use of computing resources. The advantage of such an arrangement is that no implicit structure of coordinate lines is imposed by the grid – hence the name unstructured – and the mesh can be easily concentrated where necessary without wasting computer storage. Moreover, control volumes may have any shape and there are no restrictions on the number of adjacent cells meeting at a point (2D) or along a line (3D). Generating the mesh in the current study is performed in GAMBIT. The advantage of choosing an unstructured mesh is that it allows the calculation of heat flows in or around the borehole without having to spend a long time on mesh generation and mapping. Grid generation is fairly straightforward with triangular grids and mesh refinement and adaption to improve resolution in regions with large gradients are much easier in unstructured triangular meshes. In the current model, since the multiple borehole geometry does not fit into

Cartesian or cylindrical coordinates, unstructured mesh with triangular and triangular prism elements is chosen for the three-dimensional geometry (Figure 6-2). The vertical section domain may be discretized using structured grids due to relatively uniform vertical structure, as shown in Figure 6-3. The governing equations on the individual control volumes are integrated to construct algebraic equations for the discrete dependent variable, i.e. temperature. The discretized equations are linearized and solved to yield updated values of the dependent variables (Versteeg and Malalasekera 2007).

One of the disadvantages of numerical approaches is their computation time for long-term system performance. The diameters of the U-tubes in the borehole are fairly small, on the order of 10^{-2} m, while the size of the solution domain, which depends on the duration of system operation and its heating/cooling load, is approximately on an order of 10 m, making the domain extremely disproportionate. As a result, a large number of mesh elements is required for simulation of a single borehole and its surrounding soil. To achieve an inaccuracy of 2% or less for the steady state heat transfer analysis of boreholes, a minimum number of approximately 18 elements describing any circular shape of a horizontal cross section is needed (Bauer et al. 2011). In modelling the soil surrounding the borehole, a domain of a certain size can work well for one model, while it can be too small for another model requiring more boreholes, longer system performance durations or higher heating injection/removal rates. At the outer edge of the domain, a constant farfield temperature condition equal to the initial temperature is often applied. The sensitivity of the solution results to this boundary should always be examined and avoided by increasing the size of the domain. In three-dimensional modeling of a borehole system with typical flow velocities, a vertical element size of 2 m or less should often be applied to avoid inaccuracies of greater than 2% (Bauer et al. 2011).

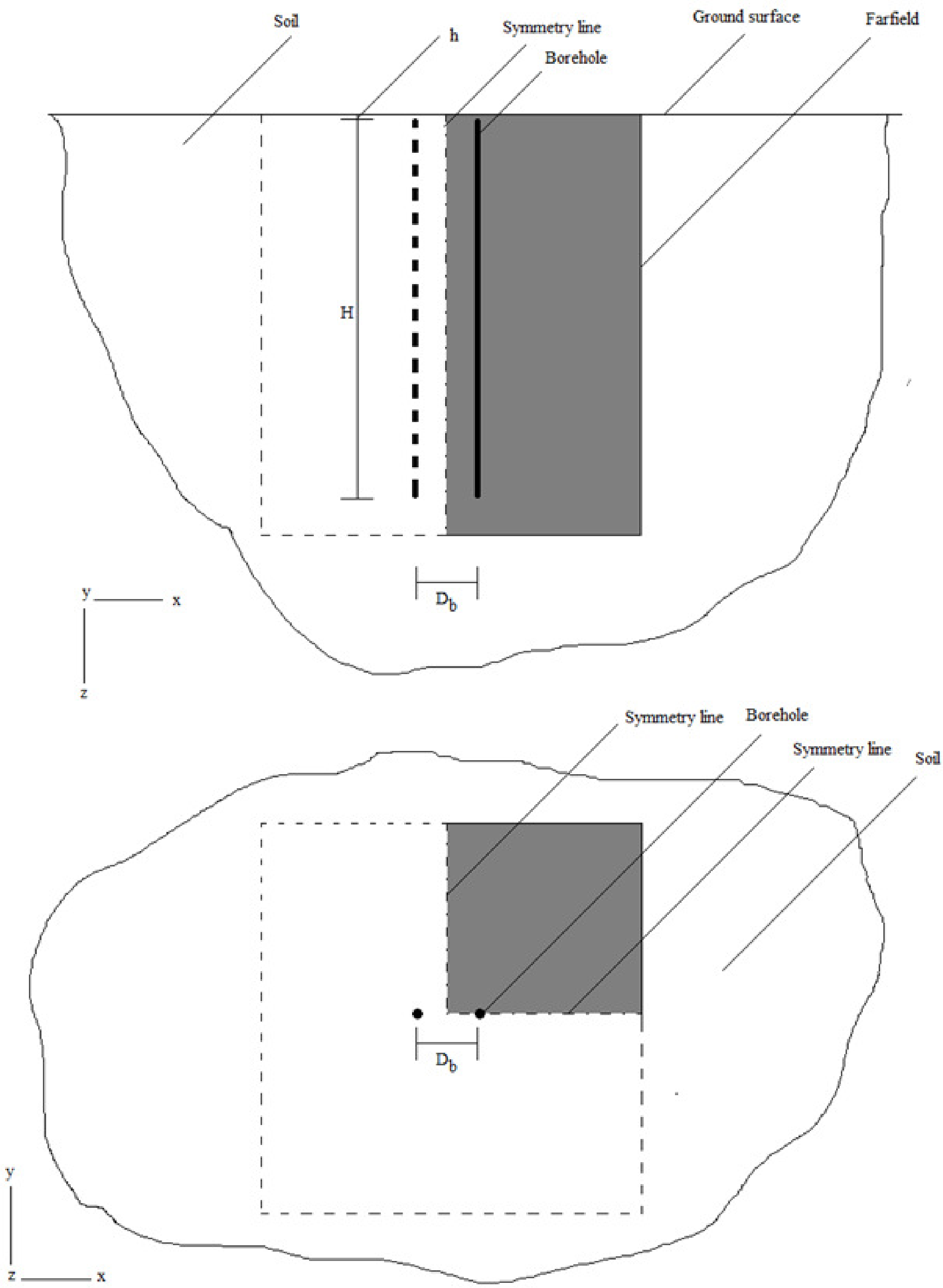

Figure 6-1 Solution domain.

To save computation time, the heat transfer symmetry about the two vertical planes shown in Figure 6-1 is utilized. Therefore, only one fourth of the borehole field is modelled and the solution domain (soil) is enclosed by the farfield, the ground surface and two symmetry planes. Theoretically, an adiabatic wall boundary condition is replaced on the symmetry line. In Figure 6-1, the grey area is the solution domain, the results of which can be replicated to the other areas drawn with dashed lines due to their symmetry. In addition, the temperature gradient in the domain between the borehole wall and the farfield changes gradually from large to small ones. Therefore, to reduce computer memory and computational time, the size of the mesh cells is chosen based on this gradual change. Applying all these techniques, a three-dimensional 15 m × 15 m × 60 m domain may require mesh sizes of the order of 1,000,000 elements to simulate multiple boreholes of 50 m length.

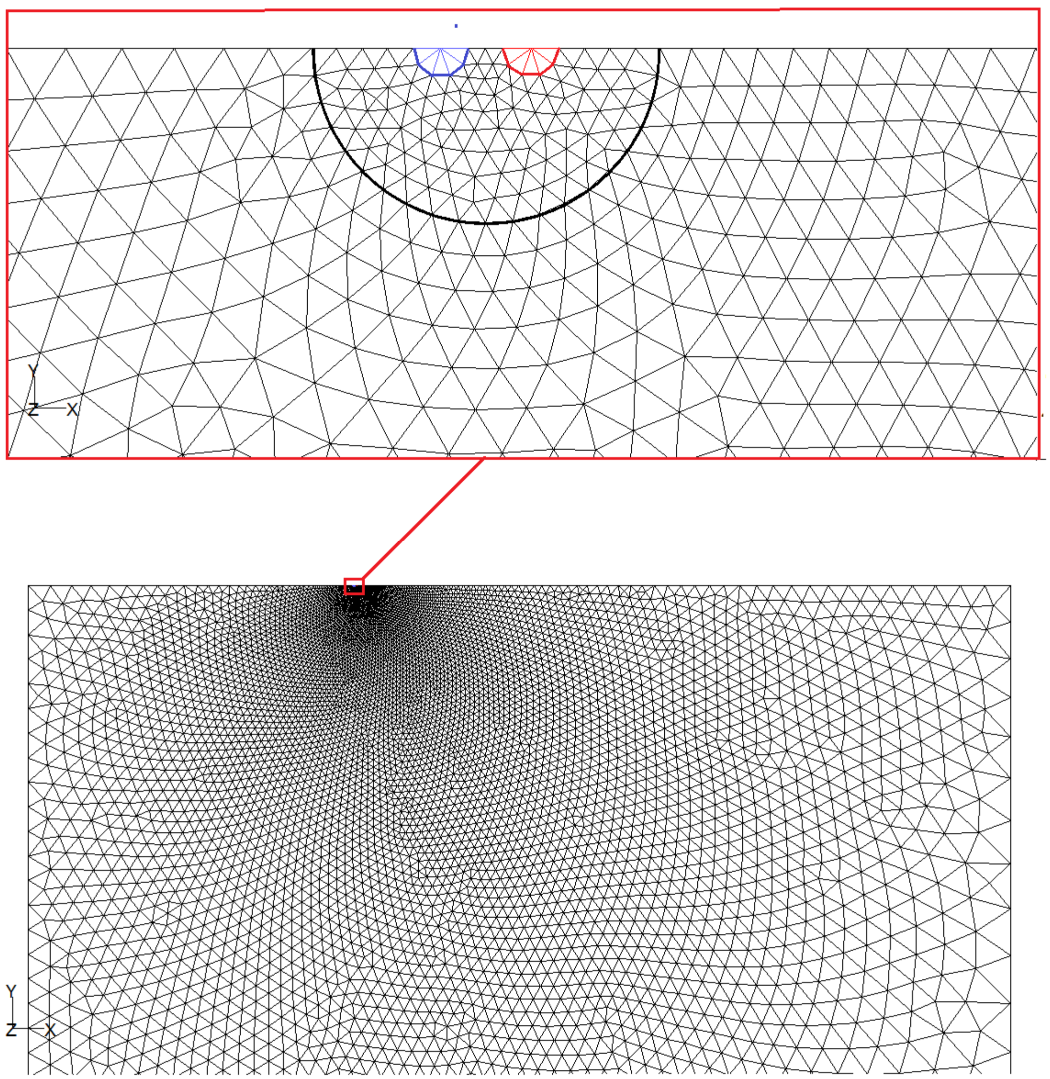

Figure 6-2 Computational triangular grids used in the solution domain in *xy* cross section.

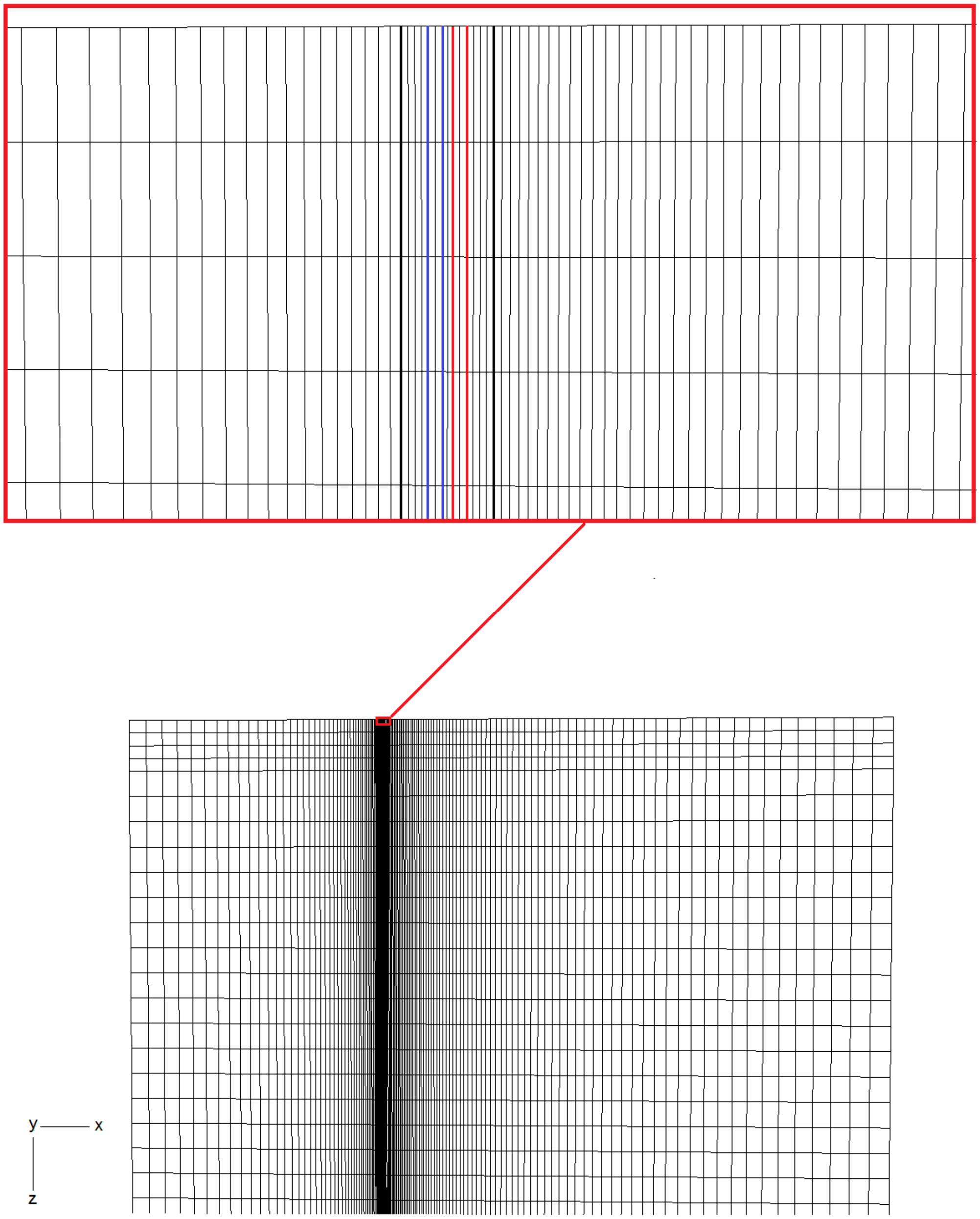

Figure 6-3 Computational triangular grids used in the solution domain in *xz* cross section.

To define the control volumes in unstructured meshes, a cell-centered control volume technique is applied by ANSYS FLUENT. In the cell-centered method, the nodes are placed at the centroid of the control volume, as illustrated in Figure 6-4, while the boundary nodes reside at the center of boundary cell-faces.

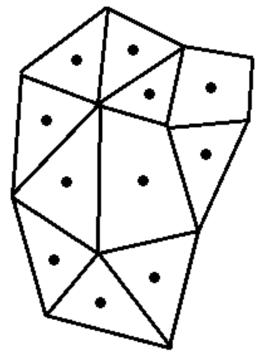

Figure 6-4 Cell-centered control volume construction in 2D unstructured meshes.

6.2 Discretization

The discretization in unstructured meshes can be developed from basic control volume technique where the integral form of the conservation equation for transport of a scalar quantity Φ is used as the starting point:

$$\int_{CV}\frac{\partial\rho\phi}{\partial t}dV+\oint\rho\phi\vec{v}\cdot d\vec{A}=\oint\Gamma_{\phi}\nabla\phi\cdot d\vec{A}+\int_{CV}S_{\phi}dV \tag{6-1}$$

where ρ is density, $\vec{v}$ is the flow velocity vector, Γ_{ϕ} is the diffusion coefficient for Φ, and S_{Φ} is source of Φ per unit volume. The terms on the left-hand side of Eq. (6-1) are the conservative form of transient derivative of transported variable Φ and the convection terms, respectively, and the diffusion and source terms appear on the right-hand side. Discretization of Eq. (6-1) yields the following general form:

$$\frac{\partial\rho\phi}{\partial t}V+\sum_{i}^{N_{faces}}\rho\phi_i\vec{v}_i\cdot\vec{A}_i=\sum_{i}^{N_{faces}}\Gamma_{\phi}\nabla\phi_i\cdot\vec{A}_i+S_{\phi}V \tag{6-2}$$

where $\vec{A}_i$ is the area of surface i, V is cell volume and N_{faces} is the number of faces enclosing a cell which depends on the cell topology. Face values of Φ are required for the convection term in Eq. (6-2) and must be interpolated from the cell center values using a second-order upwind scheme. The firs-order upwind scheme is used when the flow is aligned with the mesh. In the current study, since the mesh is in triangular prism shape, the flow crosses the mesh lines obliquely at the U-tube turn and first-order convective discretization may increase the numerical discretization error. To obtain more accurate results, the second-order discretization is used. In this approach, quantities at cell faces are computed through a Taylor series expansion of the cell-centered solution about the cell centroid. Thus when second-order upwinding is selected, the face value Φ_i is computed using the following expression:

$$\phi_i = \phi + \nabla\phi \cdot \vec{r} \tag{6-3}$$

where ϕ and $\nabla\phi$ are the cell-centered value and its gradient in the upstream cell, and $\vec{r}$ is the displacement vector from the upstream cell centroid to the face centroid. Eq. (6-2) is non-linear with respect to the unknown scalar variable Φ at the cell center as well as in surrounding neighbor cells (Φ_{nb}). A linearized form of Eq. (6-2) can be written as

$$a_P\phi = \sum_{nb} a_{nb}\phi_{nb} + b \tag{6-4}$$

where a_p and a_{nb} are linearized coefficients for Φ and Φ_{nb}. Similar relations with the form of Eq. (6-4) can be written for each cell in the solution domain which results in a system of algebraic equations. In ANSYS FLUENT, this system is solved via a Gauss-Seidel method (ANSYS FLUENT 12.0 theory guide 2013).

6.3 Pressure-Based Solver

The current problem consists of three regions: soil, grout and the running fluid. The soil and grout region are solid regions and, therefore, the only mode of heat transfer is heat conduction. The running fluid region, however, employs all conservation equations of mass, momentum and energy. In solving these equations, special practices are employed in discretization of the continuity and momentum equation. Using the discretization scheme described in Section 6.2, the *x*-momentum equation can be obtained as

$$a_P u = \sum_{nb} a_{nb}u_{nb} + \sum p_i \vec{A}\cdot\hat{i} + S \tag{6-5}$$

Equation (6-5) requires the value of the pressure, P_i, at the face between neighboring cells c_0 and c_1. If the pressure field is not known when solving Eq. (6-5), an interpolation scheme is required to compute the face values of pressure from the cell values. Since in the current study, the pressure variation between the cells is expected to be smooth, the pressure profile is not expected to have a high gradient at a cell face and, therefore, the following standard pressure interpolation scheme is used:

$$P_i = \frac{\dfrac{P_{c_0}}{a_{p,c_0}} + \dfrac{P_{c_1}}{a_{p,c_1}}}{\dfrac{1}{a_{p,c_0}} + \dfrac{1}{a_{p,c_1}}} \tag{6-6}$$

The continuity equation may be discretized as

$$\sum_{i}^{N_{faces}} \rho v_i A_i = 0 \tag{6-7}$$

Here, it is necessary to relate the face values of velocity, v_i, to the stored values of velocity at the cell centers. ANSYS FLUENT uses momentum-weighted averaging, using weighting factors based on the a_p coefficient from Eq. (6-5) to obtain the face flux ρv_i in Eq. (6-7). Hence,

$$\rho v_i = \rho \hat{v}_i + d_f \left(p_{c_0} - p_{c_1} \right) \tag{6-8}$$

where contains the influence of velocities in cells c_0 and c_1.

$$\hat{v}_i = \frac{a_{p,c_0} v_{n,c_0} + a_{p,c_1} v_{n,c_1}}{a_{p,c_0} + a_{p,c_1}} \tag{6-9}$$

p_{c_0}, p_{c_1}, v_{n,c_0} and v_{n,c_1} are the pressures and normal velocities, respectively, within the two cells on either side of the face i. The term d_f is a function of $\overline{a}_P$, the average of the momentum equation a_P coefficients for the cells on either side of face i.

To couple the pressure and velocity in continuity and momentum equations, Eq. (6-8) is used to derive an additional condition for pressure by reformatting the continuity equation [Eq. (6-7)]. In the current study, the flow problem is solved in a pressure based segregated manner by using the SIMPLE algorithm. The SIMPLE algorithm uses a relationship between velocity and pressure corrections to enforce mass conservation and to obtain the pressure field. In this algorithm, the momentum equation [Eq. (6-5)] is solved using a guessed pressure field, p^*, resulting in face flux ρv_i^* that is computed from Eq. (6-8). Therefore,

$$\rho v_i^* = \rho \hat{v}_i^* + d_f \left(p_{c_0}^* - p_{c_1}^* \right) \tag{6-10}$$

If this face flux is not does not satisfy the continuity equation, a correction $\rho v_i'$ is added to the face flux ρv_i^*, so that the corrected heat flux,

$$\rho v_i = \rho v_i^* + \rho v_i' \tag{6-11}$$

satisfies the continuity equation. In order to correct the initial guessed pressure, p^*, the SIMPLE algorithm assumes that the face flux correction, $\rho v_i'$, be written as

$$\rho v_i' = d_f \left(p_{c_0}' - p_{c_1}' \right) \tag{6-12}$$

where p' is cell pressure corrections. The flux correction equations [Eqs. (6-11) and (6-12)] are, then, substituted into the discrete continuity equation [Eq. (6-7)] to obtain a discrete equation for the pressure correction p' in the cell:

$$a_P p' = \sum_{nb} a_{nb} p'_{nb} + \sum_{i}^{N_{faces}} \rho v_i^* A_i \tag{6-13}$$

where the second term on the right-hand side of Eq. (6-13) is the net flow rate into the cell. The solution of Eq. (6-13) can be used in correcting cell pressure and the face flux:

$$p = p^* + \alpha_p p' \tag{6-14}$$

$$\rho v_i = \rho v_i^* + d_f \left(p_{c_0}' - p_{c_1}' \right) \tag{6-15}$$

where α_p is the under-relaxation factor for pressure. The corrected face flux, ρv_i, satisfies the discrete continuity equation identically during each iteration.

Since the current study involves transient operation of boreholes, the governing equations must be discretized in time in addition to discretization in space. For time-dependent flows, the pressure-based solver in ANSYS FLUENT uses an implicit discretization of the transport equation. Therefore, every term in the differential equations is integrated over time step Δt. In the pressure-based solver, the overall time-discretization error is determined from two sources of error: temporal discretization and the manner in which the solutions are advanced to the next time step (time-advancement scheme).

A second-order implicit temporal discretization is used to replace the time integrals in the current study which appears in the following format:

$$\frac{3\phi^{n+1} - 4\phi^{n} + \phi^{n-1}}{2\Delta t} = F\left(\phi^{n+1}\right) \tag{6-16}$$

where the function *F* incorporates any spatial discretization. Note that Φ_{n+1} is used in evaluating F due to the implicit method, i.e. all convective, diffusive, and source terms are evaluated from the fields for time level *n+1*. Thus, Φ_{n+1} cannot be expressed explicitly in terms of the existing solution values, Φ_n. The implicit equation can be solved iteratively at each time level before moving to the next time step. The advantage of this scheme is that it is unconditionally stable with respect to time step size and introduces $O\left[(\Delta t)^2\right]$ truncation error.

The segregated solution process by which the equations are solved one by one introduces splitting error. In ANSYS FLUENT, there are two approaches to the time-advancement scheme depending on how the splitting error is controlled: iterative time-advancement scheme and non-iterative time-advancement scheme. Comparing the two methods, the first scheme is chosen for the time advancement in the current study since, in this scheme, non-linearity of the individual equations and inter-equation couplings are fully accounted for, eliminating the splitting error. All the equations are solved iteratively, for a given time-step, until the convergence criteria are met. More specifically, the Frozen Flux Formulation is used in the time advancement scheme. This formulation addresses the non-linear terms resulting from implicit discretization of the convective part of transport equation and provides an optional way to discretize the convective part of transport equation using the mass flux at the cell faces from the previous time level *n*. This reduces the non-linear character of the discretized transport equation without compromising the accuracy and improves the convergence within each time step.

When including heat transfer within the running fluid region in the model, the pressure-based solver does not include the pressure work or kinetic energy when solving incompressible flow. Furthermore, in the current the pressure-based solver, viscous dissipation terms in the energy equation, which describe the thermal energy created by viscous shear in the flow, are not included in the energy equation because viscous heating is negligible in the current problem. The details of the derivation of the energy equation in the soil and grout regions are given in Appendix A.

6.4 Initial and Boundary Conditions

A uniform initial temperature of 282 K (equal to the undisturbed ground temperature) is assumed to be effective over the entire borefield. At the outer edge of the domain, a constant farfield temperature condition is applied (282 K).

The temperature and heat flux distributions on the borehole wall cannot be decided due to the dynamic nature of the heat exchange process between the pipes in the borehole and the borehole wall.

In some cases of the current study where only the heat flows in the soil region are studied, a constant or variable borehole wall heat flux is assumed at the borehole wall. In order to compare the results obtained by line source theory with the results from the numerical solution, an equivalent heat flow rate per unit area of the borehole wall q'' (W/m^2) to that of the line source theory q' (W/m), resulting in the same amount of total heat conducted in the soil, is calculated for the numerical solution. The following energy balance is used:

$$\dot{Q}_{borehole\ wall} = \dot{Q}_{Line\ source\ theory} \tag{6-17}$$

where $\dot{Q}_{borehole\ wall}$ (W) and $\dot{Q}_{Line\ source\ theory}$ (W) are the total heat rates conducted in the soil from the borehole wall and the line source, respectively. Therefore,

$$q''\,(2\,\pi\,r_b)\,H = q'H \tag{6-18}$$

where r_b is the borehole radius, and H is the active borehole length, i.e. the length in which heat flow is noticed. For example, if an arbitrary heat flux of 10 W/m^2 at the borehole walls is chosen in the numerical solution, its equivalent heat flow rate per unit length would be $q' = 3.1415$ W/m for the line source theory.

To fully account for the conjugated thermal process occurring in the borefield, the inlet temperature and flow rate of the fluid are specified as boundary conditions (see

Section 4.3.1). The inlet running fluid temperature, $T'_f(t)$, varies according to the temperature of the U-tube surrounding (grout) to maintain the required amount of heat flow rate during system operation.

To maintain the required ground heat load, q', the inlet temperature of the running fluid varies according to the following relation:

$$T'_f = \frac{q'H}{\dot{m}c_p} + T_{out} \tag{6-19}$$

In Eq. (6-19), the inlet running fluid temperature, T'_f, needs to be updated at every time step for a constant heat flow rate per unit length since, as the system operates, surrounding soil temperature rises/drops gradually resulting in a rise/drop in the outlet running fluid temperature, T_{out}. If the average heat flow rate per unit length of borehole is transient, the inlet running fluid temperature will change according to the variation in outlet fluid temperature and the ground heat flow rate per unit length. The transient heat flow and running fluid temperature cannot be readily defined in ANSYS FLUENT. Therefore, in the current study, a user defined function is programmed in C and hooked to the pressure base solver. Details on the algorithm that is used in this code are given in Section 6.5 and the code can be found in Appendix D.2.

The ground heat load depends on many parameters such as climate averages, type of the building (residential, recreational and industrial structures), its size, the number of people in the building, the ground heat pump specifications etc. Climate averages are used to summarize or describe the average climatic conditions of various locations. The temperature usual values and extremes for Canadian locations are available in Environment Canada (2011). Average monthly temperatures throughout the year for Toronto, Ontario based on Canadian climate stations data from 1971 to 2000 are shown in Figure 6-5. It is seen that the heating and cooling load profile throughout the year varies depending on the outside air temperature.

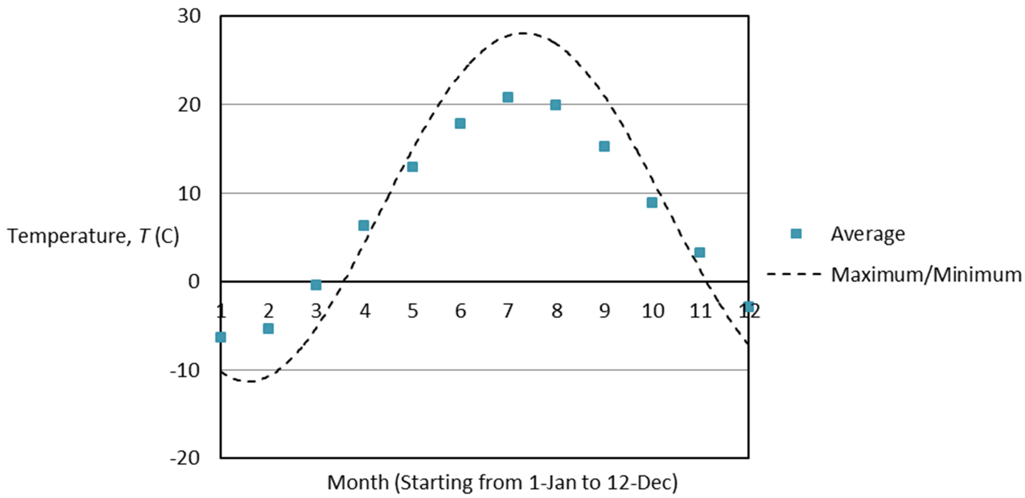

Figure 6-5 Average monthly temperatures throughout the year for Toronto, Ontario.

The effect of each parameter on the heating and cooling profiles can be examined and the dominating factors on heating and cooling profile shape will be determined in the following form:

$$\dot{Q} = f(\dot{Q}_{\max}, t) \tag{6-1}$$

where $\dot{Q}$ is the heating/cooling load at time *t*, $\dot{Q}_{\max}$ is the maximum heating/cooling which varies with the size of the building, the number of people in the building, etc., and *f* is a periodic function that best describes the shape of heating and cooling loads in a specified building type (office, residence, etc.) throughout the year. In order to examine the effects of different parameters on the building heating and cooling load profile shape which corresponds to the *f* function and size a heat pump unit, a heating and cooling load analysis can be made using programs such as HvacLoadExplorer (McQuiston et al. 2005), and the design heating and cooling loads for each month based on the varying temperature profile can be obtained. Using this data, the form of function *f* can be estimated.

The performance data of the heat pump unit (such as heating and cooling capacities, COP, power consumption, water pressure drop at the water-to-refrigerant heat exchanger) can be modeled as functions of the entrance water temperature for various circulating fluid flow rates.

Once an estimation of the heating and cooling profile shape is determined in the form of an *f* function, average monthly ground heat loads can then be defined via the heat pump power consumption and other specifications and are used in the heat boundary on the borehole wall. In order to achieve a more accurate ground heat load profile a typical heat pump system can be used and the ground heat load can be calculated experimentally or via analytical methods such as Bin method (McQuiston et al. 2005). A case study using bin method calculations to estimate the ground heat load profile is presented in Appendix C. Therefore, due to the periodic climate changes, the ground heat load profile is expected to be periodic. Here, it is assumed that the ground load profile is modeled as a simplified sinusoidal profile shown in Figure 6-6.

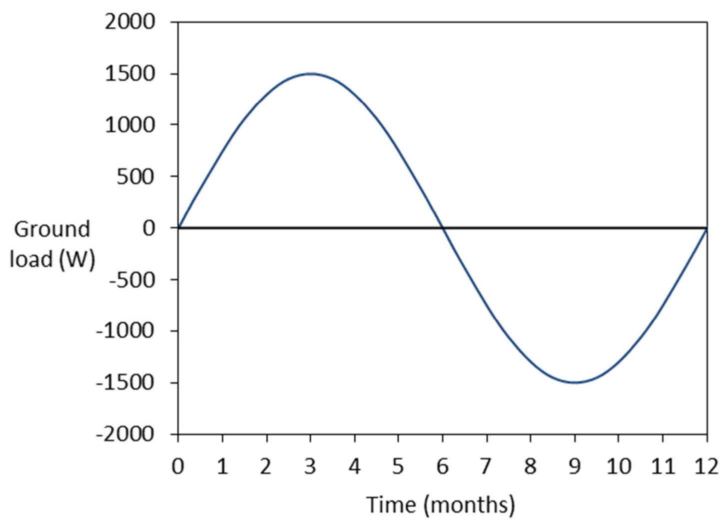

Figure 6-6 Ground load profile.

6.5 User Defined Function

To define a transient boundary condition in ANSYS FLUENT, here, the inlet running fluid temperature, a user defined function must be programmed in C and hooked to the pressure base solver. An illustration of the algorithm used in this code in order to evaluate the transient boundary condition at the running fluid inlet is shown in Figure 6-7. It is seen that in the numerical approach, the temperature of the running fluid at the U-tube exit is calculated at every time step and a new temperature for the running fluid inlet temperature is set according to the required ground heat load for the next time step. Since in order to maintain the required heat flow rate, the temperature of the inlet and outlet running fluid temperature must follow the heat flow rate occurring at the same time step, calculating the inlet running fluid temperature this way and using it as the boundary for the inlet running fluid temperature in the next time step can add some error to the solution. This method is preferred due to its relative simplicity and less computation time in ANSYS FLUENT. However, in order to minimize the error in the results of the simulation, the time steps should be chosen small enough so that the change in the required heat flow rate and, consequently, the inlet running fluid temperature is kept relatively small from one time step to the next.

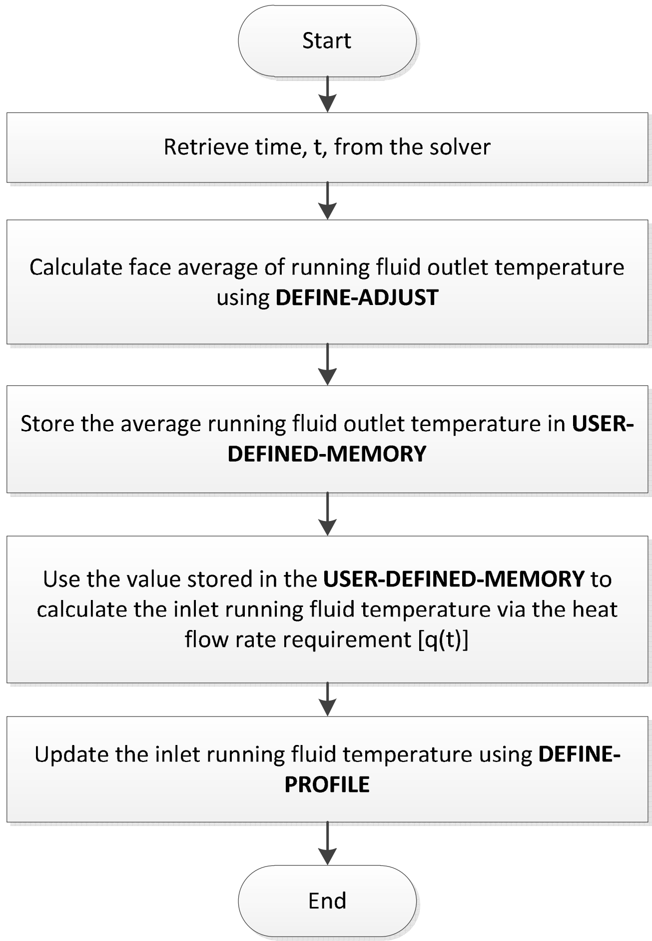

Figure 6-7 Illustration of the algorithm used in the User-Defined-Function used in the simulation.

6.6 Grid Quality

The quality of the mesh plays a significant role in the accuracy of Eq. (A-15) in estimating the temperature and stability of the numerical computation. The attributes associated with mesh quality are node point distribution, smoothness and skewness (non-orthogonality). Rapid changes in cell volume between adjacent cells translate into larger truncation errors. To improve the smoothness, the mesh should be refined based on the change in cell volume or the gradient of cell volume. The central difference used in the discretization of the governing equations is only accurate if the mesh is fully orthogonal, that is when the line joining neighboring nodes *P* and *A* and the unit normal vector n_i are in the same direction. Cell skewness is a nondimensional parameter calculated using the normalized angle and volume deviation methods. It is a measure of the difference between the shape of the cell and the shape of an equilateral cell of equivalent volume or angle. Optimal quadrilateral triangular meshes will have angles of close to 60 degrees and have all angles less than 90 degrees. Highly skewed cells can decrease accuracy and destabilize the solution. A value of 0 indicates a best case equiangular and equilateral cell, and a value of 1 indicates a completely degenerate cell which are characterized by nodes that are nearly coplanar (collinear in 2D). In the current mesh, cell skewness is reported as below for the 2D mesh shown in Appendix B.3.

Maximum equivolume cell skewness = 0.53

Maximum equiangle cell skewness = 0.64

Moreover, cell Squish is a measure used to quantify how far a cell deviates from orthogonality with respect to its faces. Therefore, the worst cells will have a Cell Squish Index close to 1. In the current mesh, cell squish is reported as below for the 2D mesh.

Maximum cell squish = 0.41

Maximum face squish = 0.28

To eliminate errors due to coarseness of a grid, a grid sensitivity study is performed. In general, the grid is made finer until less than 1% change in temperature rise calculated at the borehole wall is achieved.

6.7 Summary

In the pressure-based approach, the pressure field is extracted by solving a pressure or pressure correction equation which is obtained from continuity and momentum equations. ANSYS FLUENT will solve the governing integral equations for the conservation of mass and momentum (when appropriate), and for energy. In both cases a control-volume-based technique is used that consists of:

- Division of the domain into discrete control volumes using a computational grid.

- Integration of the governing equations on the individual control volumes to construct algebraic equations for the discrete dependent variables ("unknowns") such as temperature.
- Linearization of the discretized equations and solution of the resultant linear equation system to yield updated values of the dependent variables.

Each iteration consists of the steps illustrated in Figure 6-8 and summarized below:

- Update fluid properties (e,g, density, viscosity, specific heat) on the current solution.
- Allocate a User-Defined-Function for running fluid inlet temperature.
- Update boundary conditions using DEFINE-PROFILE macro.
- Solve system of Continuity, Momentum and Energy equations for the running fluid model.
- Solve Energy equations for the grout and soil models.
- Check for the convergence of the equations.

After each irritation, the simulation time is checked and if, the simulation should continue, the temperature boundary condition at the running fluid inlet should be updated according to the new running fluid outlet temperature and the required heat flow rate.

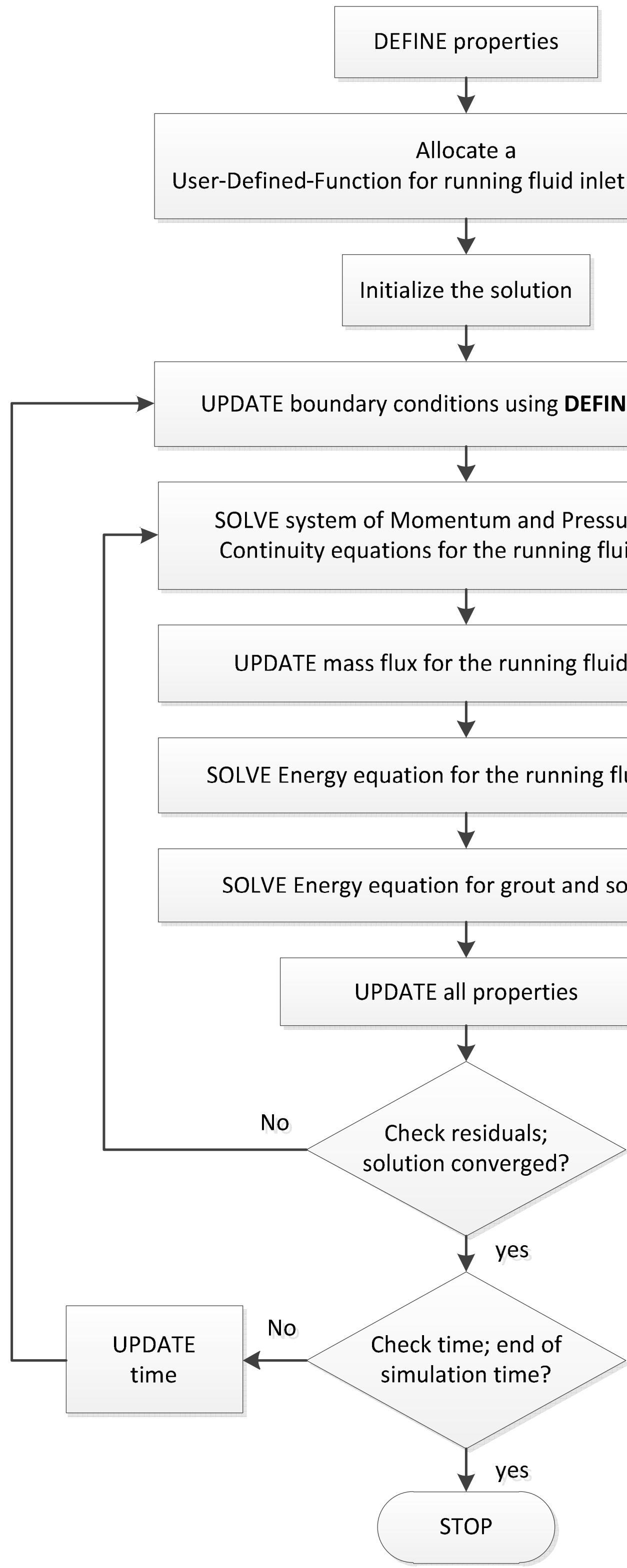

Figure 6-8 Solution procedure in ANSYS FLUENT.

Chapter 7 RESULTS AND DISCUSSION

In the current chapter, the results of various simulation models corresponding to various objectives of the current study are presented. In Section 7.1, a preliminary sensitivity study is introduced and the effect of various parameters on temperature rise in the soil surrounding the boreholes is discussed. In addition, some aspects of the analytical and numerical approaches are validated by comparing the results of the two models. After validation of the numerical approach in Section 7.1 with results of the well-known line source theory, Section **Error! Reference source not found.** focuses on the results of a two dimensional numerical model that is able to estimate the heat flows in the soil surrounding neighboring systems of boreholes. The results of this section can be used towards environmental analysis of such systems and their impact on nearby eco systems in their long term operation. Section 7.3 presents results of a full numerical simulation including the soil region surrounding the boreholes as well as the grout and running fluid inside the borehole. This Section discusses the effect of thermal interaction between the borehole systems on their heat pump performance.

7.1 Sensitivity Check and Comparison between Analytical and Numerical Approaches

When examining negative environmental effects of borehole systems, only the heat flow patterns outside the borehole are of interest. Therefore, the results of two-dimensional numerical simulation in the soil region outside the boreholes are discussed. In Section 7.1.1, a degree of confidence is achieved by comparing the results of a two-dimensional numerical model with the well-know and already-validated results of the line source theory for a single borehole. In addition, the results of a numerical model for two neighbor systems are discussed. The results are compared with analytical ones to validate superposition of single line source solutions to evaluate temperature rise of multiple boreholes in their surrounding soil. Effect of various parameters on soil area experiencing temperature rise and on thermal interaction is discussed in Section 7.1.2. In order to examine the validity of the heat flows in a two-dimensional domain, the results of the two-dimensional analysis are compared with ones from three-dimensional analysis in Section 7.1.3. In Section 7.1.4, the effect of heating strength variation along the borehole length due to the varying running fluid temperature is discussed. Finally, in Section 7.1.5, the variation of the temperature rise in the soil surrounding borehole system with soil thermal conductivity is studied. It should be noted that the simulations and geometries used in obtaining the results presented in Section 7.1 can be found in Appendix B. The models may vary with the models presented in Chapter 5 and Chapter 6 .

7.1.1 Comparison of Results of Two-dimensional Numerical Solution and Kelvin's Line Source Theory

In this section, results of the two-dimensional numerical solution are compared with results corresponding to Kelvin's line source theory. The two solution methods are applied on single and multiple borehole models and the two-dimensional numerical solution results for the temperature rise in the soil around the borehole is validated with the analytical solution results. The borehole is assumed to have a constant and steady heat flow rate of 3.14 W/m along its length. Since the simulations in this section are performed to examine the validity of the numerical solution setup with the results of the well-known line source solution, a somewhat smaller heat flow rate per unit length is chosen here to reduce the size of the solution domain and computation time. Typical values of heat flow rate per unit length for borehole heat exchangers are within 30-60 W/m and require a much larger computational domain. Note that the analytical model for the case of multiple boreholes uses a superposition of single borehole thermal responses evaluated with line source theory in order to evaluate the temperature of the soil around the boreholes. In addition, comparing the results of the superposed line source theory solution and the numerical solution, one can determine the validity of the superposition method used in the analytical method.

Figure 7-1 shows the temperature response of the soil around a single borehole calculated with the analytical and numerical methods. The temperature rise in the soil is evaluated for 6 months of system operation with 3.1 W/m of heat flow rate per unit length of borehole. As can be seen, the temperature reaches a maximum at the borehole wall and decreases with the distance from the borehole wall. The results show that the numerical values for the temperature around the borehole agree with the analytical ones. This validates the numerical setup in estimating the temperature rise in the soil surrounding the borehole.

The temperature of the soil just beside the borehole wall is calculated as 290.2 K for the numerical solution. This temperature is calculated as 289.6 K for the analytical solution. Similarly, the affected region in the soil, i.e. where the temperature excess in the soil exceeds 0.1 K, after 6 months of heat injection into the ground is about 5 m for both solution methods. The area of the effected region, however, depends highly on the heat flow rate per unit length of the borehole; for typical borehole heat flow rates, a larger affected area is expected.

Figure 7-2 and Figure 7-3 show the temperature contours in the soil around two boreholes at t=1 month and 6 months, respectively. Note that the affected region around the two boreholes (temperature excess of more than 0.1 K) grows with time (from 3 m at t=1 month to 6 m at t=6 months). Furthermore, the temperature of the soil immediately outside the borehole wall increases from 288 K at t=0 to 289.9 K after 1 month and 290.7 K after 6 months of heat injection into the soil. It is seen in Figure 7-3 (b) for both time periods that the analytical and numerical results agree well in terms of soil temperature values around the borehole. As discussed earlier, the thermal effect of two boreholes on each other is neglected when two one-dimensional analytical solutions for individual boreholes are superposed to give the temperature of the soil in the two-dimensional domain.

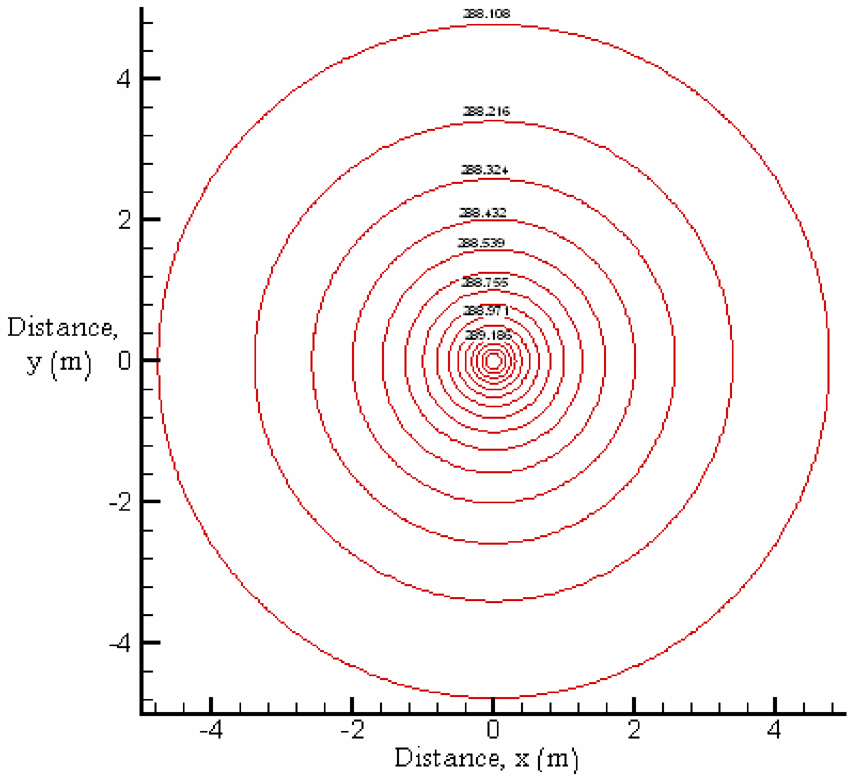

(a)

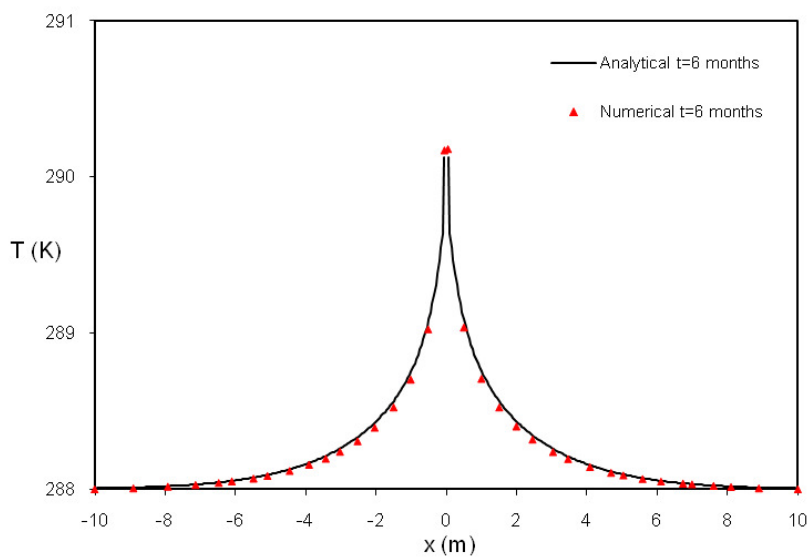

(b)

Figure 7-1 Soil temperature results (K) for a single borehole at time *t*=6 months. (a) Temperature contours (K) of the analytical solution. (b) Comparison of the analytical and numerical solutions at *y*=0.

The agreement between the analytical and numerical results here validates the application of the superposition method in solving the two-dimensional heat conduction problem in the soil in this particular case. It is also noticed that for a specific distance from each borehole, e.g. r=1 m, the temperature of the region between the two boreholes is higher (288.7 K after 1 month) than the temperature of the outer area (288.5 K after 1 month) which is due to the interacting effects of the two boreholes on each other. The temperature of the soil obtained between the two boreholes with the analytical and numerical solutions match perfectly.

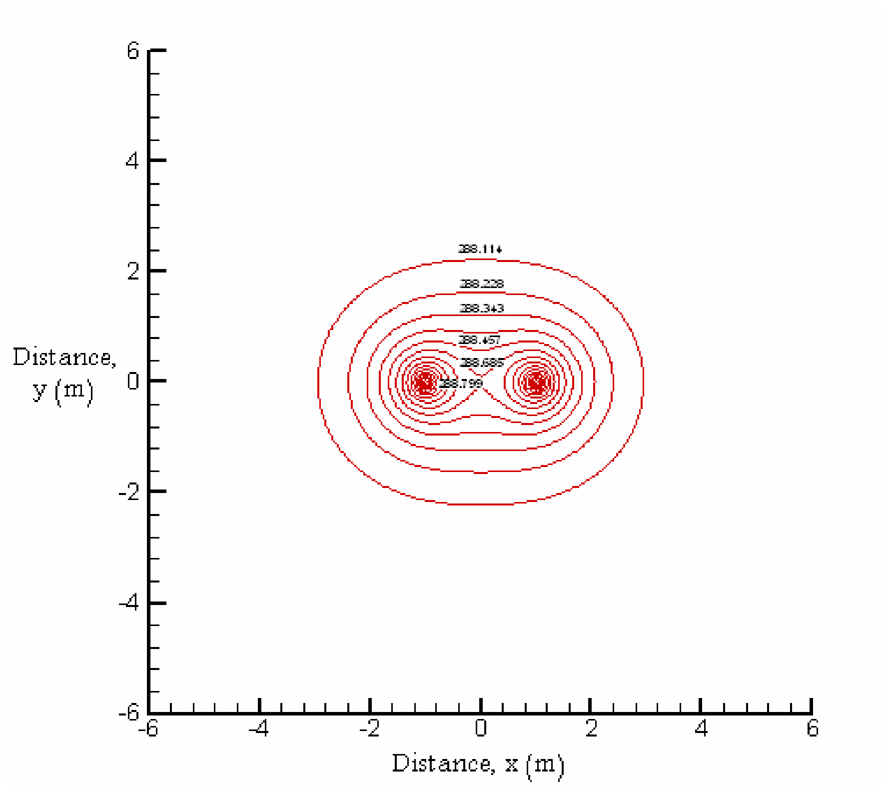

Figure 7-2 Soil temperature contours (K) of the analytical solution for multiple boreholes at time t=1 month.

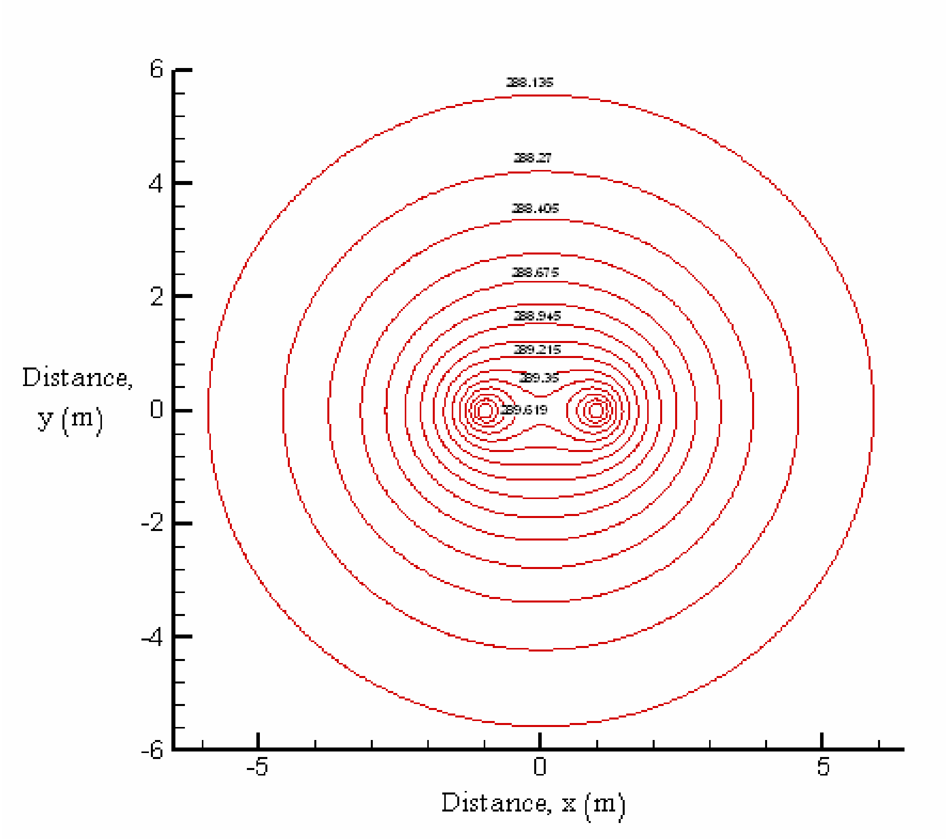

(a)

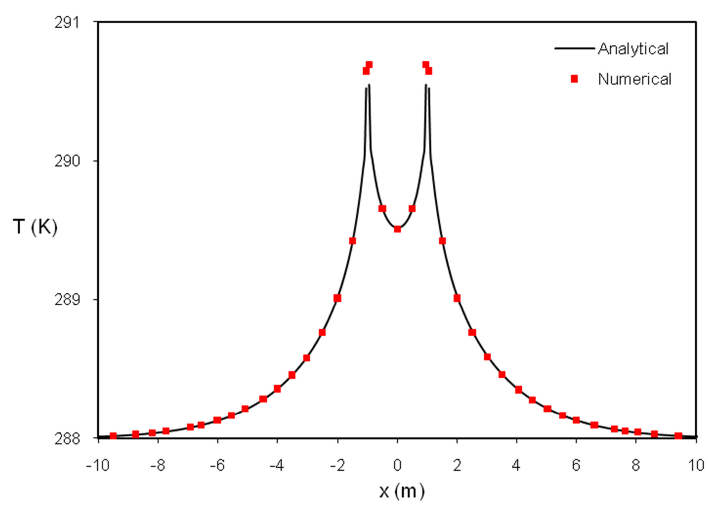

(b)

Figure 7-3 Soil temperature (K) around multiple boreholes at t=6 months. (a) Temperature contours (K) of the analytical solution. (b) Comparison of the analytical and numerical solutions at y=0 m.

7.1.2 Parameters Affecting Thermal Interactions between Multiple Boreholes

In this section, the effect of varying parameters such as time (t), distance between the boreholes (D_b), and heat flux from the borehole wall into the soil (q'') on thermal interaction between multiple boreholes are examined and compared with results of analytical solution. Similar to Section 7.1.2, the borehole is assumed to have a constant and steady heat flow. Since the objective here is to study the parameters that affect the temperature variations, a smaller heat flow rate per unit length of the borehole wall is selected (3.14 W/m along the borehole length) to reduce the size of the solution domain and computation time.

Figure 7-4 shows the growth of the affected area in the soil with time. It is seen that the temperature gradient of the soil near the boreholes tends to decrease as time increases. Furthermore, it is noticed that, for the current study with the current assumptions for borehole distance and heat flow rate at the borehole wall, the effects of thermal interaction in terms of temperature rise are noticeable after 1 week of heat input in the soil; however, the temperature increase in the soil between the two boreholes due to thermal interaction does not exceed 1 K before 1 month of constant heat input.

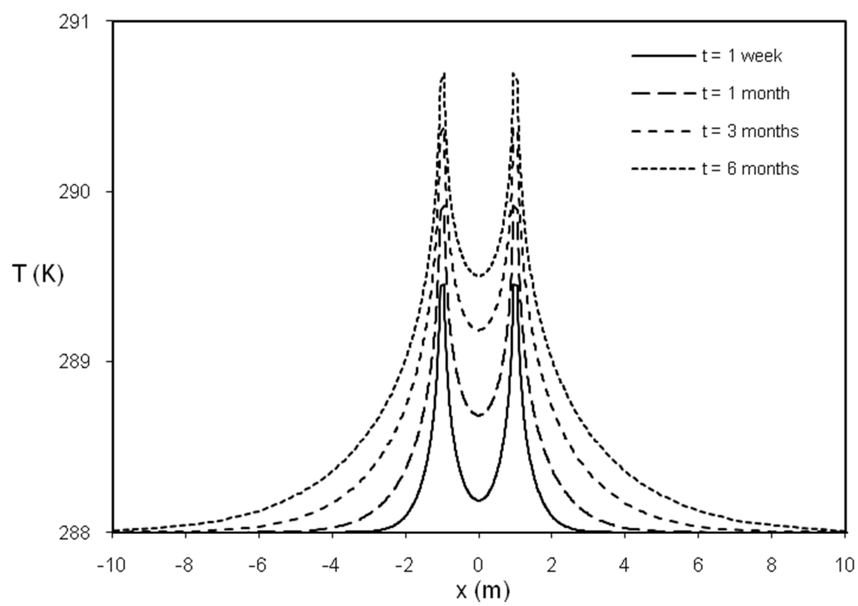

Figure 7-4 Temperature of soil (K) around multiple boreholes at different values at time t at y=0 m.

Figure 7-5 shows the effect of borehole distance (D_b) on the thermal interaction between two boreholes for analytical and numerical solutions. It is seen that, similar to the case of a 2-meter distance between the two boreholes, the analytical method shows greater soil temperatures at the borehole wall compared to the numerical one for the case of a 3-meter distance. Furthermore, a greater distance between the two boreholes (3 m distance compared to 2 m) leads to a weaker interaction between the two boreholes; the temperature of the soil between the two boreholes after 6 months decreases from 289.5 K for the case of D_b=2 m to 289.1 K for the case of D_b=3 m. The same trend is noticed for the temperature at the borehole wall, which is 290.7 K for a shorter distance (D_b=2 m) decreases to 290.5 K for a longer distance (D_b=3 m).

Figure 7-6 shows the soil temperature around the two boreholes installed at different separation distances. Note that the closer the two boreholes are installed, the stronger is the thermal interaction between them (the temperature between them reaches 290.2 K for D_b=1 m compared to 289.1 K for D_b=3 m) and the higher becomes the temperature of soil at the borehole wall (291 K for D_b=1 m compared to 290.5 K for D_b=3 m). For a specific heat flux from the borehole wall, a borehole separation distance can be calculated in order for the temperature of the soil to stay below a desired limit. It is also observed that, for a specified heat flux on the borehole wall (10 W/m^2), a greater distance between the two boreholes results in a slightly larger region in the soil experiencing temperature excess of more than 0.05 K (7.6 m for D_b=1 m compared to 8.1 m for 3 m). However, since the interaction effect is smaller for higher borehole distances, moving away from each borehole towards farfield, there is a larger temperature gradient for the boreholes with a larger spacing, i.e. the temperature excess in the soil disappears at a shorter distance from the borehole. This can also be due to less temperature rise effects from each borehole reaching to the outer soil around the other borehole.

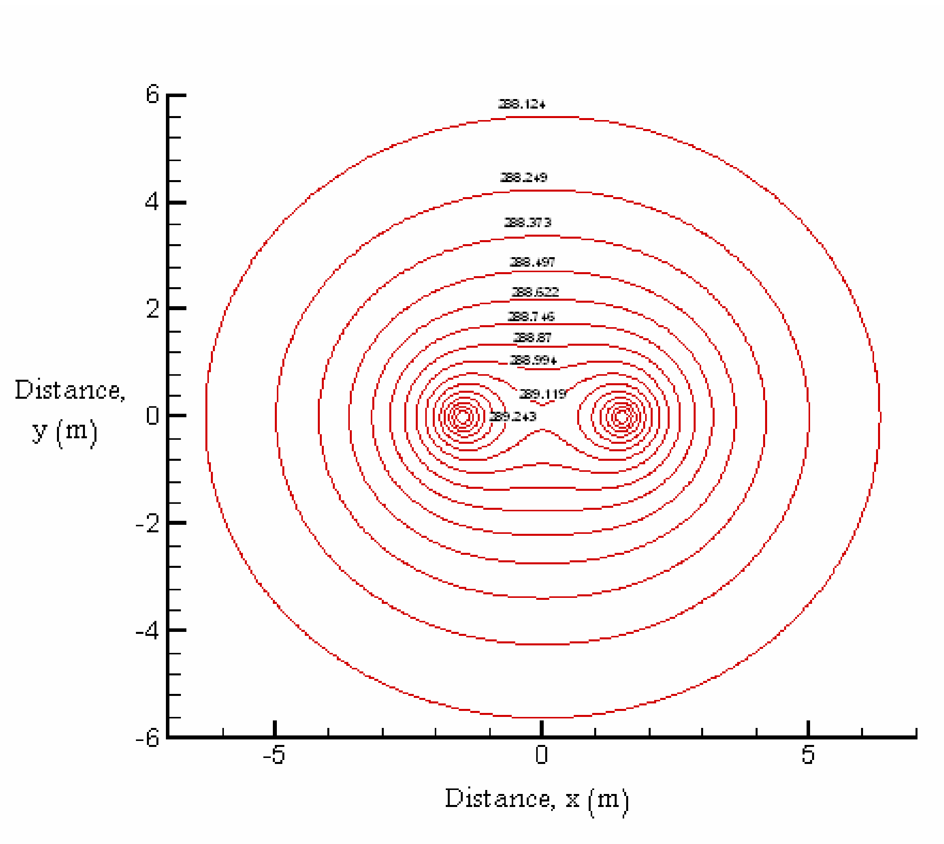

(a)

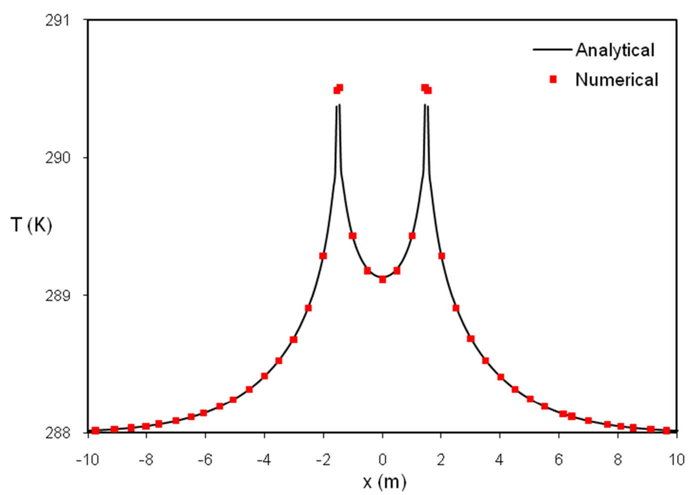

(b)

Figure 7-5 Soil temperature (K) around multiple boreholes at t=6 months and D_b=3 m. (a) Temperature contours (K) of the analytical solution. (b) Comparison of the analytical and numerical solutions at y=0 m.

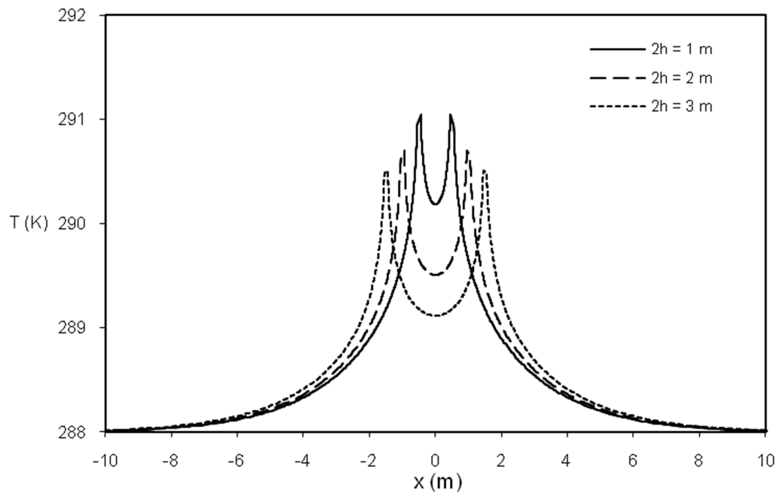

Figure 7-6 Temperature of soil (K) around multiple boreholes at several borehole distances at y=0 m.

The effect of heat flux at the borehole wall on the thermal interaction between the two boreholes for both analytical and numerical solutions is shown in Figure 7-7. It is seen that a larger heat flux results in a significant increase in the temperature of the soil at the borehole wall (301.5 K for q''=50 W/m^2) and also in the region far from the borehole wall. This results in a stronger thermal interaction between the two boreholes as well. As can be seen in Figure 7-7, the temperature of the soil between the two boreholes increases from 289.5 K in the case of q''=10 W/m^2 to 295.7 K in the case of q''=50 W/m^2. It is noticed that for a higher heat flux (q''=50 W/m^2 compared to q'' =10 W/m^2), the results of the numerical solution still match the analytical results well.

Figure 7-8 shows the effect of heat flux at the borehole wall on the temperature response of the soil around the boreholes. It is seen that a higher heat flux results in a higher temperature at the borehole wall and also a greater area around the borehole experiencing a temperature excess. A comparison of the affecting parameters on the thermal interaction between the two boreholes reveals that varying the heat flux at the borehole wall has a bigger role on the thermal interaction between the boreholes than varying borehole distances with the same ratio.

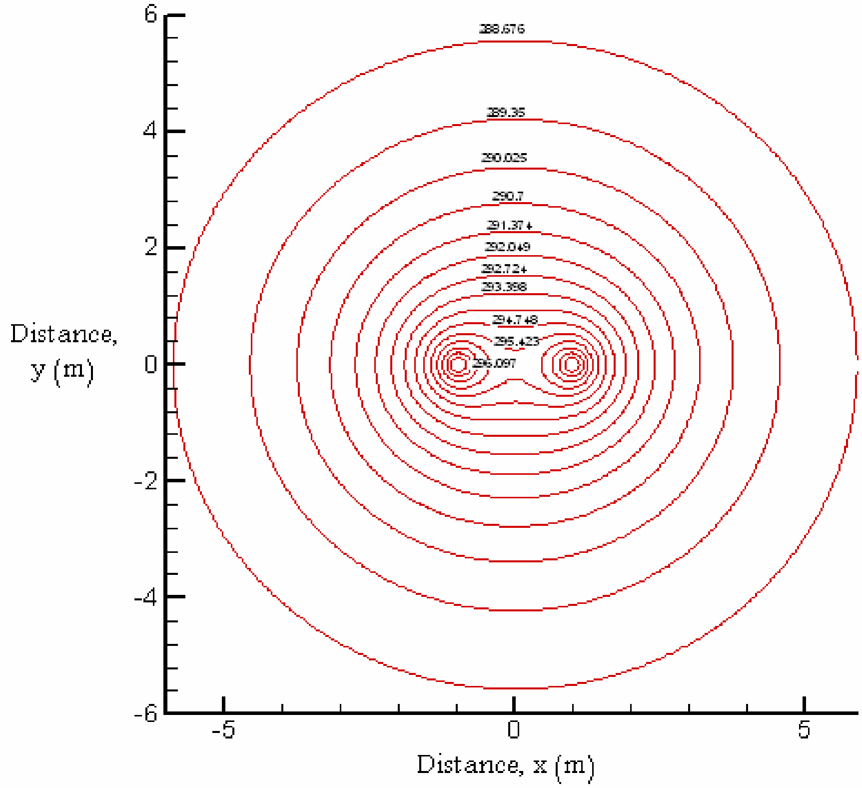

(a)

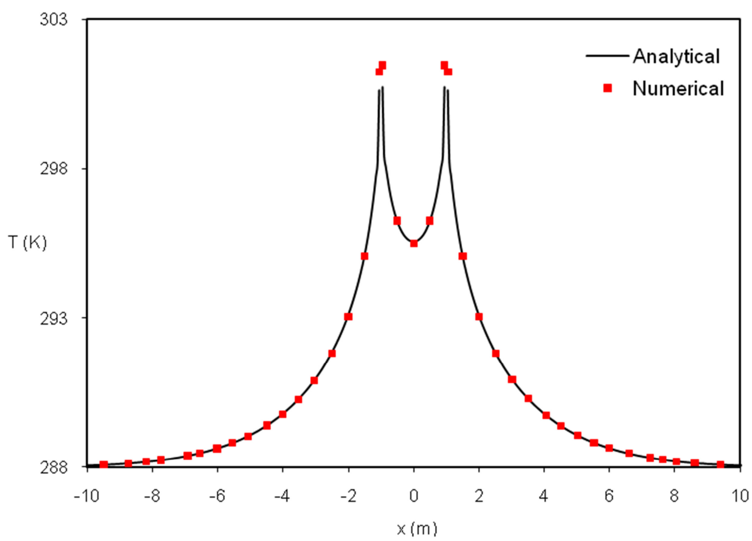

(b)

Figure 7-7 Soil temperature (K) aound multiple boreholes at q''=50 W/m^2 and t=6 months. (a) Temperature contours (K) of the analytical solution. (b) Comparison of the analytical and numerical solutions at y=0 m.

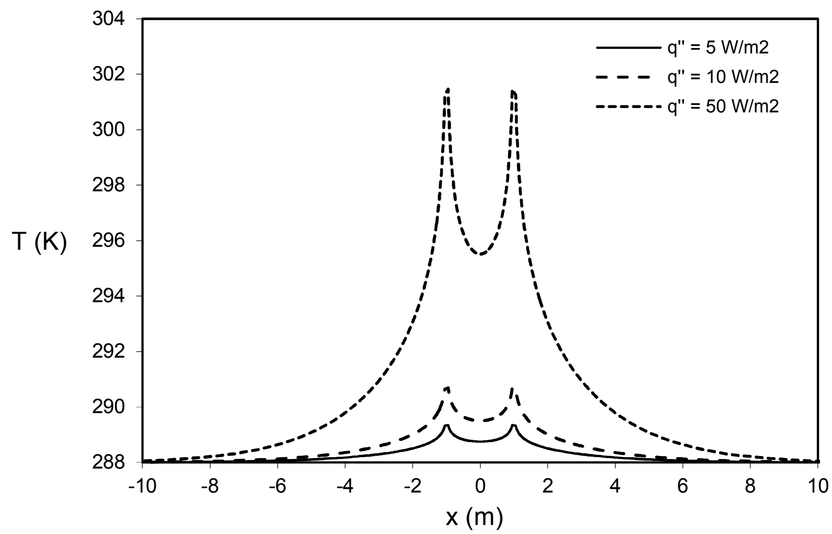

Figure 7-8 Temperature of soil (K) around multiple boreholes for various values of heat flux (q'') at the borehole wall.

Figure 7-9 shows the effect of varying heat flux from the borehole walls. It is seen that even with varying amounts of heat input in the soil, the temperature of the soil around the borehole is affected almost symmetrically in the form of circular contours at significant distances (greater than about 3 m). A comparison of the numerical and analytical results in Figure 7-9 (b) shows that except for the soil at the borehole wall, similar to the previous cases, the results match. It is seen in this figure that if the sum of heat fluxes from the two boreholes are the same, the temperature of the soil around the boreholes match after a distance of about 6 m for the case of D_b=2 m.

It is worth mentioning that the methods used for calculating the temperature profiles in the soil around two boreholes can be applied to two systems of borehole heat exchangers as well. For example, if an area of 40 m x 40 m x 200 m in the soil is occupied for one system of borehole heat exchangers, the ratio of system depth to its radial size is large enough to be treated as one cylinder or line source of heat when system interactions and temperature excess around a system in larger distances are to be accounted for. Therefore, a parametric study on two interacting boreholes can determine the results for two interacting systems of boreholes.

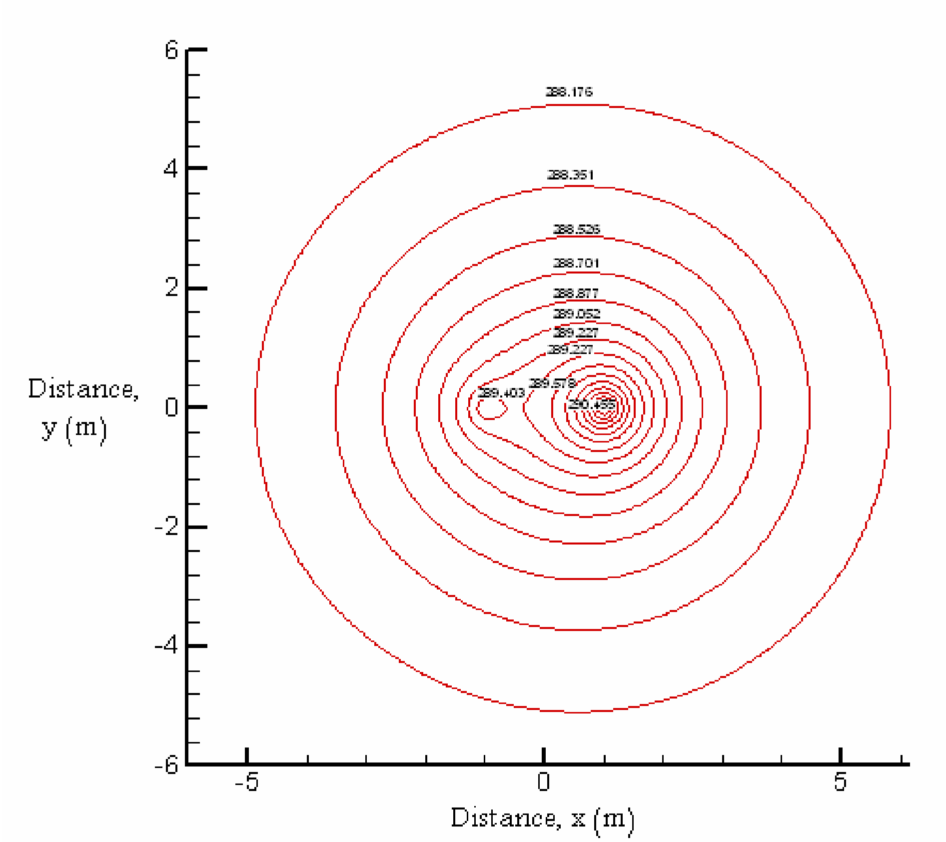

(a)

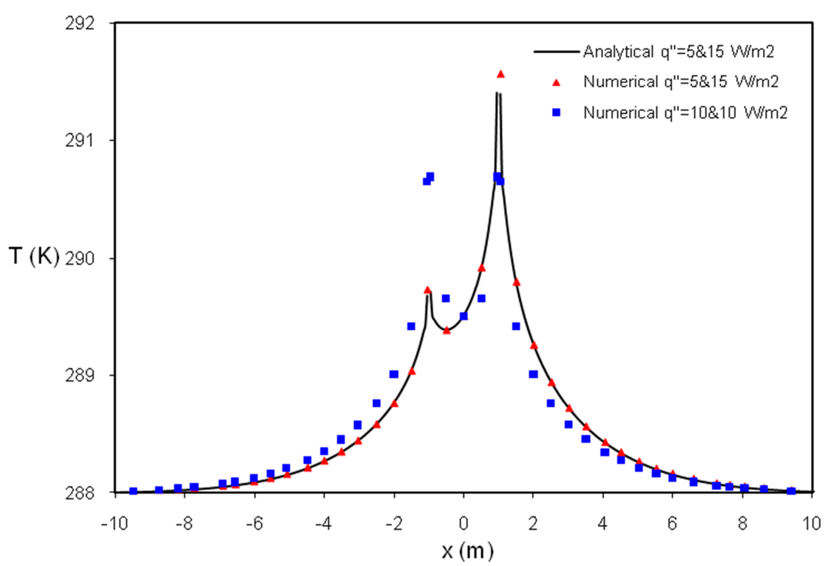

(b)

Figure 7-9 Soil temperature (K) around multiple boreholes at q''=5 and 15 W/m^2 and t=6 months. (a) Temperature contours (K) of the analytical solution. (b) Comparison of the analytical and numerical solutions at y=0 m.

7.1.3 Validation of Two-dimensional Numerical Solution with a Three-dimensional Solution

The main drawback of the two-dimensional numerical solution is that it neglects axial heat transfer effects which exist at depths near the top and bottom of the boreholes. To examine the inaccuracy associated with this simplification in the evaluation of the temperature response of the soil around the boreholes, a three-dimensional solution domain is considered in this section and the effect of borehole axial effects on the temperature profile is examined. Note that the heat flux from the borehole wall to the soil is assumed to be constant along the borehole length (q''=10 W/m^2). Since the objective of the study in this section is only to compare the two and three-dimensional solution domains, the selected heat flow rate is a relatively lower value compared to the design range (30-60 W/m) to reduce the solution domain size and computation time. Also, the results presented in this section are obtained for a three-dimensional geometry that is shown in Figure B-3. More details regarding the three-dimensional model can be found in Section B.2. Figure 7-10 compares the temperature profiles around multiple boreholes evaluated by the two-dimensional solution with the ones evaluated by the three-dimensional one at distances in the middle of the borehole length (z=0) and 4 m away from the bottom of the borehole (z=96 m). It is seen that the temperature values calculated by the two-dimensional method agree well with the results gained by the three-dimensional method for about 96% of the borehole length (less than 1% error in soil temperature). Therefore, it can be concluded that the two-dimensional method, having a comparatively lower computational time, is valid for calculating the temperature response of the soil around 96% of the borehole length.

The temperature response of the soil around multiple boreholes evaluated by the three-dimensional solution at various borehole depths is compared in Figure 7-11. It is shown that the temperature rise in the soil around the borehole decreases at the very end of borehole length where axial heat transfer effects come into play. The maximum amount of temperature rise due to thermal interaction of multiple boreholes in a six-month period of heat transfer from the borehole into the soil occurs in the middle of the borehole length (z=0). Therefore, with the objective of limiting boreholes' operations and sizes in order to prevent their thermal interaction, the middle length of the boreholes is the critical area. This is true when the heat flux from the borehole wall to the surrounding soil does not change significantly along the borehole length and the assumption of constant heat flux from the borehole wall is valid.

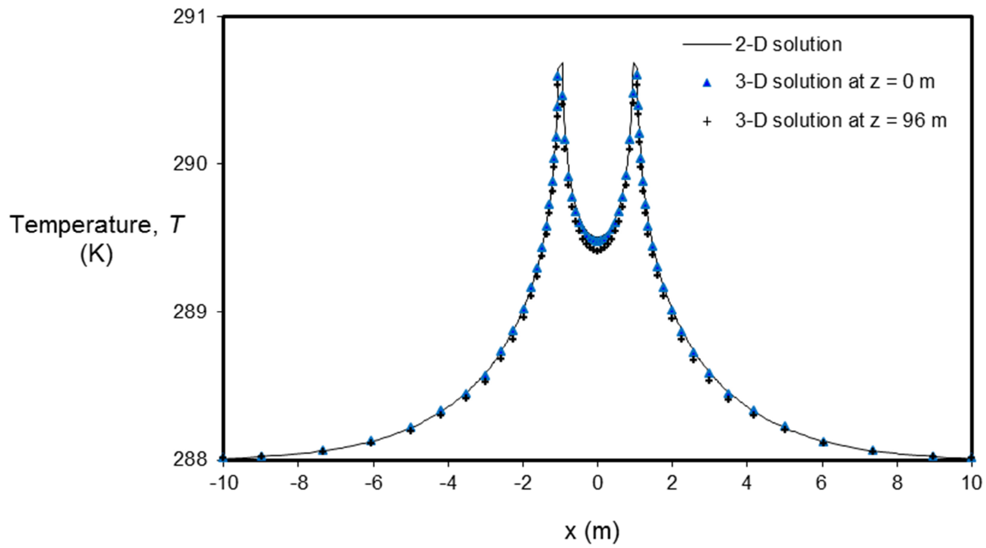

Figure 7-10 Soil temperature (K) around multiple boreholes at q''=10 W/m^2 and t=6 months, and comparison of the two-dimensional solution and the three-dimensional solution at various borehole depths.

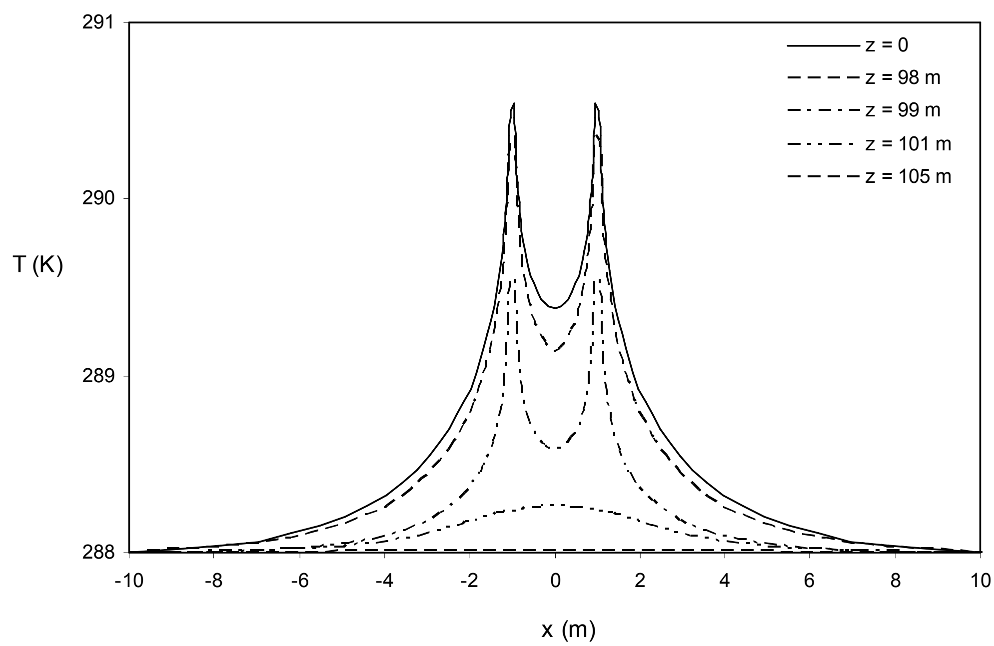

Figure 7-11 Soil temperature (K) around multiple boreholes at q''=10 W/m^2 and t=6 months, and temperature response of the soil at various borehole depths in the three-dimensional analysis.

In order to examine the validity of the two-dimensional results for a higher heat flux from the borehole wall, Figure 7-12 shows the results of a three-dimensional analysis for q''=20 W/m^2. It is seen that, although a larger temperature rise around the boreholes and a larger thermal interaction between them exist for this case, the temperature profile around the boreholes does not change in the middle of the borehole length (z=0 m) and until about 4 m away from the boreholes' top and bottom (z=96 m). Therefore, similar to the previous case (q''=10 W/m^2), axial heat transfer effects are negligible for about 96% of the borehole length and the two-dimensional analysis can be applied for temperature evaluation of the soil around the boreholes. It can be concluded that the length of the borehole for which axial heat transfer effects are negligible and two-dimensional analysis can be applied does not vary with the change in the amount of heat flux from the borehole wall into the soil.

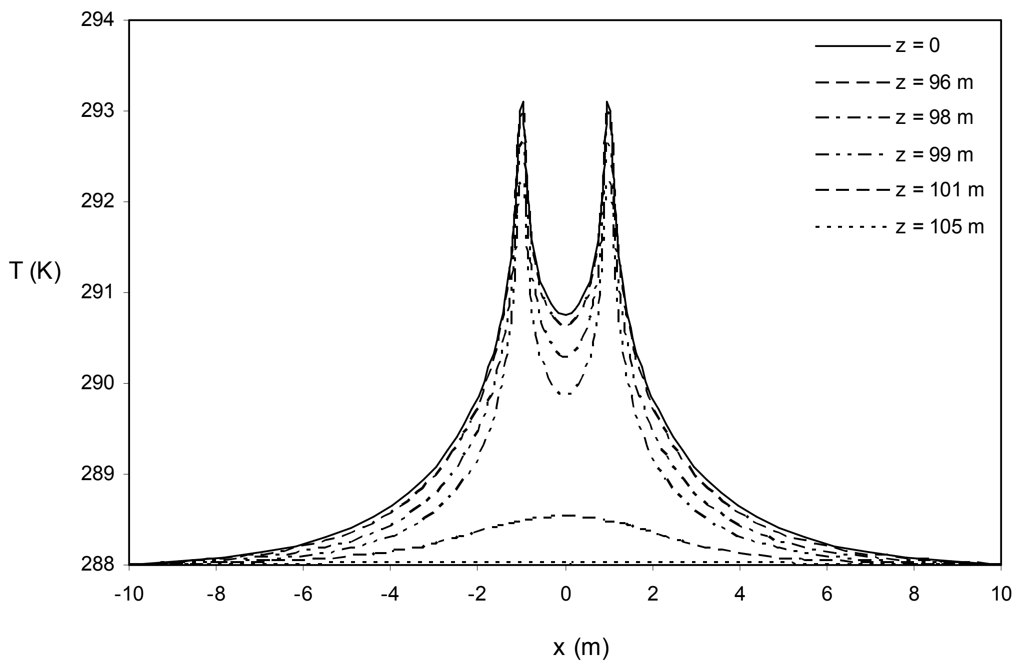

Figure 7-12 Soil temperature (K) around multiple boreholes at q''=20 W/m^2 and t=6 months, and temperature response of the soil at various borehole depths in the three-dimensional analysis.

7.1.4 Heat Flux Variation along the Borehole Length

A limitation in the models presented in the previous section is the assumption of uniform heat input along the borehole length to the ground, when the borehole is assumed as a line source of heat. In reality, however, the temperature and heat flux distributions on the borehole wall can only be decided by accounting for the heat exchange process between the tubes in the borehole and the borehole wall. A variable heat flux (VHF) along the borehole is calculated by defining the temperature profiles of the fluid running along the tubes in the borehole.

It should be noted that the current section focuses only on the variation of heating strength along the borehole length. Since only the existence of such a variation is intended to be discussed, the current section does not provide typical values for the borehole spacing and the heat flux on the borehole wall and lower values are chosen in order to keep the solution domain size smaller in the numerical solution. It should also be noted that the temperature of the soil at the borehole wall which is used in coupling the model inside the borehole with the one outside the borehole in the current problem is assumed to be constant throughout the whole operation time. Therefore, the current solution is only valid for low temperature variations in the soil surrounding the boreholes which is only gained by assuming lower heat flux values on the borehole wall. Modifying the current problem to one with typical industrial values for ground heat pump systems will need the soil temperature to be assumed variable and is subject of Section 7.3. Appendix D examines the importance of choosing a variable borehole wall temperature when coupling the models for inside and outside the borehole by using a method that updates this value at every time step and one that does not.

A three-dimensional model of transient conduction of heat in the soil around multiple GHEs is presented in this section. A domain consisting of two vertical borehole heat exchangers having a distance of D_b from each other is considered.

The temperature responses of the soil around multiple boreholes evaluated by the VHF model at various borehole depths are compared in Figure 7-13 and Figure 7-14 (a). It is shown in Figure 7-13 that the maximum temperature rise due to thermal interaction of multiple boreholes in a six-month period of heat transfer from the borehole into the soil occurs at the top 3% heating length of the borehole and it decreases along the borehole length as the heat flux from the borehole wall into the soil decreases. Therefore, with the objective of limiting boreholes' operations and sizes in order to prevent their thermal interaction, the top length of the boreholes (about 3% total length) is the critical area. Also, as expected the maximum temperature rise in the soil occurs at the borehole wall (x=0.95 m and x=1.05 m).

Since the current study is not using typical conditions such as typical values for borehole spacing, heat flux on the borehole wall, etc., a minimum value of spacing is not suggested in this study. An extension of the current study to typical industrial values may require the assumptions of constant borehole wall temperature and constant ground surface temperature made in the current model to be modified to be variable and is subject of ongoing research by the authors. In such a case, using the current solution method, it is possible to gain a minimum value of spacing or maximum amount of heat input to the ground to avoid thermal interactions between boreholes under typical conditions.

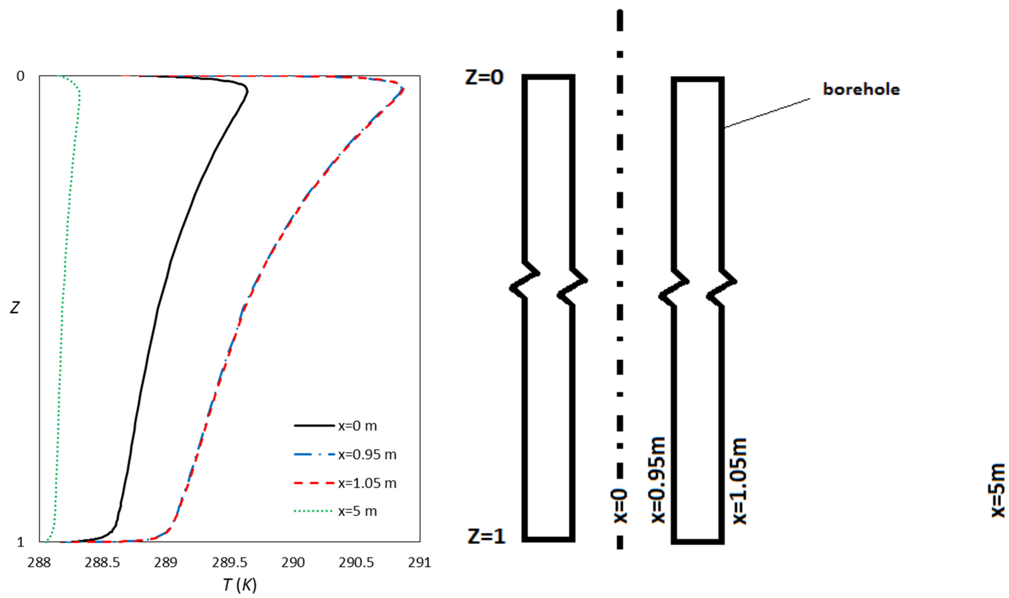

Figure 7-13 Soil temperature (K) around multiple boreholes in *xz* plane in *t*=6 months, at various distances from borehole wall for VHF model.

It is shown in Figure 7-14 (a) that the thermal interaction between the boreholes is at its minimum at the bottom of the borehole (z=-99.9 m) where the heat flux to the soil is lowest. This is not true for the case of constant heat flux from the borehole wall to the surrounding soil along the borehole length [Figure 7-14 (b)]. It is seen in Figure 7-14 (b) that the greatest thermal interaction occurs at top of the borehole, but remains at its maximum amount along the borehole length. For this case, the critical length of the borehole would be almost 95% of the borehole length. However, as discussed earlier, the case of constant heat flux is only a simplification to the VHF problem and does not present the problem as accurate as the VHF problem. Note that in order to compare the results gained by constant heat flux model with the results gained by the

VHS model, an equivalent inlet temperature ($T_f' = 290.6\,\mathrm{K}$) for the VHS model, resulting in the same total heat conduction in the soil, can be assumed. The total heat flow rate is calculated by integrating the heat flow rate along the borehole.

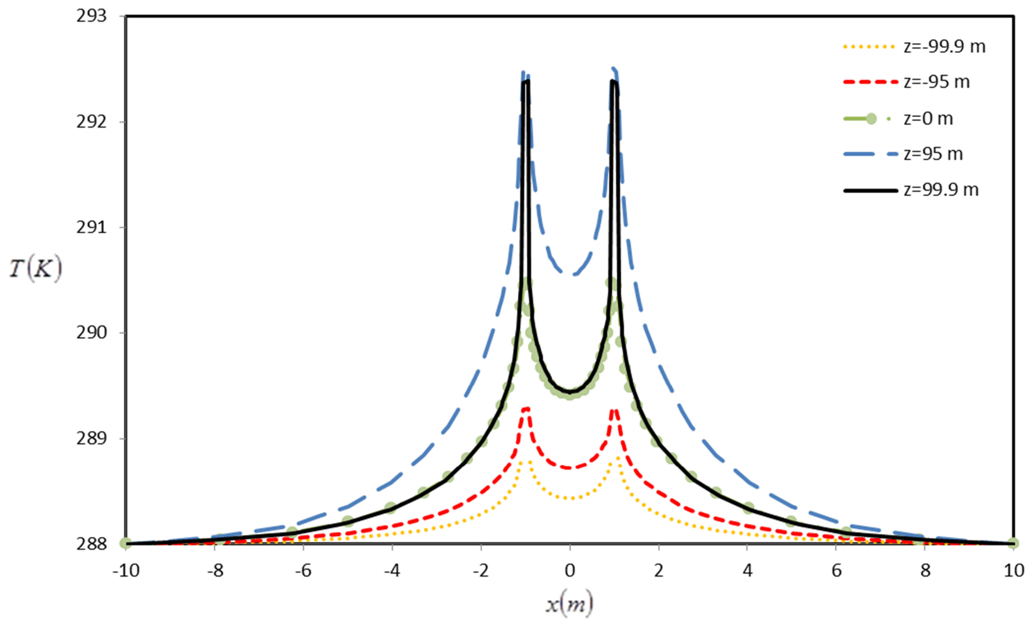

(a)

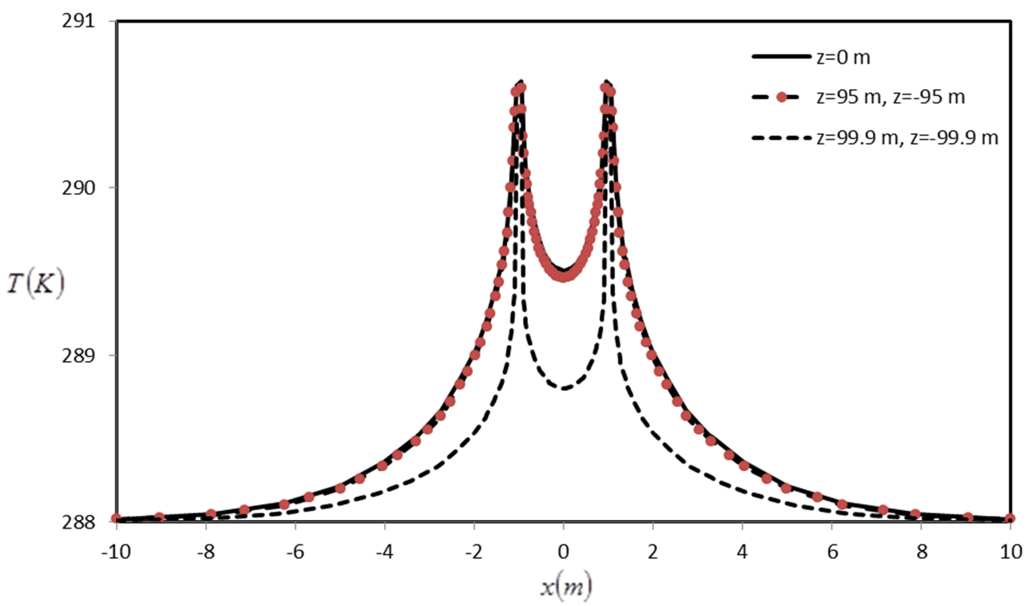

(b)

Figure 7-14 Soil temperature (K) around multiple boreholes in t=6 months, at various borehole depths for (a) VHF model, and (b) constant heat flux model.

Another notable characteristic of Figure 7-14 is the decrease in the thermal interaction in the lengths of z=99.9 m when one moves from z=95 m towards the top end of the borehole. Specifically for the case of VHF (Figure 9a), there is higher heat flux as one moves towards the top end and one expects greater thermal interactions. In both cases, the temperature rise in the soil around the borehole declines at the very end of borehole length, and this can be due to axial heat transfer effects which become notable only at the very ends of borehole lengths.

The results of the VHF model and constant heat flux model are compared in Figure 7-15. It is seen in Figure 7-15 (a) that the assumption of constant heat flux on the borehole wall introduces numerous inaccuracies especially when dealing with the temperature rises in the soil at the very top and bottom of the borehole. Figure 7-15 (b) shows that, by using varying heat flux method, the heat flux on the borehole is spread along the borehole in a way that the middle area remains similar to its average amount. It can be concluded that using the constant heat flux method is only valid for the middle length of the boreholes and moving any further to the top or bottom of the borehole, the temperature rises evaluated become increasingly inaccurate. Quasi-three-dimensional models reveal drawbacks of two-dimensional models and are thus preferred for design and analysis of GHEs, as they provide more accurate information for performance simulation, analysis and design.

It should be noted that the effect of temperature rise due to one borehole on the other is neglected by applying the superposition method. This effect is examined for a two-dimensional numerical domain in Section 7.1.1 by comparing the results of the numerical solution with analytical results of line source theory where the superposition method is used to account for the temperature rise in the soil surrounding multiple boreholes. It was shown that these effects are minor in comparison to the order of the temperature rise in the soil due to the individual performance of the boreholes. Since the objective in the current section is to examine at what depths the thermal interaction among boreholes creates a critical temperature rise, the focus is mostly on introducing a heat flow rate profile along the borehole length which can be coupled to the numerical or line source model outside the borehole to show the effect of varying heat flux along borehole length on temperature rise in the soil. In Figure 7-16, comparison is made between the two methods and it is shown that the temperature rise in the soil caused by both methods agree well. Therefore, it can be concluded that the results of analytical method presented Section 5.3.1 can present as accurate results as a numerical method.

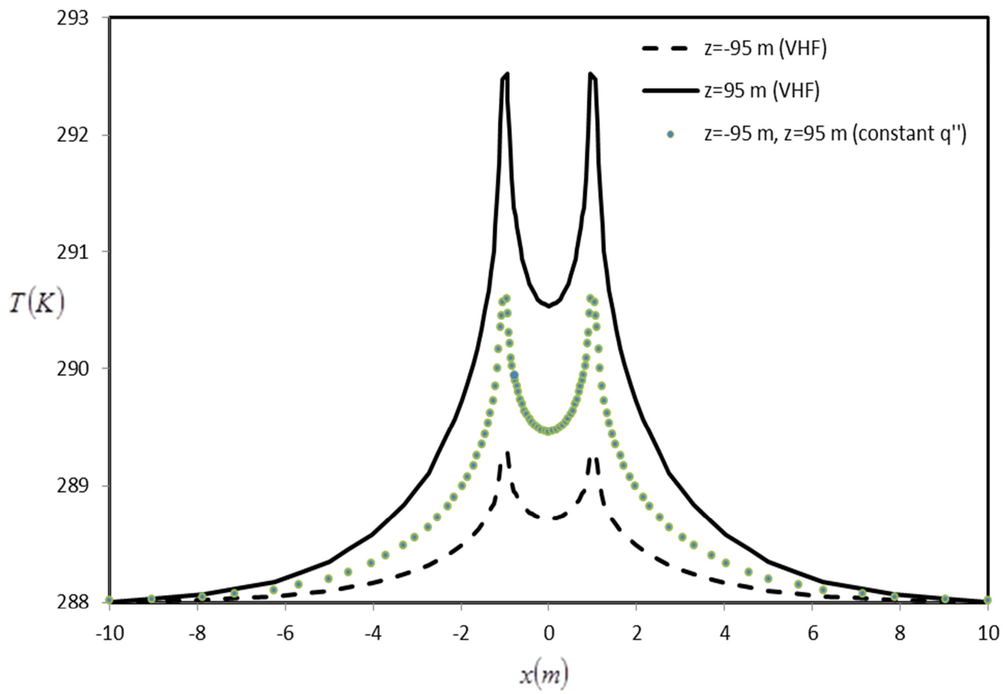

(a)

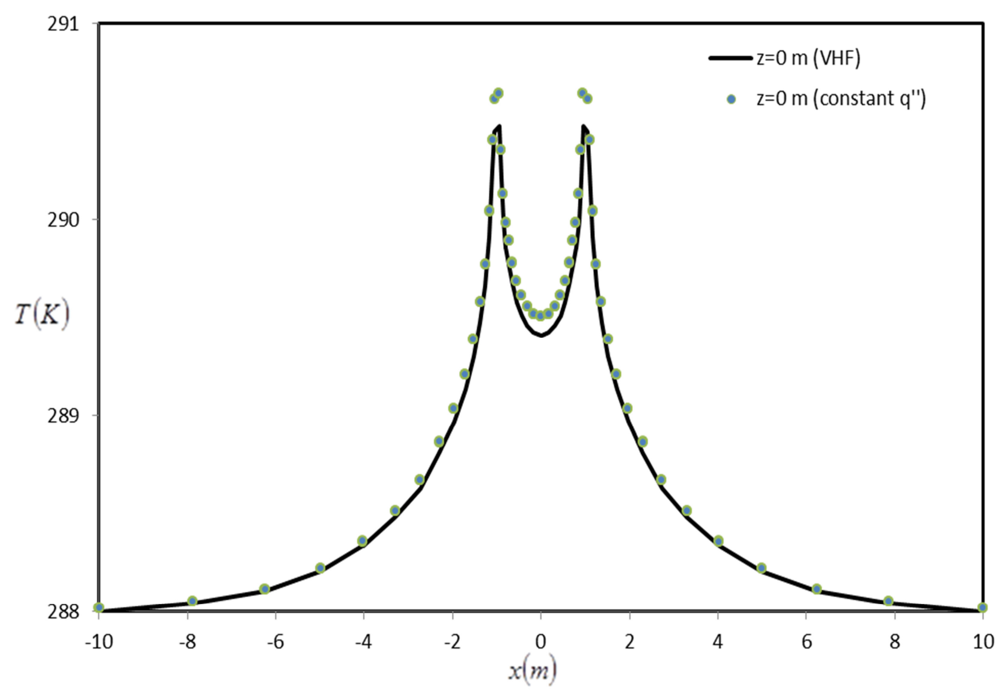

(b)

Figure 7-15 Comparison of soil temperature (K) around multiple boreholes at t=6 months for VHF and constant heat flux models, at (a) z=95 m and z=-95 m, and (b) z=0 m.

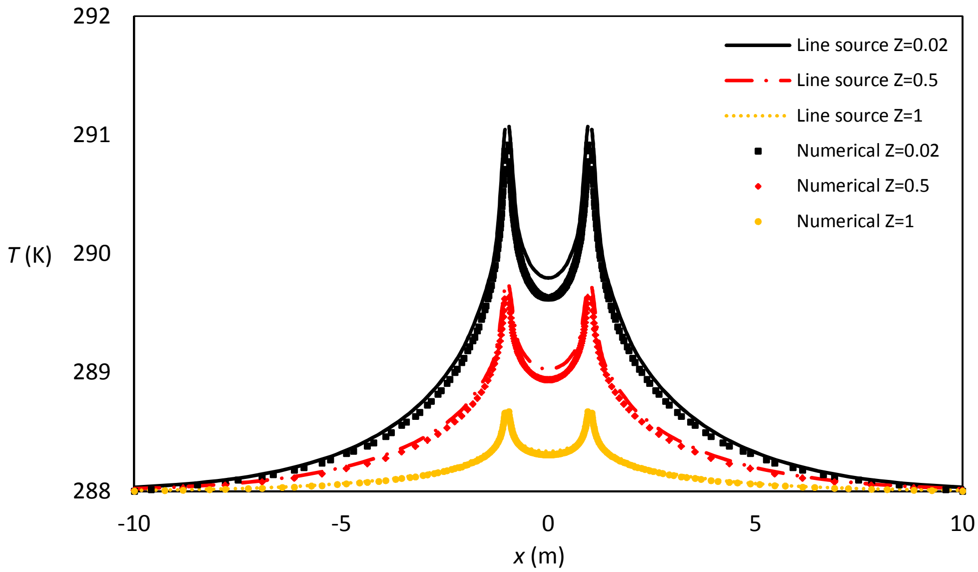

Figure 7-16 Soil temperature (K) around multiple boreholes in t=6 months for line source and numerical models at various borehole depths.

7.1.5 Impact of Soil Thermal Conductivity Sensitivity

Thermal characteristics of the soil play an important role in evaluating heat flows in the soil surrounding a borehole. One property that can affect the conduction of heat in the soil surrounding the boreholes is the soil thermal conductivity. In order to study the variation of temperature rise at the borehole wall with soil thermal conductivity, various types of soil are considered in this section (Table 7-1). In the figures in this section, the variation in temperature of certain points in the soil with various thermal conductivities is presented.

Table 7-1 Soil thermal characteristics

Property	Soil type 1	Soil type 2	Soil type 3	Soil type 4
Thermal conductivity, k (W/mK)	1.0	1.5	2	2.5
Specific heat (J/kgK)	1550			
Density (kg/m^3)	1950			

A two-dimensional model of transient heat conduction in the soil around multiple ground heat exchangers is presented in this section. A domain consisting of several borehole systems, each consisting of 16 vertical boreholes is considered (Figure 7-17). The borehole systems are placed at every 100 m and the boreholes are installed at 6-meter distances.

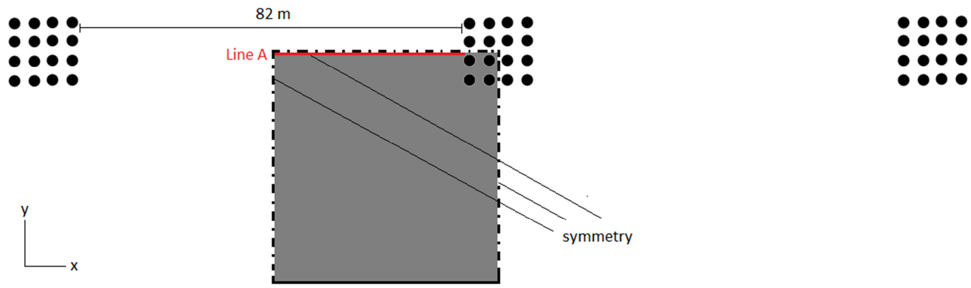

Figure 7-17 Solution domain.

Due to the periodic climate changes, the ground heat load profile for each borehole is expected to be periodic. Here, it is assumed that the ground load profile is modeled as a simplified sinusoidal profile delivering/removing a maximum of 30 W/m of heat (Figure 7-18). This heat flow rate per unit length of the borehole is within the range of the heat flow rates that are often chosen by system designers. Using this heat boundary at the borehole wall, the temperature of the soil surrounding the boreholes can be determined using a finite volume method. Details of this method and the geometry of the solution domain can be found in Appendix B.3.

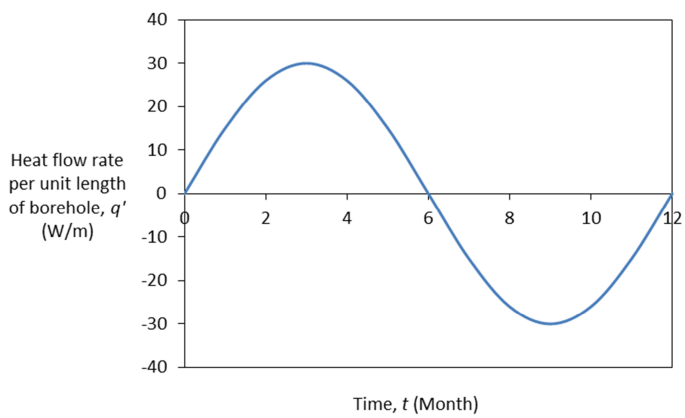

Figure 7-18 Heat flow rate at the borehole wall.

The temperature at the borehole wall of Borehole 4 (Figure 7-24) is chosen as a representative of the temperature at the four boreholes and its variation with time for various soil thermal conductivities is shown in Figure 7-19. It is seen that the temperature variations at the borehole wall are periodic. This is expected since the ground heat flow at the borehole wall varies periodically. It is also noticed that for soils with higher thermal conductivity, the temperature of the soil at the borehole wall is lower in the ground heat delivery mode and higher in the ground heat removal mode. This is due to the ability of soils with higher thermal conductivity to conduct heat than to store it. An example of a soil with high thermal conductivity is soil that contains pieces of rocks which has a high thermal conductivity. On the other hand, soils containing air gaps are not good conductors of heat; therefore, a borehole installed in such soil types may experience a higher temperature at its wall in the heat delivery mode and a lower temperature at the borehole wall in the heat removal mode. For higher heat pump efficiencies, lower temperatures at the borehole wall in heat delivery mode and higher temperatures at the borehole wall in the heat removal mode are preferred. Therefore, a heat pump couples with boreholes that are installed in soils with a higher thermal conductivity are expected to have a higher efficiency. This is discussed in more detail in Section 7.3.

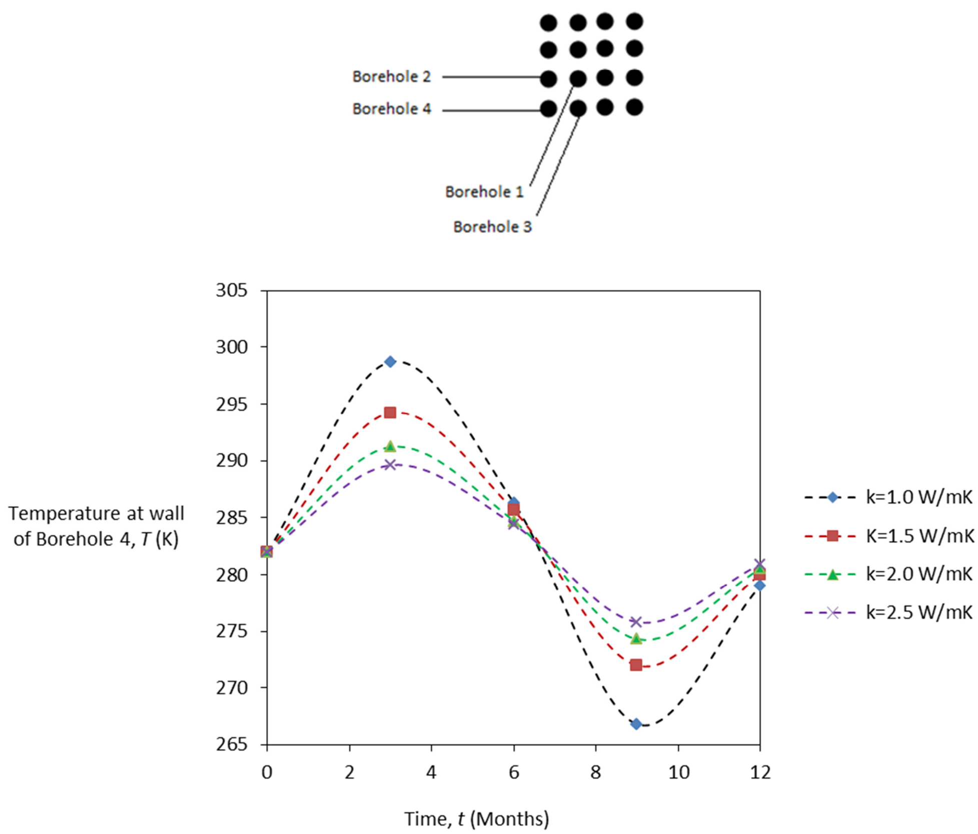

Figure 7-19 Variation of the temperature of the borehole wall with time.

Figure 7-20 shows the temperature on an arbitrary line, Line A in Figure 7-17, after three and nine months of system operation. These two times are chosen since the ground heat delivery/removal peaks at these times and it is expected that noticeable temperature rises occur at these times. By observing soil temperatures on Line A, the size of the soil area outside the borefield experiencing temperature rise can be determined. It is seen in Figure 7-20 that boreholes that are installed in soils with higher conductivity can cause temperature rise in a larger area of soil surrounding them in their yearly operation. This could mean that a borehole that is installed in a more conductive soil could have larger negative impacts on its surrounding sensitive systems than a borehole installed in soil with lower thermal conductivity. Observing the temperature contours in the soil surrounding the boreholes that are shown in Figure 7-21 and Figure 7-22 could give a better understanding of the above statements. It is seen that although thermal conductivity of the soil does have a noticeable effect on the temperature rise in the soil surrounding the borehole, the change in the size of the soil area surrounding the boreholes that experience a temperature rise of over 0.1 K is less that 3 m in the current case. To complete this discussion, a long-term study of the system should be performed to examine the growth of the soil area experiencing a temperature rise over few years. This is discussed in more detail in Section 7.2.

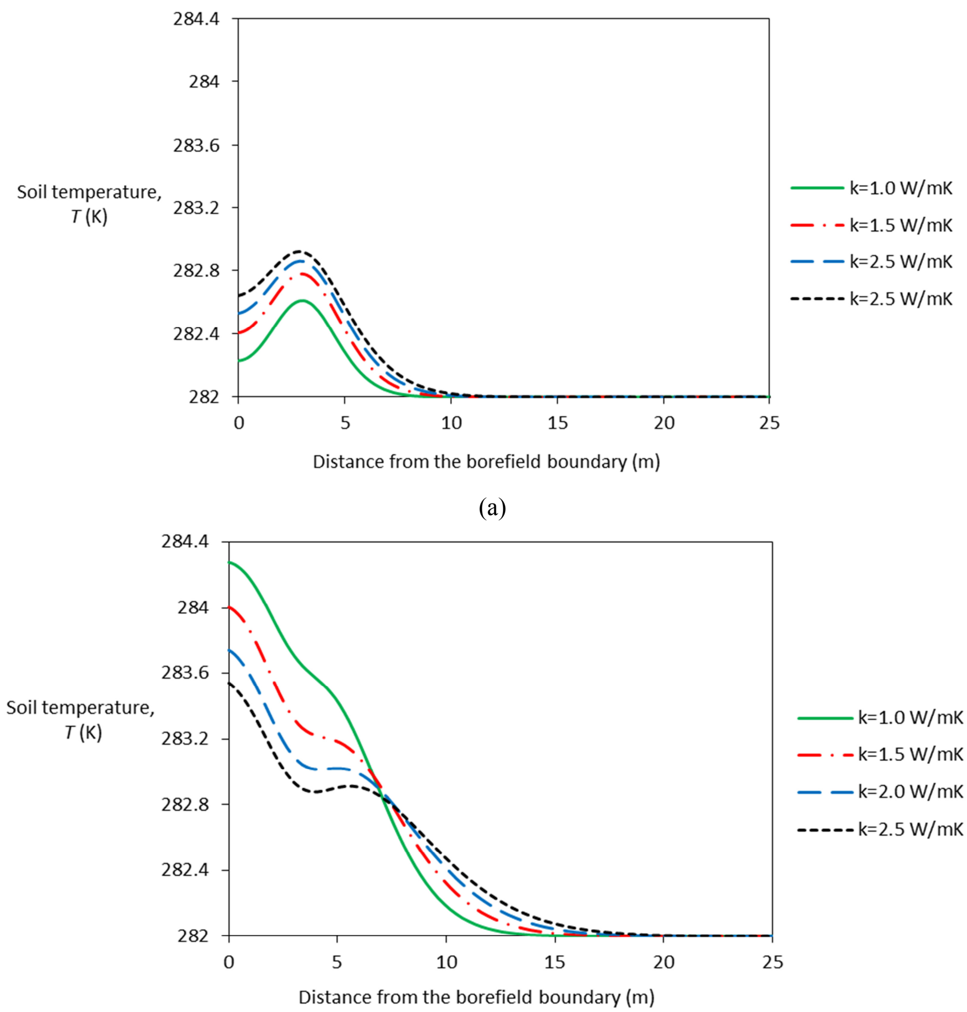

(b)

Figure 7-20 Soil temperatures outside of borefield boundary after (a) 3 months and (b) 6 months of system operation.

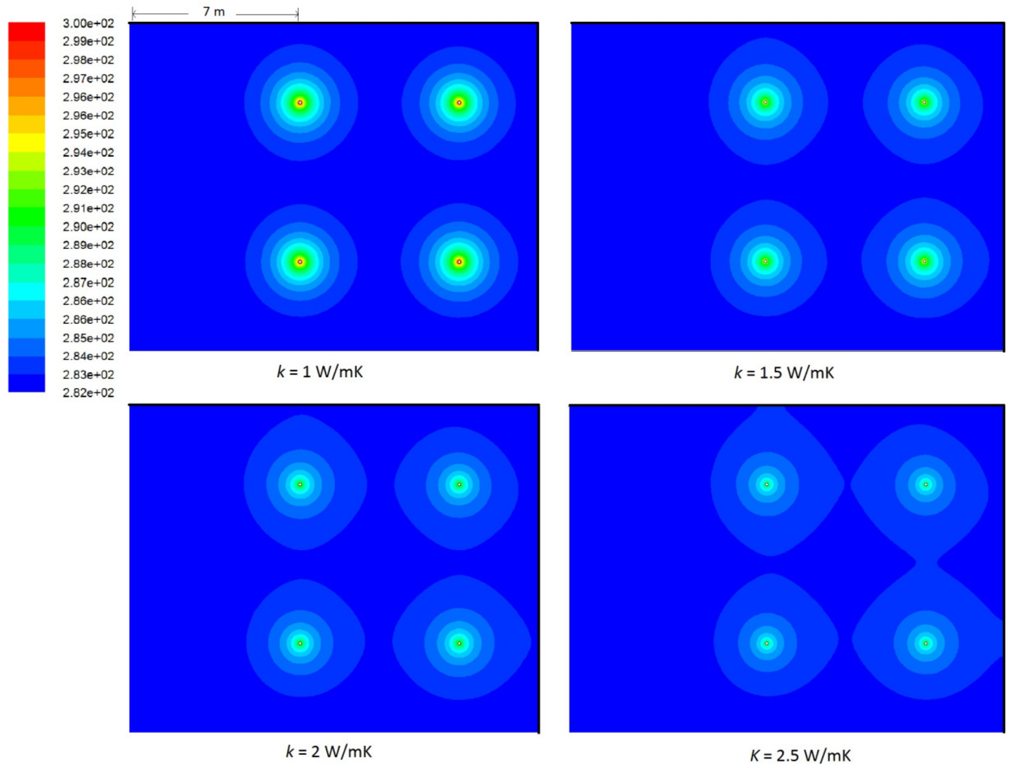

Figure 7-21 Soil temperatures contours after 3 Months.

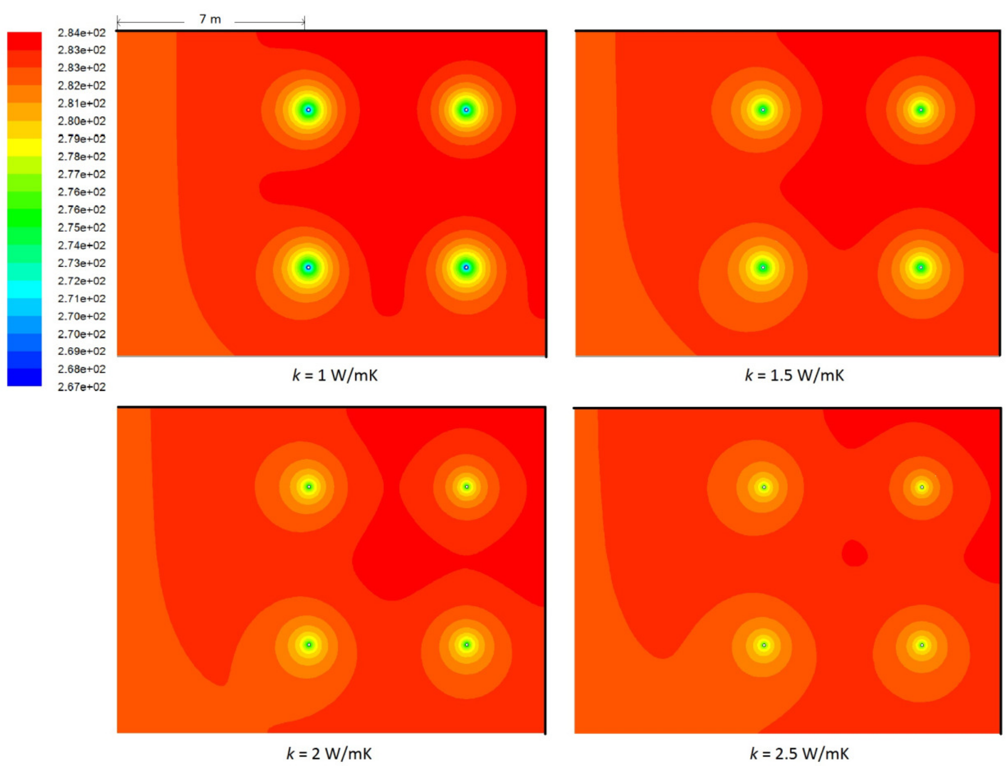

Figure 7-22 Soil temperatures contours after 9 Months.

7.2 Long-term Environmental Effects

In evaluating the temperature rise in the soil due to installation of GHEs, a key step is to define the heat flux from the surface of the heat exchanger to the soil. This can be very complicated due to the dynamic nature of the heat transfer from the fluid flowing in the U-tubes within the borehole to the borehole wall. For simplicity, the U-tube configuration in the borehole is not simulated in the model and the boundary condition at the borehole wall is set to the heat flux. This is done since, when studying the heat flows in the soil surrounding the boreholes and their possible negative effect of the eco systems near the system, their inner dynamic heat exchange processes can be of second priority compared to the heat dissipation in the soil surrounding them. Furthermore, it is assumed that the inlet temperature of the circulating fluid running in the U-tube inside the borehole will be adjusted according to the building heating needs. The transient nature of geothermal systems responding to the needs of buildings is discussed in a case study here. The weather annual periodic variation is correlated with the heat flux at the wall of the heat exchanger, here, at the borehole wall (Figure 7-23). The details of calculation of the ground heat load profile are included in Appendix C. In the heat flux profile, and the heat flux profile is balanced, i.e. the total amount of heat delivered to the soil in the cooling period is the same as the heat that is removed in the heating period. This assumption is made since, in the design stage of these systems, they are aimed to have a balanced heat flow profile in order to avoid temperature rise or drop after the their yearly cycle due to an unbalanced heat flux. Since it was shown in Section 7.1.3 that using results of a two-dimensional model are valid for analysis of heat flows in the soil surrounding the borehole, a two-dimensional model of transient heat conduction in the soil surrounding multiple GHEs is presented in this section. A domain consisting of several borehole systems, each consisting of 16 vertical boreholes, is considered (Figure 7-24). The borehole systems are placed at every 100 m and the boreholes are installed at 6-meter distances.

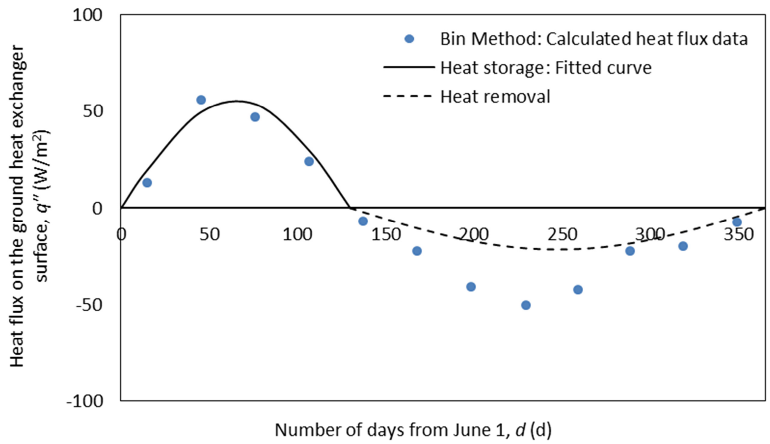

Figure 7-23 Variation of heat flux on the ground heat exchanger wall.

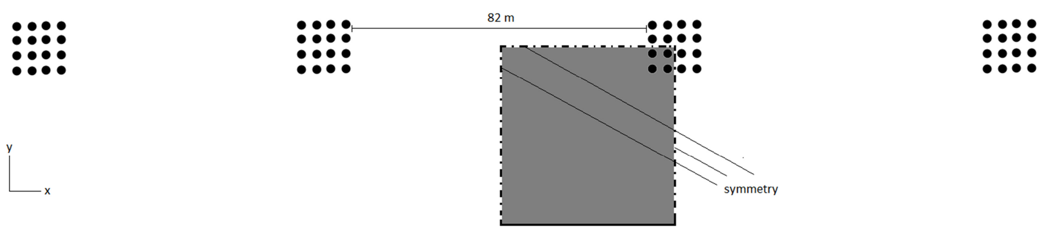

(a)

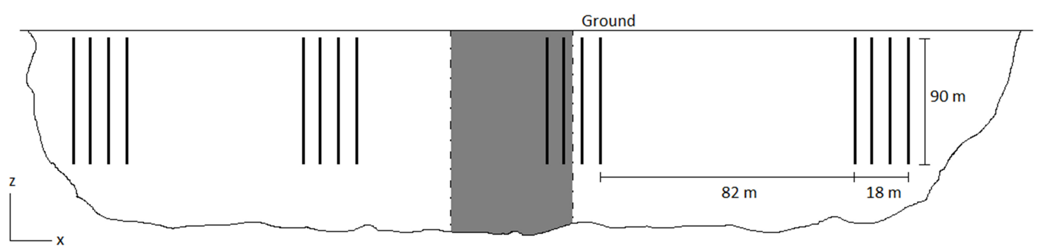

(b)

Figure 7-24 Solution domain: (a) horizontal cross section (*xy*), and (b) horizontal cross section (*xz*).

The annual temperature variations of the borehole wall for the four boreholes are shown in Figure 7-25. It is seen that the temperature response of the borehole wall for the different borehole placements does not vary greatly (i.e., variations are less than 0.2%). This might be due to the stronger dependence of the borehole temperature on the heat flux on the wall than borehole placement. The slight variation that is noticed between the temperature rise of the boreholes is due to their relative location. The boreholes that are surrounded by other boreholes (Borehole 1) experience a slightly higher temperature in the heat delivery mode and, therefore, their temperature drop in the heat removal mode is lower than other boreholes. Comparing the temperature variations with the heat flux variations in Figure 7-23, it is noticed that the temperature variation of the borehole wall has some similarities to the transient variation of the heat flux with its maximum and minimum values being in the second and ninth months, respectively.

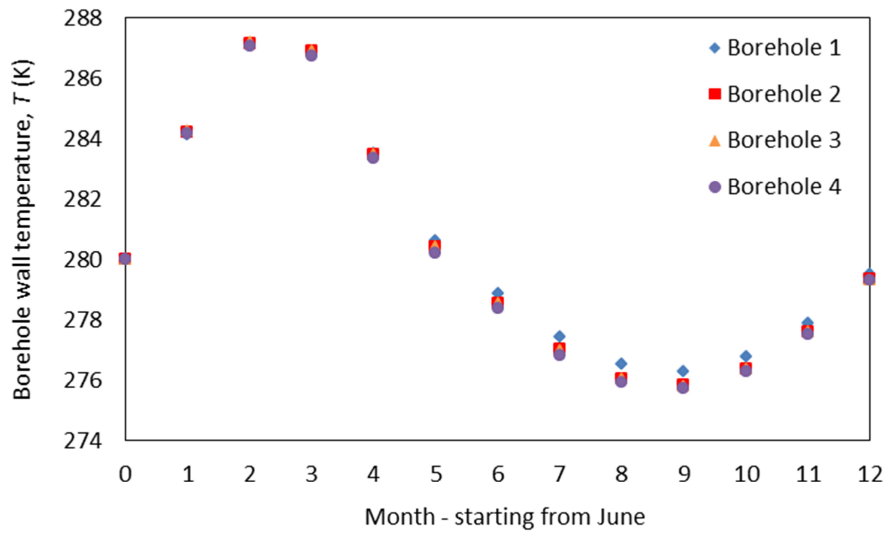

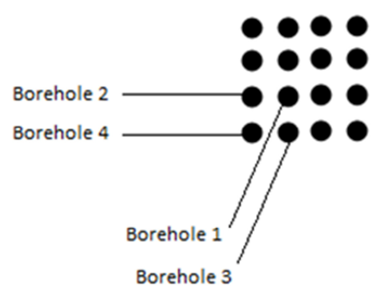

Figure 7-25   Annual temperature variations of the borehole wall.

Figure 7-26 shows the temperature contours in the soil surrounding the boreholes for one year. It is seen that the maximum temperature occurs in the soil immediately outside of the borehole wall and when the heat flux is at its maximum. Furthermore, it is noticed for the current problem that the thermal plume from the system reaches its furthest extent at the end of Month 10.

The temperatures for the two symmetry lines which intersect in the center of the system (Figure 7-24) are shown in Figure 7-27. Figure 7-27 shows the soil temperature outside the borefield on the two symmetry lines that intersect in the centre of the borefeild: one that goes towards another borefield (symmetry y=0) and one that goes towards farfield (symmetry x=0). It is seen that considering temperature rises of no more than 0.2ºC in the soil, the thermal plume in the soil caused by the system extends about 10 m from the outer edge of the borefield (x=9 m) and does not have any interaction with its neighboring system. It can be concluded that, if the borehole spacing and the distance of neighboring borehole systems are kept at a certain distance, for a certain amount of heat flux, here given in Figure 7-23, there should not be any thermal interaction between neighboring systems nor should there be any thermal plume flowing away from the system.

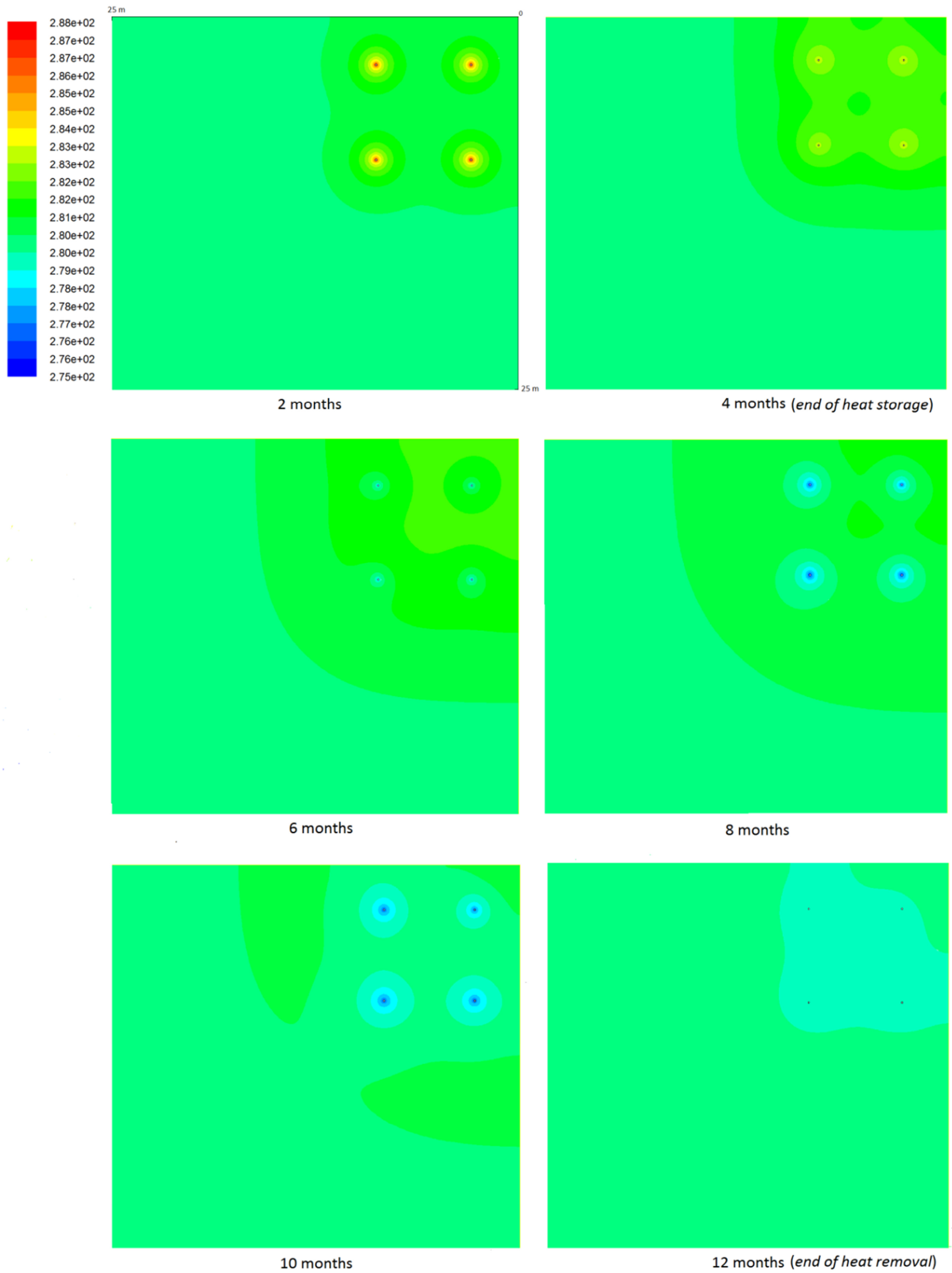

Figure 7-26 Temperature contours in the soil surrounding 4 of the 16 boreholes in the system (the holes surrounded with the highest temperature gradient shown in the figure) in Year 1 (Note: 4 boreholes are shown here due to symmetry.)

It is also observed in Figure 7-27 that the temperature of the soil is reduced by about 0.2ºC at the borefield boundary, followed by a temperature rise of 0.3ºC in the 10-meter region outside of the borefield. The temperature rise is due to heat conduction in the soil, which extends to about 10 m outside the borefield even after the heat exchanger heat injection phase. When the heat extraction phase begins at the beginning of the fifth month, the temperature of the soil immediately beyond the borehole wall reduces to about 4ºC and, therefore, the direction of the heat conduction in the soil changes towards the borefield resulting in a temperature drop in the borefield and around it.

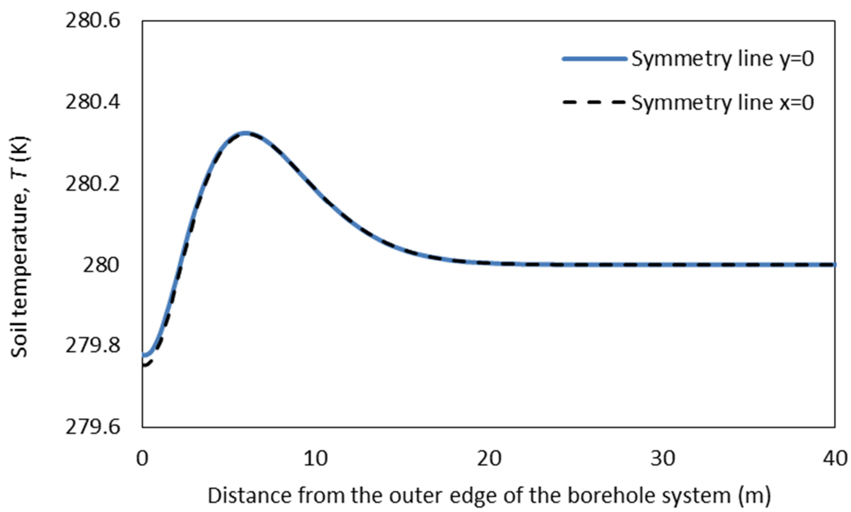

Figure 7-27 Soil temperature outside the borehole field after 10 months of system operation.

Figure 7-28 shows borehole wall temperatures for Borehole 1 and Borehole 4 during a three-year period of heat storage and removal. It is seen that the temperatures of the borehole walls fall on the same path every year. It can be concluded that for a balanced system where borehole spacing, system spacing and the heat flow rate per unit area are kept at the recommended values and there is no temperature rise or fall after the first year of system performance, there should not be any accumulation of heat in the long term if the same heat storage and removal pattern is followed every year. Even the smallest amounts of temperature rise or fall in the soil after the first year operation can result in unacceptable temperature changes in the long term (Figure 7-29). Figure 7-29 shows the effect of the minor temperature reduction in the soil after the first year operation over five years. It is seen that the temperature at the borehole walls reduces every year and it is estimated that this pattern can affect the heat pump operation over the system's lifetime.

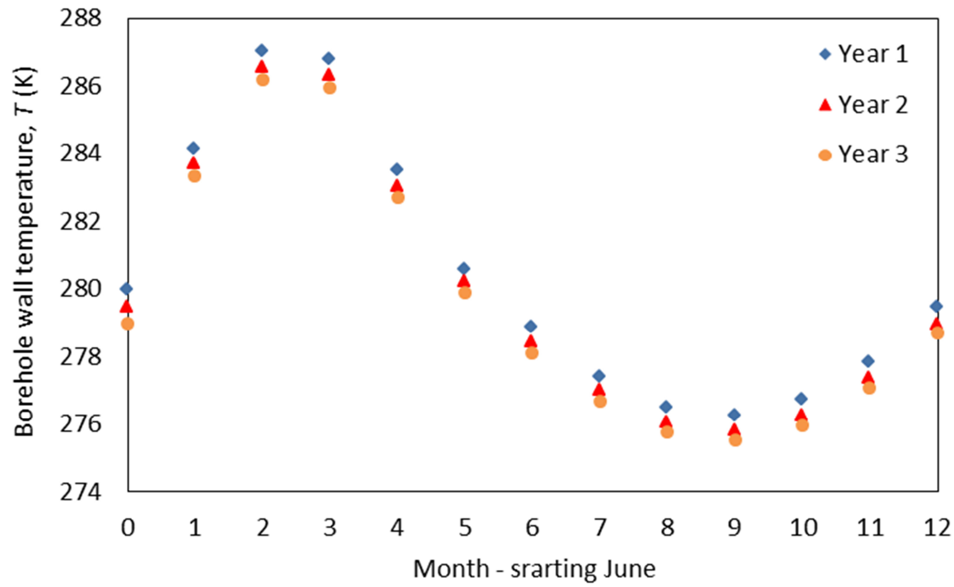

(a)

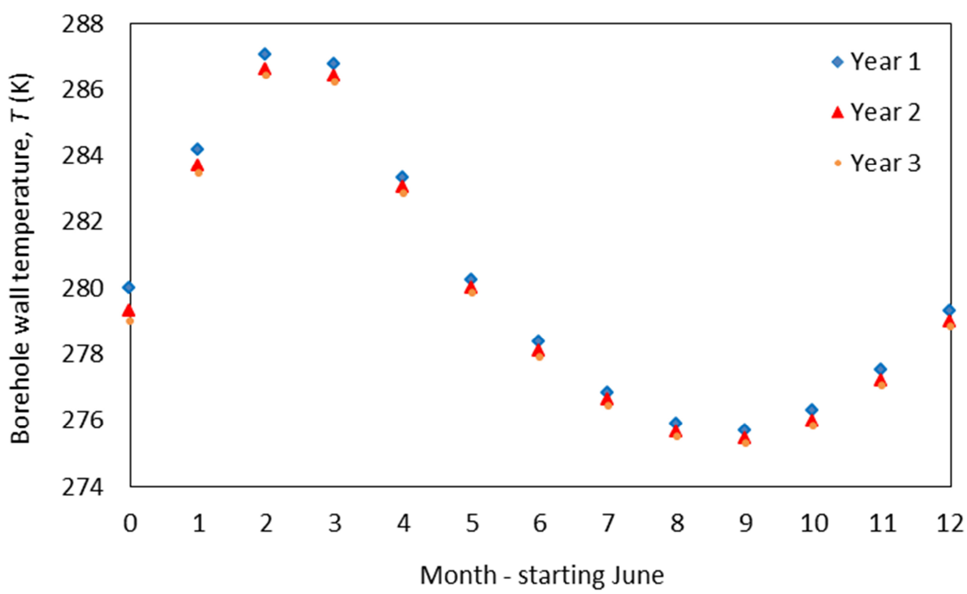

(b)

Figure 7-28 Borehole wall temperatures: (a) Borehole 1, (b) Borehole 2.

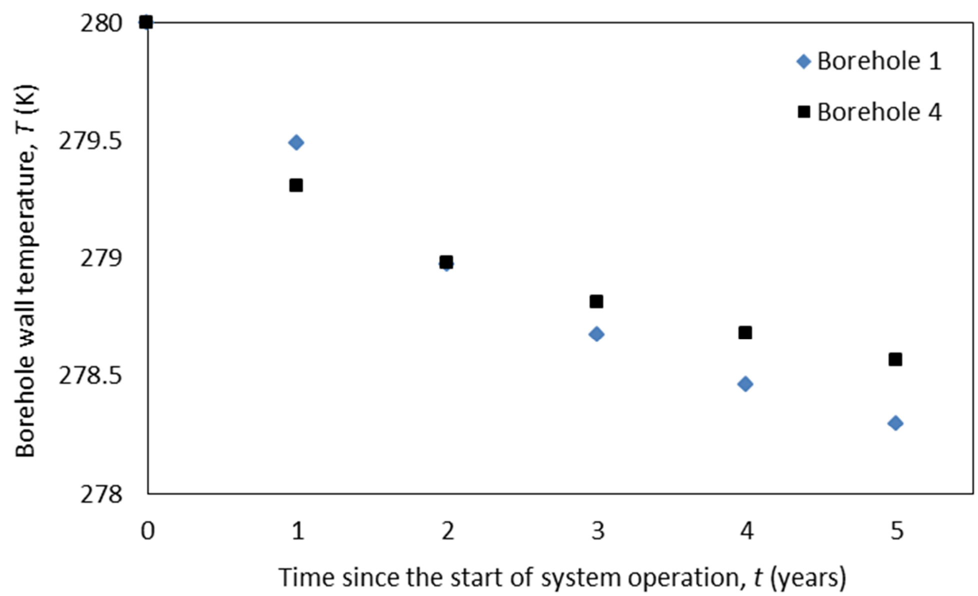

Figure 7-29 Borehole wall temperatures of Borehole 1 and Borehole 2 over five years of system operation.

Figure 7-30 shows the temperature contours in the soil surrounding the boreholes at the end of every year in a 5-year period. It is seen that all the heat is stored in the ground, is collected through the GHE. In this case, a small amount of extra heat is also collected which causes a slight temperature reduction in the soil at the end of the first year. This temperature reduction adds up every year and will be doubled by the end of the fifth year of system operation. It can be concluded that even the slightest amount of excess heat storage or removal, which in some cases can be noticed after the first year operation, can cause a temperature rise or reduction in the long term and affect the sustainability of the system. However, no significant heat escape is noticed in the case of the current balanced system. This effect is also noticed in a recent study by Wang et al. (2012). In their study, there was a slightly more heat extraction from than injection into the borehole heat exchanger than required to keep the heat storage and removal in the ground balanced. Consequently, the temperature of borehole heat exchanger reduced very slightly year over year (0.8ºC after 15 years).

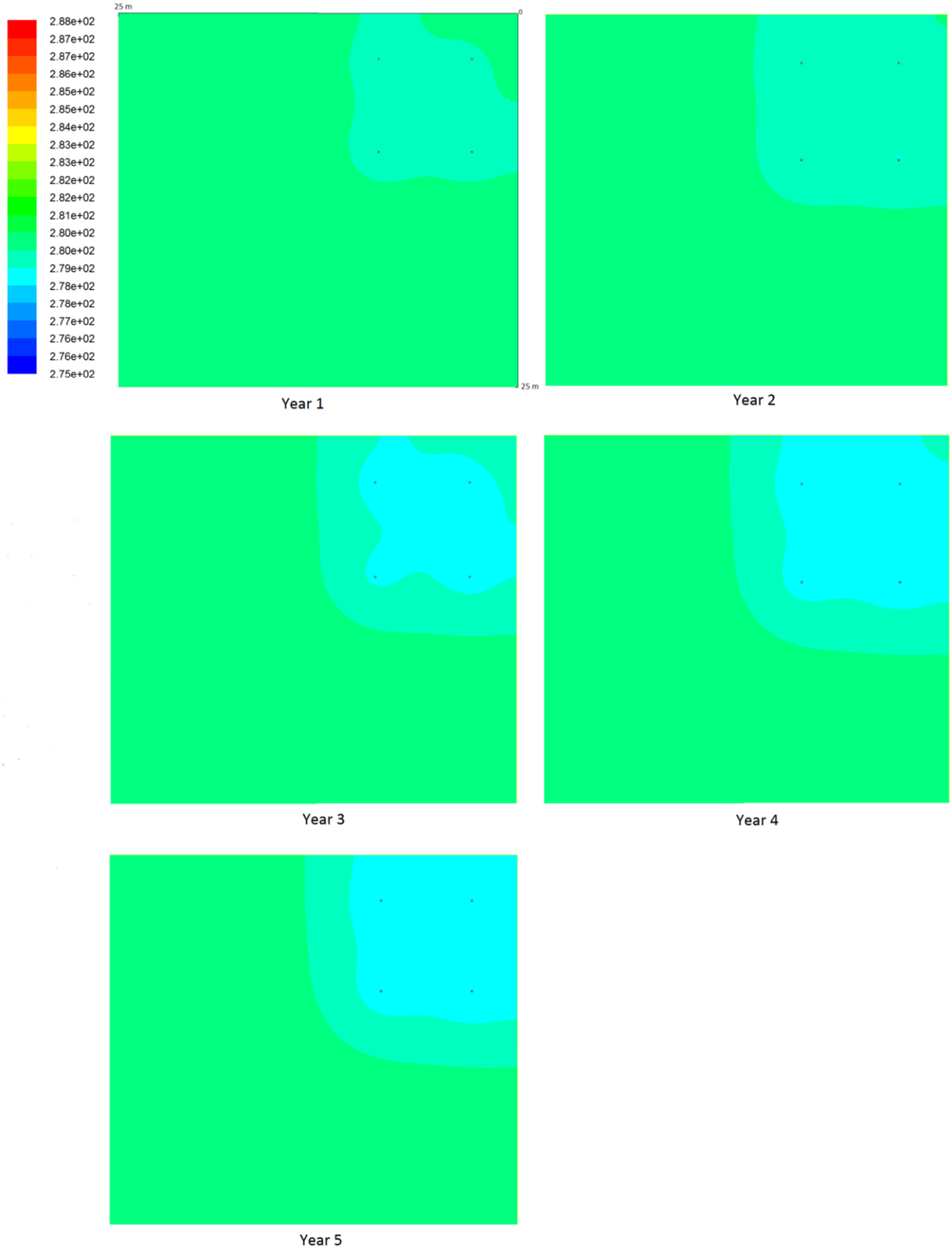

Figure 7-30 Temperature contours in the soil surrounding 4 of the 16 boreholes in the system (the holes surrounded with the highest temperature gradient shown in the figure) in Year 1 to 5. (Note: 4 boreholes are shown here due to symmetry.)

7.3 Thermal Interaction

One limitation in the previous models is using a heat flux boundary condition on the borehole wall. As mentioned previously, it is assumed that the inlet temperature of the fluid circulating in the U-tube inside the borehole will be adjusted according to the ground heat load. Since the circulating fluid temperature is one of the key parameters in the heat pump operation and efficiency, it cannot be adjusted to values that result in low efficiency of the heat pump. Using a heat flux boundary condition can cause the temperature of the ground to rise infinitely without a stop in system operation. In reality, if the temperature of the soil surrounding a borehole becomes close to or higher than the inlet temperature of the circulating fluid exiting the heat pump, the system will not be able to deliver the desired heat to the ground and will automatically stop operating until the heat around it is dissipated away and the temperature drops to a lower value. In order to overcome such a limitation, the periodic heat boundary on the borehole wall can be replaced with a temperature boundary or the heat boundary that is related to the running fluid temperature and can be updated at short time steps with respect to the soil temperature. This is possible if the heat transfer model for outside of the borehole is coupled to the model inside the borehole.

In this section, some of the results of the analytical model, that is presented in Section 5.3.2 are discussed and validated with a finite volume numerical method (Chapter 6). The results are for two neighboring boreholes based on some typical properties given in Table 4-1. There are studies in the literature that focus on methods to find optimum system specifications such as optimum mass flow rate or borehole length (Li and Lai 2013). The ground load profile is modeled as a simplified sinusoidal profile (Figure 6-6).

Figure 7-31 shows the change in the borehole wall temperature and running fluid inlet and outlet temperature with the heat load profile that is shown in Figure 6-6. It is seen that as the system experiences a periodic profile of ground heating and cooling load (Figure 6-6), the temperature of the borehole wall also experiences a periodic profile with a time lag; the maximum temperature of the borehole wall occurs some time after maximum heat input in the soil. This is due to the thermal capacitance of the borehole grout that results in a slower response to the change in its thermal environment. In the analytical method, the change in the borehole wall temperature with time sets a new temperature for the running fluid inlet and outlet temperature in order to deliver/remove a required heat load to/from the ground. It is seen that the difference between the running fluid inlet and outlet temperature varies over time. This is due to the variable ground heat profile of the borehole. Comparison between the analytical and the numerical results for the borehole wall temperature and the running fluid inlet and outlet temperature shows error of less than 1% using the following relation for calculation of error.

$$Error = \frac{T_{numerical} - T_{analytical}}{T_{numerical}} \tag{7-1}$$

The error noticed in the results of borehole wall temperature could be due to the simplifying assumptions in the analytical approach such as heat transfer from a line source of heat to the surrounding soil. In this assumption, the thermal properties of grout in the borehole are not accounted for when calculating the borehole wall temperature. Instead, to estimate the borehole wall temperature at R=0.1 m, it is assumed that the line source of heat is surrounded by soil from R=0 up to R=R_b=0.1 m. Due to the small errors involved in the estimation of the borehole wall temperature and the inlet and outlet running fluid temperature, it can be concluded that the analytical approach is capable of coupling the soil temperature to the running fluid temperature when the ground load is known.

In the numerical approach, the temperature of the running fluid at the exit is calculated at every time step and a new temperature for the running fluid inlet temperature is set according to the required ground heat load for the next time step. In this approach, since the temperature of the inlet fluid is updated one time step after the outlet fluid temperature is calculated, the time steps should be chosen small enough so that the change in the inlet running fluid temperature is kept relatively small.

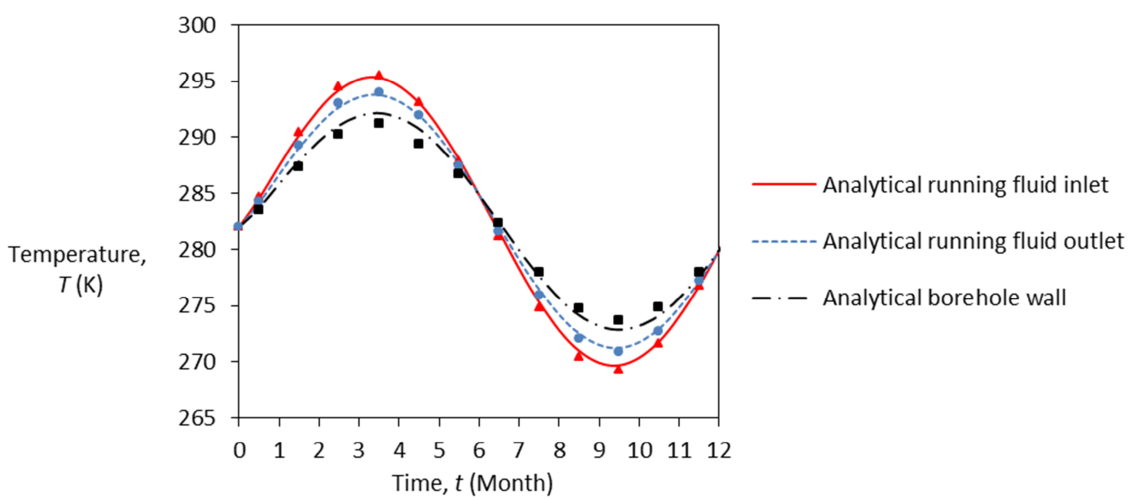

Figure 7-31 Transient temperature of the borehole wall and inlet and outlet running fluid temperature for numerical and analytical solutions.

The circulating fluid temperatures of the two analytical and numerical models after 2.5 months of system operation are compared in Figure 7-32. It is seen that the temperature of the running fluid is 294.5 K at its inlet and, by losing heat to the surrounding soil, its temperature decreases along the U-tube length and drops to about 293.0 K at the outlet. A comparison of the temperatures resulting from both numerical and analytical models shows good agreement (less than 0.5 K difference). Therefore, both models are able to estimate the temperature of the running fluid along the borehole length. Note that the largest differences in the temperature results of the numerical and analytical model appear at higher heat loads in Months 2-4 and 8-10 (Figure 6-6) and the maximum 0.5 K temperature difference between the numerical and analytical results is true for the whole system operation period.

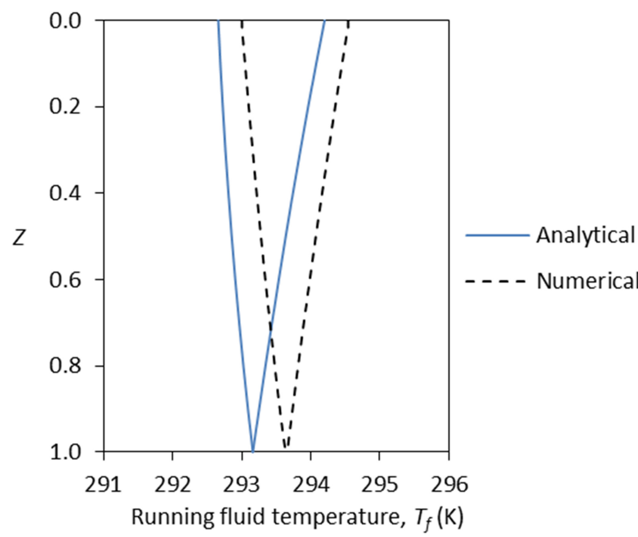

Figure 7-32 Running fluid temperature profile along the borehole of numerical and analytical solutions.

Figure 7-33 illustrates the variation in COP_{rev} with running fluid temperature for heat delivery and removal modes based on the analytical relations. As the system operates in the heat delivery mode, the temperature of the soil surrounding the borehole and, consequently, the temperature of the running fluid both increase over time. In the heat removal mode, the temperature of the soil and, therefore, the running fluid decreases as the system operates. It is seen that for various coil temperatures and for both heat delivery and removal modes, the change in COP decreases as the system operates over time when the borehole wall temperature variation is already high. This could mean that the effect of borehole wall temperature change due to thermal interaction, if there is any, becomes minimal on the performance of the heat pump if the temperature rise occurs when the borehole wall temperature is already high (in the heat delivery mode) or low (in the heat removal mode).

Figure 7-33 shows the COP_{rev} variation of the current system, with the geometrical specification summarized in Table 4-1, with the periodic variations of the running fluid temperature that is shown in Figure 7-31. It is seen that in the cooling season (ground heat delivery), the operation of the heat pump will cause the temperature of the borehole wall and, consequently, the temperature of the running fluid to increase. An increase in the running fluid temperature will result in a drop in the heat pump COP as the heat pump has to deliver the heat to an environment with a higher temperature [Eq. (5-21)]. In the heating season (ground heat removal), the system operation results in a temperature drop in the soil surrounding the borehole and, consequently, a drop in the borehole wall and the running fluid temperatures. The coefficient of the heat pump is lower when it collects heat from a lower-temperature environment, which is the lower temperature of the running fluid here [Eq. (5-22)].

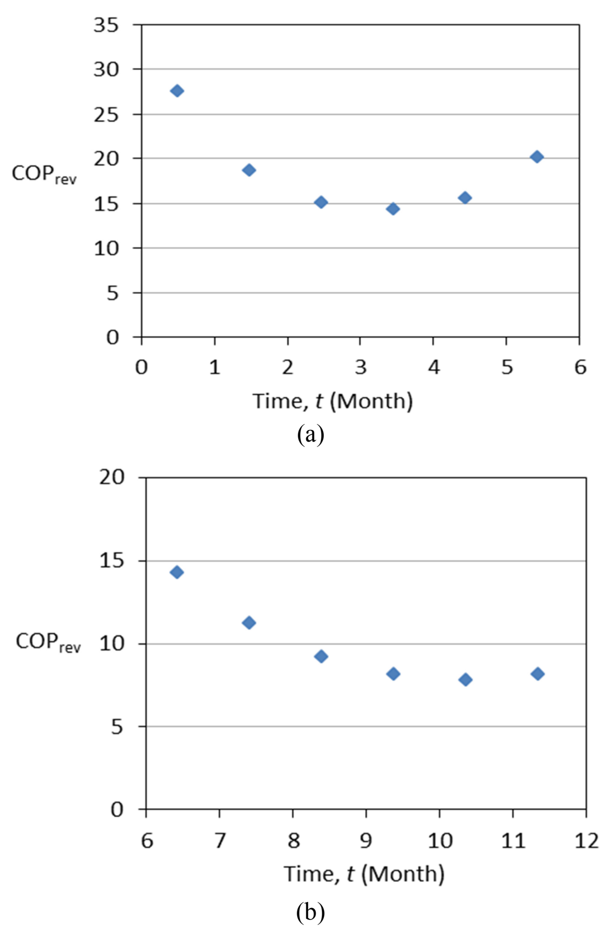

Figure 7-33 Heat pump COP_{rev} variations with time for (a) ground heating load and (b) ground cooling load.

In the current case, with the geometrical specification summarized in Table 4-1, there will not be a large thermal interaction between the two systems with the ground heat load given in Figure 6-6. However, if the boreholes are installed closer to each other, thermal interaction is noticed. For example, if the borehole spacing is decreased from 10 m in the current model to 6m and then 4 m, thermal interaction occurs between the boreholes in the form of a temperature rise/drop of less than 0.3 K and 0.6 K on the borehole wall, respectively, due to the operation of the other system. The temperature rise due to thermal interaction on the borehole wall can be calculated in the current model and is shown for different borehole distances in Figure 7-34. It is seen that as the system experiences a periodic profile of ground heating and cooling load (Figure 6-6), the temperature of the borehole wall also experiences a periodic profile with a time lag and also the temperature rise due to a neighbor system is a periodic profile. The maximum temperature rise due to a neighboring system depends on the distance between the two systems. The closer the two systems, the higher the temperature rise. In addition, the maximum temperature rise due to a neighboring system occurs with a delay after the neighboring system experiences its peak heat load due to the thermal capacitance of the surrounding soil. If both systems operate with similar heat load profiles, the system experiences its peak temperature rise due to the neighboring system with a delay after it experiences its peak borehole wall temperature. Depending on the distance between the two systems this delay may vary. If the boreholes are installed relatively close to each other, this delay will be shorter and the maximum temperature rise due to the neighboring systems occur shortly after the maximum borehole temperature rise on the borehole wall due to the system itself. In this case, the temperature rise that the system is experiencing due to the operation of another system occurs when the borehole wall temperature and the running fluid temperature is already high close to its maximum.

From Figure 7-35 (a), it can be expected that COP_{rev} drop due to this temperature rise will not be great (drop of less than 4% in COP in the 295-300 K running fluid temperature range). However, when the boreholes are installed further apart, it takes longer until the temperature rise due to maximum ground heat input from the neighboring system reaches the system. When this occurs, the neighboring system may not be at its maximum borehole wall temperature and running fluid temperature. In that case, from Figure 7-35 (a) it can be expected that the system experiences a larger COP_{rev} drop due to this temperature rise (drop of about 10% in COP in the 282-285 K range). A similar discussion can be made when heat is being removed from the soil. In this case, thermal interaction can be interpreted as the rise or drop in the borehole wall temperature and, consequently, in the running fluid temperature. In the current system with characteristics given in Table 1, the system will experience a small temperature rise in Months 6 to 12 due to the neighboring system. This will result in a minor increase in the running fluid temperature which could actually increase the performance of the heat pump. This will also be the case for boreholes that are installed 8 m and 6 am apart. Oppositely, it is seen in Figure 7-34 that in a borehole distance of 4 m, the system experiences a minor temperature drop in Month 12 when the system is in heat removal mode and any temperature drop can decrease the performance of the heat pump; in this case, at running fluid temperature of 278.9 K by 3%.

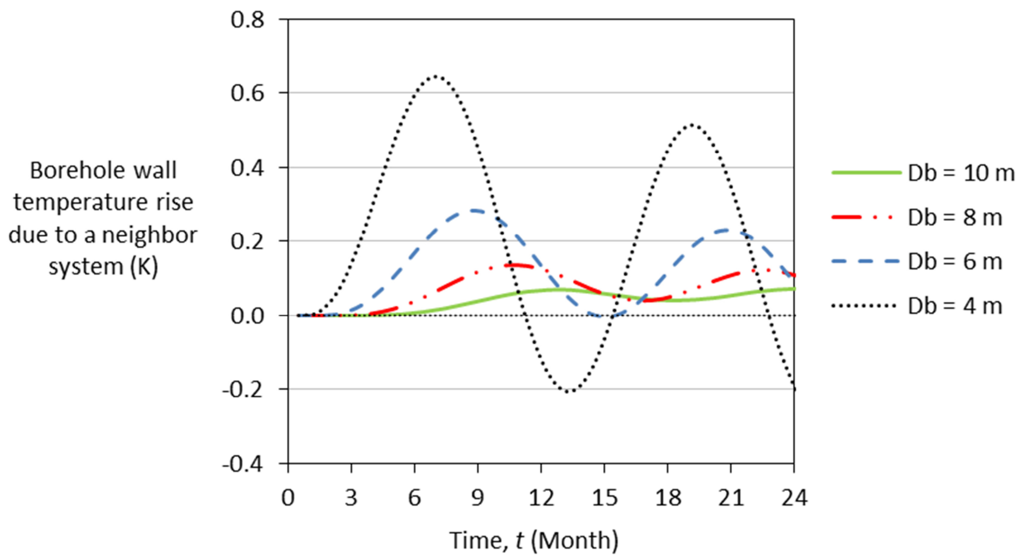

Figure 7-34 Borehole wall temperature rise due to operation of a neighboring system for various borehole distances (D_b).

In summary, it can be concluded from Figure 7-34 and Figure 7-35 that the possibility of thermal interaction between two neighboring systems exists when systems are installed relatively close to each other. It is estimated, however, that the thermal interaction between the systems that are installed closely will not be large enough to cause COP_{rev} drops of more than 10%. Furthermore, the thermal interaction between systems and its effect on the COP_{rev} of the neighboring system depends highly on the cycle of the periodic heat input profile of the systems and the distance between borehole systems. This information determines if the temperature rise/drop of a neighboring system reaches the system of study when it is sensitive to a temperature change or not and if it actually has a negative effect on the COP_{rev} of the system of study. For example, the temperature rise in the soil surrounding one system can dissipate towards the other system with a delay of more than 2-3 months and may actually be advantageous to the neighboring system if it is in its heat removal mode. This effect is examined in the longer run over the system's lifetime (30 years); the temperature rise on the borehole wall due to a neighboring system at distance D_b is shown in Figure 7-36. It is seen that the temperature rise oscillates about an average temperature rise that tends to become zero in the second half of the system operation life. The variation of this average temperature is due to the system reaching a steady state after the first several years of operation.

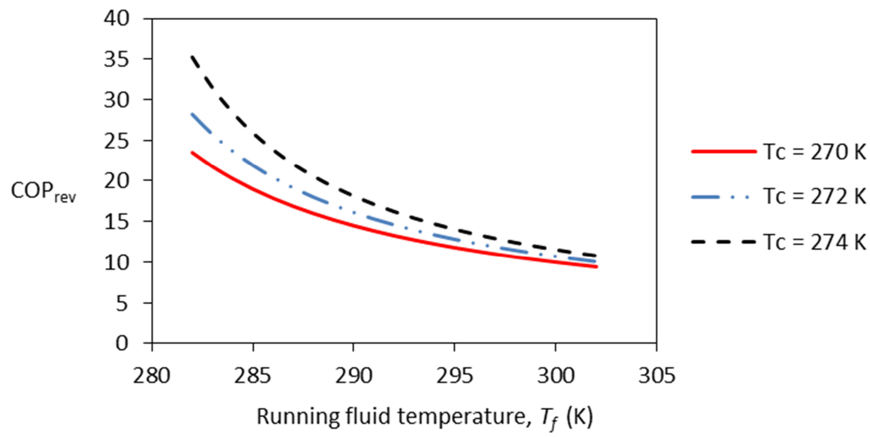

(a)

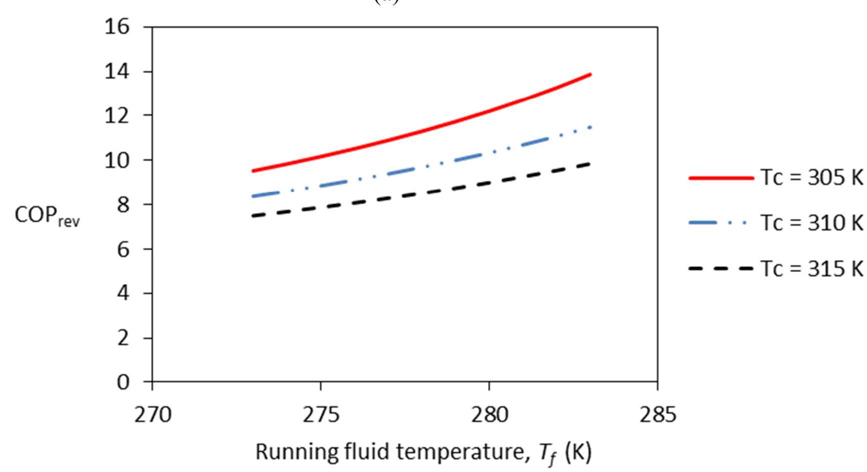

(b)

Figure 7-35 Variation of COP of a reversible heat pump with the running fluid temperature in (a) heat delivery mode, and (b) heat removal mode for various coil temperatures (T_c).

It is also seen that although the oscillations occur between varying temperatures, they occur in the same time periods if the ground heat load is kept constant; i.e. if the temperature rise due to thermal interaction between two boreholes that are 4 m apart occurs in Month 7 of system operation, it is expected to occur repeatedly every year in Month 7. Therefore, a temperature rise noticed in Figure 7-34 in the ground heat removal mode, which is found to be advantageous to heat pump operation, is expected to exist in the same manner during systems lifetime.

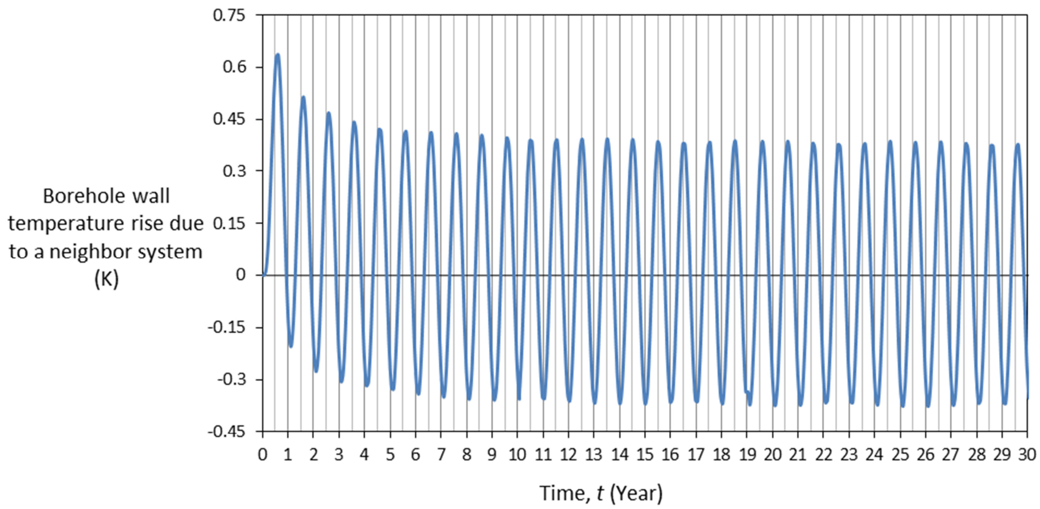

(a)

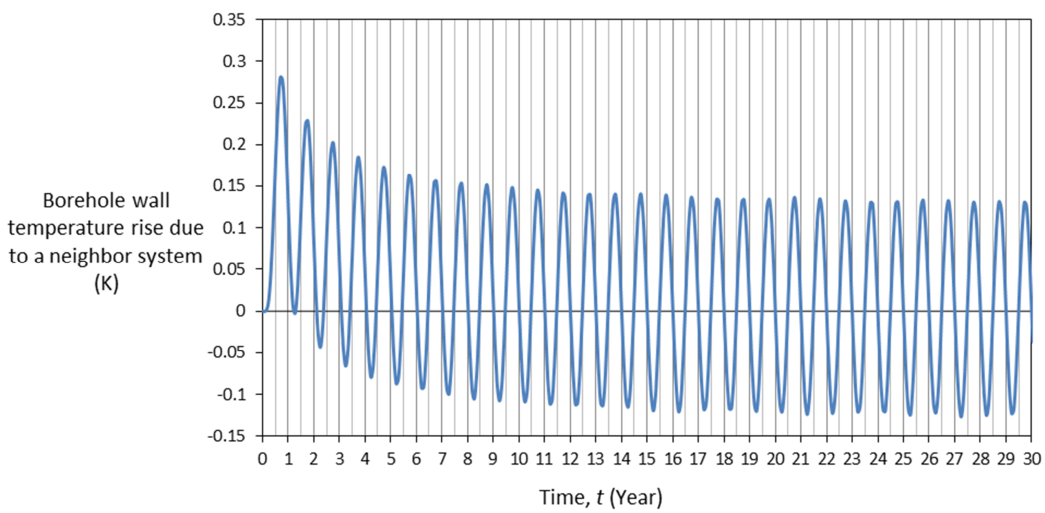

(b)

Figure 7-36 Borehole wall temperature rise due to operation of a neighboring system borehole at a distance (D_b) of (a) 4 m and (b) 6 m.

It should be noted that GHEs are usually installed at system distances further than 10 m. In larger systems with more than one borehole or with a higher ground heat load, the property area that the system is being installed in is usually large enough to provide enough distance between the system and its neighbors. However, in cases where the distance between borehole system installations are lower than typical or the system operates with a larger heat load profile, the method presented in the current study can be applied to estimate if there is a thermal interaction between the systems and how it affects heat pump COP.

Chapter 8 CONCLUSIONS AND RECOMMENDATIONS

Due to their good efficiency, the use of geothermal energy is often encouraged; however, two issues arise in the long-term use of ground for thermal purposes: the sustainability and impact of these systems on the environment. Numerical and analytical modeling of vertical GHEs allow study of these effects. In this chapter, the main contributions, principal findings, conclusions and recommendations for future work are given.

8.1 Summary of Main Accomplishments and Contributions

In the present study, a review of heat transfer models is provided for ground heat exchangers, and the main analytical and numerical models of vertical heat exchangers, are described and compared, and recent model developments are discussed.

A finite volume numerical model is developed in ANSYS FLUENT. A computer code was developed and hooked to the ANSYS FLUENT model to enable original analysis of system parameters from the numerical results. This analysis includes the study of potential thermal interaction among systems in their operating life time as well as the heat flow patterns in areas further away from the systems that can result in negative environmental impacts.

The sensitivity of temperature rise in the soil surrounding vertical ground heat exchangers to parameters such as system spacing and system heat flow rate per unit length is examined.

An analytical approach is presented for a complete analysis of the system by coupling the parameters from the heat pump model to the ground heat exchanger model and the heat exchanger model to the surrounding soil domain. The transient borehole wall temperature is chosen as the coupling parameter between the ground model and the heat exchanger model. The coil temperature is chosen as the coupling parameter between the heat exchanger model and the heat pump model. Another addition to this model is its ability to evaluate the temperature variations in the soil when the heat input to the ground varies periodically. Thus, the heat delivery and removal profile of the system for long-term system operation is modeled. A computer code is developed for coupling the models and evaluation of the analytical expressions. The results of this model are compared to the numerical results from the numerical model.

Several topics which aid the solution and analysis of the problem but are not central to the main subject of the study are investigated:

- The sensitivity of the results of the numerical model to two-dimensional and three-dimensional domains is examined.
- Providing estimates to the transient boundary conditions at the heat exchanger wall and the ground surface.
- Analysis and comparison of the complexities and benefits of the analytical approach presented in the current study and the numerical model.

8.2 Summary of Principal Findings

The finite volume numerical model developed in ANSYS FLUENT leads to several findings:

- For various heat pump coil temperatures and for both heat delivery and removal modes, the change in ground heat pump COP decreases as the system operates over time when the borehole wall temperature variation is already high.
- The thermal interaction between systems and its effect on the COP_{rev} of the neighboring system depends highly on the cycle of the periodic heat input profile of the systems and the distance between borehole systems.
- In the absence of thermal interaction, the temperatures of the borehole walls fall on the same path every year. It can be concluded that for a balanced system where system spacing and the heat flow rate per unit area are kept at the recommended values and there is no temperature rise or fall after the first year of system performance, there should not be any accumulation of heat in the long term if the same heat storage and removal pattern is followed every year.

- In analysis of heat flows and temperature rise in the soil to examine environmental impacts, no significant heat escape or temperature rise in borefield distances more than 10 m is noticed in the case of the current balanced system. This conclusion is drawn based on the 30-60 W/m heat flow on borehole walls that is common to borehole designers and the typical soil thermal characteristics chosen for the current study.

A comparison between the analytical and the numerical results for the borehole wall temperature and the running fluid inlet and outlet temperature shows error of less than 1%. Note that this error is calculated based on the 30-60 W/m heat flow on borehole walls that is a common selection to borehole designers and the typical soil thermal characteristics chosen for the current study. The proposed analytical approach is capable of coupling the soil temperature to the running fluid temperature when the ground load is known. Note that this error is calculated for the two analytical and numerical approaches used in the current study considering the assumptions presented in Section 4.2.

A comparison between the results of two-dimensional and three-dimensional numerical analyses of heat conduction in the soil around multiple boreholes shows that the two-dimensional results are valid for about 96% of the borehole length. The values of the two-dimensional analysis differ from those of three-dimensional analysis at the top and bottom of the borehole length where axial heat transfer effects exist.

8.3 Conclusions

As a result of a preliminary sensitivity study, the effect of various parameters on temperature rise in the soil surrounding the boreholes is discussed. The following conclusions are drawn:

- The use of superposition of analytical solutions for single boreholes when discussing heat flows and temperature rise/drop in the soil surrounding multiple boreholes is verified.
- The distance between two boreholes or two systems of boreholes, the heat flux from the borehole wall and the time of system operation all affect directly the amount of thermal interaction between the systems.

- A numerical two-dimensional domain can be used in analysis of the temperature rise and heat flows in the soil surrounding boreholes for about 96% of the borehole depth.

In the preliminary models mentioned above, a constant heat flow rate per unit length of borehole is used as the boundary condition. How the temperature variation in the soil surrounding the boreholes, such as thermal interaction in the surrounding soil, can affect the running fluid temperature and the performance of the heat pump coupled to them can be discussed only if the heat transfer inside the borehole is modelled as well. Therefore, a model for heat transfer inside the borehole should be utilised as the boundary condition for the three-dimensional transient heat transfer analysis outside the borehole in order to evaluate the temperature rise in the soil surrounding multiple boreholes and their interaction. Two approaches are chosen in coupling the model outside the borehole to the model inside the borehole in the current study and the following conclusions are drawn:

- The maximum temperature rise due to thermal interaction of multiple boreholes occurs at the top of the borehole (about 3% total length) and it decreases along the borehole length as the heat flux from the borehole wall into the soil decreases. Therefore, with the objective of limiting boreholes' operations and sizes in order to prevent their thermal interaction, the top length of the boreholes is the critical area.
- The assumption of uniform heat flux along the borehole is only valid for the middle length of the boreholes and moving any further to the top or bottom of the borehole, the temperature rise evaluations become increasingly inaccurate. It is shown that closely installed systems experience the maximum temperature rise due to a neighboring system shortly after their peak borehole wall temperature while systems that are installed further apart may experience a lower temperature rise due to the neighboring system and longer after their peak borehole wall temperature. The heat pump COP_{rev} drop due to this delayed temperature rise from a neighboring system depends on borehole wall temperature and its associated running fluid temperature when thermal interaction is experienced.
- The possibility of thermal interaction between two neighboring systems exists when systems are installed relatively close to each other. It is estimated, however, that the thermal interaction between the systems that are installed closely will not be large enough to cause COP_{rev} drops of more than 10%.

- Ground heat exchangers are usually installed at borefield distances further than 10 m; a residential building in the smaller range would be away from its neighbor by at least this distance and would require a smaller size heat exchanger corresponding to lower heating/cooling needs. In larger systems with more than one borehole or with a higher ground heat load, the property area that the system is being installed in is usually large enough to provide enough borefield distance between the system and its neighbors and thermal interaction is unlikely.
- Given the large computation time related to the numerical simulation, it can be concluded that the analytical model may be a better choice in delivering the results with an acceptable degree of accuracy. These results presented can be employed to model GHEs in order to examine the possibility of thermal interaction among multiple neighboring systems as well as its effect on running fluid temperature and heat pump efficiency.

Another objective of the current study is to study the migration of thermal plumes away from the systems in the long run which might be disruptive or problematic for ecosystems or living organisms in the ground in long run. A numerical finite volume model in a two-dimensional meshed domain is developed and used to evaluate the temperature response in the soil surrounding multiple borehole systems. A case study is considered in order to formulate an annual profile for heat injection/extraction to/from the soil. The 5-year simulation of the system shows that for a system that has a balanced heat injection and extraction into the soil, if the borehole spacing, the distance of neighboring borehole systems and the heat injection/extraction rate are designed within acceptable limits, there should not be any thermal interaction between neighboring systems nor should there be any thermal plume flowing away from the system. Any temperature rise or decrease in the soil surrounding the GHE that is noticed after the first year operation needs to be compensated for during the second year operation so that the system can operate sustainably.

8.4 Recommendations

The current study presents an assessment of the temperature rise in the soil surrounding multiple borehole heat exchangers as well as the heat pump efficiency variation related to the temperature variations. The results of the current study could be improved to achieve higher accuracy via the following tasks:

- Improve the ground surface boundary; in the current model, like many other studies on vertical heat exchanger analysis, the ground is assumed to be isothermal to its average yearly temperature. To improve this boundary condition, a periodic temperature profile can be chosen for the ground surface. Furthermore, a heat balance on the ground surface including parameters such as solar radiation, ambient air temperature and relative humidity, rainfall, snow cover, and wind speed could help improve the numerical model in the current study. Inclusion of all these effect in the analytical model may not be a wise choice given how complex the problem will become.
- Improve the current analytical model by better estimating the heat flow rate along the borehole wall. In the current model, it is shown that the heat flow rate strength varies along the borehole wall due to the varying circulation fluid temperature. As mentioned in Section 5.3.1, it is assumed that the borehole wall temperature is constant throughout system operation period. Using the coupling procedure introduced in Section 5.3.2, this model may be improved to a more general and accurate form by assuming a transient borehole wall temperature when the transient heat flow rate along the borehole and running fluid temperature variation along the borehole are accounted for.
- Improve the current model considering the variation in the ground temperature and thermal properties with depth. In the current model, the ground temperature and its thermal properties are assumed to be constant in the entre domain. This assumption can be improved to account for the temperature variation in the soil in varying depths as well as the variation in its thermal properties.
- Study the current objectives for various soil thermal characteristics. Soil characteristics can have a large impact on the ranges of the temperatures in the soil surrounding the borehole.

The results of the current study can guide proper site characterization, system design, construction and operation so that these systems minimally impact the environment as well as other neighboring systems. Systems with different sizes have different heating and cooling loads. Once the ground heat load for a system is estimated, the current model can be used to estimate the temperature rise in the soil and find the optimum borehole spacing between the system and its neighboring systems. For systems that are already installed, the results of the current study can be used to estimate the heat flows and temperature rise surrounding the system in the long term. In cases where the distance between borehole installations are lower than typical or the system operates with a larger heat load profile, the method presented in the current study can be applied to estimate if there is a thermal interaction between the systems and how it affects heat pump COP. This is particularly important since using the procedure presented in the current study, one can predict the potential system malfunction due to thermal interaction after few years of system operation and prevent it. Also, the temperature rise surrounding the system and further away from the system can be estimated to examine negative effects on eco-systems nearby.

The future research on this topic could focus on the following:

- Modify the mathematical model to reduce simulation time without compromising its accuracy;
- Modify the analytical model and introduce non-dimensional parameters for general system discussion.
- Study the current objectives in presence of moisture migration;
- Study the current objectives in presence of groundwater flow;
- Study the current objectives but with unbalanced ground heating and cooling periods;
- Perform a similar study on horizontal heat exchangers to discuss thermal interaction of these systems and their environmental impacts.
- Perform an estimation of ecological impacts based on mutual interaction established from the simulation data.

REFERENCES

Andrushuk, R., P. Merkel. 2009. "Performance of ground source heat pumps in Manitoba." *GeoConneXion Magazine*, Summer:15-16.

ANSYS FLUENT 12.0 theory guide, http://www.sharcnet.ca/Software/Fluent12/html/th/main_pre.htm, Accessed on Aug. 01, 2013.

Awwa Research Foundation, Contaminant transport through aquitards: A state of the science review, 2006a.

Awwa Research Foundation, Contaminant transport through aquitards: Technical guidance for aquitard assessment, 2006b.

Bandyopadhyay, G., W. Gosnold, M. Mannc. 2008. "Analytical and semi-analytical solutions for short-time transient response of ground heat exchangers." *Energy and Buildings* 40(10):1816–1824.

Bauer, D., D. Heidemann, H.-J.G. Diersch. 2011. "Transient 3D analysis of borehole heat exchanger modeling." Geothermics 40:250–260.

Bernier, M., A. Pinel, P. Labib, R. Paillot. 2004. "A multiple load aggregation algorithm for annual hourly simulations of GCHP systems." *HVAC&R Research* 10(4):471–487.

Bose, J. E., J.D. Parker, F.C. McQuiston. 1985. *Design/Data Manual for Closed-Loop Ground Coupled Heat Pump Systems*. Oklahoma State University for ASHRAE. Oklahoma: Stillwater, 1985.

Canadian GeoExchange Coalition. 2010. The state of the Canadian geothermal heat pump industry: Industry Survey and Market Analysis.

Carslaw, H.S., J.C. Jaeger. 1946. *Conduction of Heat in Solids.* Oxford UK: Claremore Press.

Cengel, Y.A., M.A. Boles. 2006. *Thermodynamics: An Engineering Approach*, fifth ed. New York: McGraw-Hill.

Chiasson, A.D., S.J. Rees, J.D. Spitler. 2000. "A preliminary assessment of the effects of groundwater flow on closed-loop ground-source heat pump systems." *ASHRAE Transactions* 106(1):380–393.

Claesson J., A. Dunand. 1983. *Heat extraction from the ground by horizontal pipes: a mathematical analysis*. Stockholm: Swedish Council for Building Research.

Claesson, J., G. Hellström. 2011. "Multipole method to calculate borehole thermal resistances in a borehole heat exchanger." *HVAC&R Res*. 17:895–911.

Coskun, S., E. Pulat, K. Unlu, R. Yamankaradeniz. 2008. "Experimental performance investigation of a horizontal ground source compression refrigeration machine." *International Journal of Energy Research* 32:44–56.

Cui, P., H. Yang, Z.H. Fang. 2006. "Heat transfer analysis of ground heat exchangers with inclined boreholes." *Applied Thermal Engineering* 26:1169–1175.

Diao, N.R., H.Y. Zeng, Z.H. Fang. 2004a. "Improvement in modeling of heat transfer in vertical ground heat exchangers." *HVAC&R Research* 10(4):459–470.

Diao, N.R., Q. Li, Z.H. Fang. 2004b. "Heat transfer in ground heat exchangers with groundwater advection." *International Journal of Thermal Sciences* 43: 1203–1211

Esen, H., M. Inalli, M. Esen. 2007a. "Numerical and experimental analysis of a horizontal ground-coupled heat pump system." *Building and Environment* 42(3):1126–1134.

Esen, H., M. Inalli, M. Esen, K. Pihtili. 2007b. "Energy and exergy analysis of a ground-coupled heat pump system with two horizontal ground heat exchangers." *Building and Environment* 42:3606–3615.

Eskilson, P. 1987. "Thermal analysis of heat extraction boreholes." Doctoral thesis, Lund, Sweden: University of Lund, Department of Mathematical Physics, 1987.

Environment Canada, Canadian climate normals, http://www.climate.weatheroffice.gc.ca/ climate_normals/index_e.html, Accessed on Apr. 25, 2011.

Fang, Z.H., N.R. Diao, P. Cui. 2002. "Discontinuous operation of geothermal heat exchangers." *Tsinghua Science and Technology* 7(2):194–197.

Ferguson, G. 2009. "Unfinished business in geothermal energy." *Ground Water* 47(2):167-167.

Ferguson, G., A.D. Woodbury. 2005. "Thermal sustainability of groundwater-source cooling in Winnipeg, Manitoba" *Canadian Geothechnical* 42:1290-1301.

Ferguson, G., A.D. Woodbury. 2006. "Observed thermal pollution and post-development simulations of low-temperature geothermal systems in Winnipeg, Canada." *Hydrogeology* 14(7):1206-1215.

Fisheries and Oceans Canada, Ontario-Great Lakes Area (DFO-OGLA), Fish Habitat and Fluctuating Water Levels on the Great Lakes, Report, August 2009.

Florides, G., S. Kalogirou. 2007. "Ground heat exchangers - A review of systems, models and applications." *Renewable Energy* 32(15):2461–2478.

Gao, J., X. Zhang, J. Liu, K. Li, J. Yang. 2008. "Numerical and experimental assessment of thermal performance of vertical energy piles: An application." *Applied Energy* 85: 901–910.

Gehlin, S.E.A., G. Hellström. 2003. "Influence on thermal response test by groundwater flow in vertical fractures in hard rock." *Renewable Energy* 28(14):2221–2238.

Geothermal Heat Pump Consortium, http://www.geoexchange.org, Accessed on Aug 03, 2013.

Gu, Y., D.L. O'Neal. 1998. "Development of an equivalent diameter expression for vertical U-tube used in ground-coupled heat pumps." *ASHRAE Transactions* 104:347–355.

Hart, D.P., R. 1986. Couvillion, Earth coupled heat transfer. Publication of National Water Well Association, Dublin, Ohio.

He, M., S. Rees, L. Shao. 2009. "Simulation of a domestic ground source heat pump system using a transient numerical borehole heat exchanger model." *Proc. 11th*

International Building Performance Simulation Association Conference, Glasgow, Scotland. 607-614.

Hepbasli, A., O. Akdemir, E. Hancioglu. 2003. "Experimental study of a closed loop vertical ground source heat pump system." *Energy Conversion and Management* 44: 527–548.

Hecht-Mendez, J., N. Molina-Giraldo, P. Blum, P. Bayer. 2010. "Evaluating MT3DMS for heat transport simulation of closed geothermal systems." *Ground Water* 48(5):741–756.

Hellström, G. 1991. Ground heat storage: Thermal analyses of duct storage systems. Doctoral thesis, Lund, Sweden: Department of Mathematical Physics, University of Lund.

Hikari, F., I. Ryuichi, I. Takashi. 2004. "Improvements on analytical modeling for vertical U-tube ground heat exchangers." *Geothermal Resources Council Transactions* 28:73–77.

Hillel, D. 1982. *Introduction to soil physics*. San Diego: Academic Press.

Incropera, F.P., D.P. DeWitt. 2000. *Introduction to Heat Transfer*. New York: Wiley; 3rd Ed.

Ingersoll, L.R., O.J. Zobel, A.C. Ingersoll. 1954. *Heat Conduction with Engineering, Geological, and other Applications.* New York: McGraw-Hill, 1954.

Ingersoll, L.R., H.J. Plass. 1948. "Theory of the ground pipe heat source for the heat pump." *ASHVE Transactions* 47:339-348.

Inalli, M., H. Esen. 2004. "Experimental thermal performance evaluation of a horizontal ground source heat pump system." *Applied Thermal Engineering* 24(14–15):2219–2232.

Jacovides, C.P., G. Mihalakakou, M. Santamouris, J.O. Lewis. 1996. "On the ground temperature profile for passive cooling applications in buildings." *Solar Energy* 57:167-75.

Jun, L., Z. Xu, G. Jun, Y. Jie. 2009. "Evaluation of heat exchange rate of GHE in geothermal heat pump systems." *Renewable Energy* 34(12):2898-2904.

Kavanaugh, S.P. 1985. “Simulation and experimental verification of vertical ground coupled heat pump systems.” Doctoral Thesis, Oklahoma State University, USA.

Kavanaugh, S.P. 1992. “Simulation of ground-coupled heat pumps with an analytical solution.” *Proceedings of the ASME International Solar Energy Conference*, New York, 1:395–400.

Lamarche, L., B. Beauchamp. 2007. “A new contribution to the finite line source model for geothermal boreholes.” *Energy and Building* 39(2):188–198.

Lee, C.K., H.N. Lam. 2008. “Computer simulation of borehole ground heat exchangers for geothermal heat pump systems.” *Renewable Energy* 33(6):1286–1296.

Leong, W.H., V.R. Tarnawski. 2010. “Effects of simultaneous heat and moisture transfer in soils on the performance of a ground source heat pump system.” *ASME-ATI-UIT Conference on Thermal and Environmental Issues in Energy Systems*, Sorrento, Italy.

Leong W.H., C.J. Lawrence, V.R. Tarnawski, M.A. Rosen. 2006. “Evaluation of a ground thermal energy storage system for heating and cooling of an existing dwelling.” *IBPSA-Canada’s 4th Biennial Building Performance Simulation Conference*, University of Toronto, Toronto, Canada.

Li M., A.C.K. Lai. 2013. “Thermodynamic optimization of ground heat exchangers with single U-tube by entropy generation minimization method.” *Energy Conversion and Management* 65, 133–139.

Li, Z., M. Zheng. 2009. “Development of a numerical model for the simulation of vertical U-tube ground heat exchangers.” *Applied Thermal Engineering* 29(5-6):920–924.

Marcotte, D., P. Pasquier. 2008. “Fast fluid and ground temperature computation for geothermal ground-loop heat exchanger systems.” *Geothermics* 37:651–665.

Markle, J.M., R.A. Schincariol. 2007. “Thermal plume transport from sand and gravel pits – Potential thermal impacts on cool water streams.” *Hydrology* 338:174–195.

McQuiston, F.C., J.D. Parker, J.D. Spitler. 2005. *Heating, Ventilating, and Air Conditioning: Analysis and Design*. New York: Wiley, 6th ed.

Mei, V.C. 1986. Horizontal Ground-Coupled Heat Exchanger, Theoretical and Experimental Analysis. Oak Ridge National Laboratory: Technical Report ORNL/CON-193.

Mei, V.C., V.D. Baxter. 1986. "Performance of a ground-coupled heat pump with multiple dissimilar U-tube coils in series." *ASHRAE Transactions* 92(2):22–25.

Mihalakakou, G. 2002. "On estimating ground surface temperature profiles." *Energy and Buildings* 34:251–259.

Mihalakakou, G., J.O. Lewis. 1996. "The influence of different ground covers on the heating potential of the earth-to-air heat exchangers." *Renewable Energy* 7:33-46.

Muraya, N.K. 1995. "Numerical modeling of the transient thermal interference of vertical U-tube heat exchangers." Doctoral thesis, USA: Texas A&M University, College Station.

Nam, Y., R. Ooka, S. Hwang. 2008. "Development of a numerical model to predict heat exchange rates for a ground-source heat pump system." *Energy and Buildings* 40(12):2133–2140.

Paul, N.D. 1996. "The effect of grout conductivity on vertical heat exchanger design and performance." Master Thesis, USA: South Dakota State University.

Piechowski, M. 1999. "Heat and mass transfer model of a ground heat exchanger: Theoretical development." *Int. J. Energy Res.* 23:571–588.

Pulat, E., S. Coskun, K. Unlu, N. Yamankaradeniz. 2009. "Experimental study of horizontal ground source heat pump performance for mild climate in Turkey." *Energy* 34:1284–1295.

Rottmayer, S. P., W. A. Beckman, J. W. Mitchell. 1997. "Simulation of a single vertical U-tube ground heat exchanger in an infinite medium." *ASHRAE Transactions* 103(2):651-658.

Salah El-Din, M.M. 1999. "On the heat flow into the ground." *Renewable Energy* 18:473–490.

Shonder, J.A., J.V. Beck. 1999. "Determining effective soil formation thermal properties from field data using a parameter estimation technique." *ASHRAE Transactions* 105: 458-466.

Tarnawski, V.R. 1982. "An Analysis of Heat and Moisture Movement in Soils in the Vicinity of Ground Heat Collectors for Use in Heat Pump Systems." *Acta Polytechnica Scandinavica, Mechanical Engineering Series* 82, Helsinki.

USAF. 1978. Engineering weather data. Department of the Air Force Manual AFM 88-29. U.S. Government Printing Office, Washington, D.C.

Versteeg, H.K., W. Malalasekera. 2007. *An introduction to computational fluid dynamics, The finite volume method.* Harlow, England: Prentice Hall.

Xu, X., J.D. Spitler. 2006. "Modeling of Vertical Ground Loop Heat Exchangers with Variable Convective Resistance and Thermal Mass of the Fluid." *Proceedings of Ecostock*, Pomona, NJ.

Yang, H., P. Cui, Z. Fang. 2010. "Vertical-borehole ground-coupled heat pumps: A review of models and systems." *Applied Energy* 87(1):16-27.

Yang, W., M. Shi, G. Liu, Z. Chen. 2009. "A two-region simulation model of vertical U-tube ground heat exchanger and its experimental verification." *Applied Energy* 86:2005–2012.

Yavuzturk C., J. Spitler, 1999. "A short time step response factor model for vertical ground loop heat exchangers." *ASHRAE Trans.* 105:475–485.

Yavuzturk, C., J.D. Spitler. 2001. "Field validation of a short time step model for vertical ground-loop heat exchangers." *ASHRAE Transactions* 107(1):617–625.

Yavuzturk, C. 1999. "Modeling of vertical ground loop heat exchangers for ground source heat pump systems." Doctoral thesis, Oklahoma, USA: Oklahoma State University.

Yavuzturk, C., J.D. Spitler, S.J. Rees. 1999. "A transient two-dimensional finite volume model for the simulation of vertical U-tube ground heat exchangers." *ASHRAE Transactions* 105(2):465–474.

York, K., Z. Sarwar Jahangir, T. Solomon, L. Stafford. 1998. "Effects of a large scale geothermal heat pump installation on aquifer microbiota." *Proc. of the Second International Conference on Geothermal Heat Pump systems at Richard Stockton College*, Pomona, NJ, USA.

Younger, P.L. 2008. “Ground-Coupled Heating-Cooling Systems in Urban Areas: How Sustainable Are They?” *Bulletin of Science, Technology & Society* 28(2):174-182.

Zeng, H.Y., N.R. Diao, Fang Z. 2002. “A finite line-source model for boreholes in geothermal heat exchangers.” *Heat Transfer Asian Research* 31(7):558–567.

Zeng, H.Y., N.R. Diao, Z. Fang. 2003a. “Heat transfer analysis of boreholes in vertical ground heat exchangers.” *International Journal of Heat and Mass Transfer* 46(23):4467–4481.

Zeng, H.Y., N.R. Diao, Z. Fang. 2003b. “Efficiency of vertical geothermal heat exchangers in ground source heat pump systems.” *Journal of Thermal Science* 12(1):77–81.

Appendix A Numerical Discretization

The discretization in unstructured meshes for the grout and soil region can be developed from basic control volume technique where the integral form of the energy conservation equation is used as the starting point:

$$\int_{CV} div\left[grad(T)\right]dV = \int_{CV} \frac{1}{a}\frac{\partial T}{\partial t}dV \tag{A-1}$$

Here, ΔV is the volume. Integration of Eq. (A-1) over a time interval from t to $t+\Delta t$ gives

$$\int_{t}^{t+\Delta t}\int_{CV} div\left[grad(T)\right]dV\,dt = \int_{t}^{t+\Delta t}\int_{CV} \frac{1}{a}\frac{\partial T}{\partial t}dV\,dt \tag{A-2}$$

The volume integration in the right hand side can be conveniently evaluated as the product of the volume of the cell and the relevant centroid value of the integrand. The time integration in the current model is treated using the implicit technique.

Using Gauss's divergence theorem, which is applicable to any shape of control volume:

$$\int_{CV} div\ a\ dV = \int_{A} n\cdot a\ dA \tag{A-3}$$

The diffusive terms on the left hand side of Eq. (A-3) are rewritten as integrals over the entire bounding surface *A*:

$$\int_{t}^{t+\Delta t}\int_{A} n\cdot grad\ T\ dAdt = \int_{CV}\int_{t}^{t+\Delta t} \frac{1}{a}\frac{\partial T}{\partial t}dtdV \tag{A-4}$$

In Eq. (A-4), the order of integration and differentiation in the term on the right hand side has been changed to illustrate its physical meaning.

The surface integration must be carried out over the bounding surface *A* of the control volume CV. The physical interpretation of **n . a** is the component of the vector **a** in the direction of the outward unit vector **n** normal to infinitesimal surface element *dA*. The

2D example of the triangular control volumes is shown in Figure A-1 Typical triangular control volume.

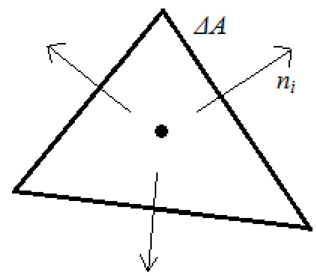

Figure A-1 Typical triangular control volume.

Note that the bounding surface or control surface of each control volume is a closed contour formed by means of a series of finite-sized straight line elements, the area of which is denoted by ΔA. In the 3D model, the control volume model would be bounded by triangular prism elements. A is the area of the entire control surface in Eq. (A-4) and dA indicates an infinitesimal surface element. The area integrations are carried out over all line segments (2D) or surface elements (3D), so they can be written as follows:

$$\sum_{i}^{all\ surfaces} \int_{t}^{t+\Delta t} \int_{\Delta A_i} n_i \cdot grad\ T\ dAdt = \int_{CV} \int_{t}^{t+\Delta t} \frac{1}{a} \frac{\partial T}{\partial t} dtdV \tag{A-5}$$

To evaluate the control surface integrations, expressions for *grad T* as well as geometric quantities n_i and ΔA_i are needed. The outward normal vector n_i and surface element area ΔA_i can be calculated using simple trigonometry and vector algebra from the vertex coordinates of the unstructured grid [Versteeg and Malalasekera, 2007]. The area integration for each of the surface elements in Eq. (A-5) is approximated by the dot product of the outward unit normal vector $\boldsymbol{n_i}$ and the diffusive flux vector (*grad T*) for the control surface element ΔA_i. The latter can be approximated easily using the central differencing method along line *PA*. Thus,

$$\int_{\Delta A_i} n_i \cdot grad\ T\ dA \cong n_i \cdot grad\ T\ \Delta A_i \cong \left(\frac{T_A - T_P}{\Delta \xi}\right)\Delta A_i \tag{A-6}$$

where $\Delta \xi$ is the distance between the centroids A and P of two neighbor grids with common surface of ΔA_i. Note that the integration in Eq. (A-6) should be carried out for all surfaces surrounding a node.

If the temperature at a node is assumed to prevail over the whole control volume, using the first-order temporal discretization, the right hand side of Eq. (A-5) can be written as

$$\int_{CV}\int_{t}^{t+\Delta t} \frac{1}{a}\frac{\partial T}{\partial t} dtdV = \frac{1}{a}\frac{T_P - T_P^0}{\Delta t}\Delta V \tag{A-7}$$

Substituting Eqs. (A-6) and (A-7) in Eq. (A-5), it can be rewritten in the following form:

$$\int_{t}^{t+\Delta t}\left[\sum_{i}^{all\ surfaces}\left(\frac{T_{nb} - T_P}{\Delta \xi}\right)\Delta A_i\right]dt = \frac{1}{a}\frac{T_P - T_P^0}{\Delta t}\Delta V \tag{A-8}$$

where nb is the node number of the adjacent cell. To evaluate the right hand side of this equation we need to make an assumption about the variation of T_P and T_{nb} with time. We could use temperatures at time t or at time $t+\Delta t$ to calculate the time integral or, alternatively, a combination of temperatures at time t and $t+\Delta t$. This approach may be generalized by means of a weighting parameter θ between 0 and 1 and write the integral I_T of temperature T_P with respect to time as

$$I_T = \int_{t}^{t+\Delta t} T_P dt = \left[\theta T_P + (1-\theta)T_P^0\right]\Delta t \tag{A-9}$$

Using this formula for T_{nb} in Eq. (A-8), and dividing by Δt throughout, we have

$$\sum_{i}^{all\ surfaces}\left[\theta\left(\frac{T_{nb} - T_P}{\Delta \xi}\right) + (1-\theta)\left(\frac{T_{nb}^0 - T_P^0}{\Delta \xi}\right)\right]\Delta A_i = \frac{1}{a}\frac{T_P - T_P^0}{\Delta t}\Delta V \tag{A-10}$$

which may be rearranged to give

$$\left[\frac{1}{\alpha}\frac{\Delta V}{\Delta t}+\theta\sum_{i}^{all\ surfaces}\frac{\Delta A_i}{\Delta\xi}\right]T_P=\sum_{i}^{all\ surfaces}\frac{\Delta A_i}{\Delta\xi}\left[\theta\, T_{nb}+(1-\theta)T_{nb}^{0}\right]+ \left[\frac{1}{\alpha}\frac{\Delta V}{\Delta t}-(1-\theta)\sum_{i}^{all\ surfaces}\frac{\Delta A_i}{\Delta\xi}\right]T_P^0 \tag{A-11}$$

Now, we identify the coefficients of T_{nb} and write Eq. (A-11) in the familiar standard form:

$$a_P T_P=\sum_{i}^{all\ surfaces}a_{nb}\left[\theta\, T_{nb}+(1-\theta)T_{nb}^{0}\right]+\left[a_P^0-(1-\theta)\sum_{i}^{all\ surfaces}\frac{\Delta A_i}{\Delta\xi}\right]T_P^0 \tag{A-12}$$

where

$$a_P=\theta\sum_{i}^{all\ surfaces}a_{nb}+a_P^0 \tag{A-13}$$

and

$$a_P^0=\frac{1}{\alpha}\frac{\Delta V}{\Delta t} \tag{A-14}$$

$$a_{nb}=\frac{\Delta A_{nb}}{\Delta\xi}$$

The exact form of the final discretized equation depends on the value of θ. In the current model, the fully implicit formulation (θ=1) is used. Therefore, Eq. (A-12) will reduce to the following form:

$$a_P T_P=\sum_{i}^{all\ surfaces}a_{nb}T_{nb}+a_P^0 T_P^0 \tag{A-15}$$

where

$$a_P=\sum_{i}^{all\ surfaces}a_{nb}+a_P^0 \tag{A-16}$$

and the constants a_P^0 and a_{nb} are introduced in Eq. (A-14).

The implicit equation can be solved iteratively at each time level before moving to the next time step. The advantage of the fully implicit scheme is that it is unconditionally stable with respect to time step size.

Appendix B Numerical Models

The heat conduction in the soil surrounding a single borehole is mainly in the radial direction assuming the variations of the borehole wall temperature in the circumferential direction due to running fluid inlet and outlet tubes are negligible. For the case of multiple boreholes, heat conduction in the circumferential direction is also noticed in the region surrounding the two boreholes. Furthermore, the heat flows in the axial direction exist, but are often assumed negligible in modeling vertical borehole heat exchangers. All numerical models that are presented in this section use a similar pressure based solver in ANSYS FLUENT that is discussed in Chapter 6 .

B.1 Two-dimensional Numerical Model

The transient governing integral equations for the conservation of energy,

$$\rho c_p \frac{\partial T}{\partial t} = k \nabla^2 T \tag{B-1}$$

is solved with a control volume method in ANSYS FLUENT for a single borehole and multiple boreholes in a two-dimensional domain. Note that instead of superposing one-dimensional solutions to account for circumferential heat transfer effects, the circumferential heat transfer effects are taken into account in the two-dimensional numerical solution. However, the two-dimensional numerical solution does not take into account the axial heat transfer effects in the soil. In Figure B-1, the grey area is the solution domain. Since the temperature gradient in the domain between the borehole wall and the farfield changes gradually from large to small, the size of the mesh cells is chosen based on this gradual change to reduce computer memory and computational time.

An initial temperature of 288 K, which is the undisturbed ground temperature, is assumed for the entire borefield. At the outer edge of the domain, a constant farfield temperature condition equal to the initial temperature (288 K) is applied. To simplify the current model, a constant heat flux of 10 W/m^2 on the borehole wall is assumed since, in order to study the thermal interaction between multiple boreholes, their inner dynamic heat exchange process can be of second priority compared to the heat dissipation in the soil surrounding them. In addition, to account for the transient term in Eq. (B-1), the time is subdivided into 4200 time steps of 3600 s which equals a time period of 6 months.

Also, the thermal properties given in Table B-1 are assumed in this model. Note that the properties of soil are approximate values for clay soil with no water content.

This model is used in obtaining the results presented in Sections 7.1.1 and 7.1.2.

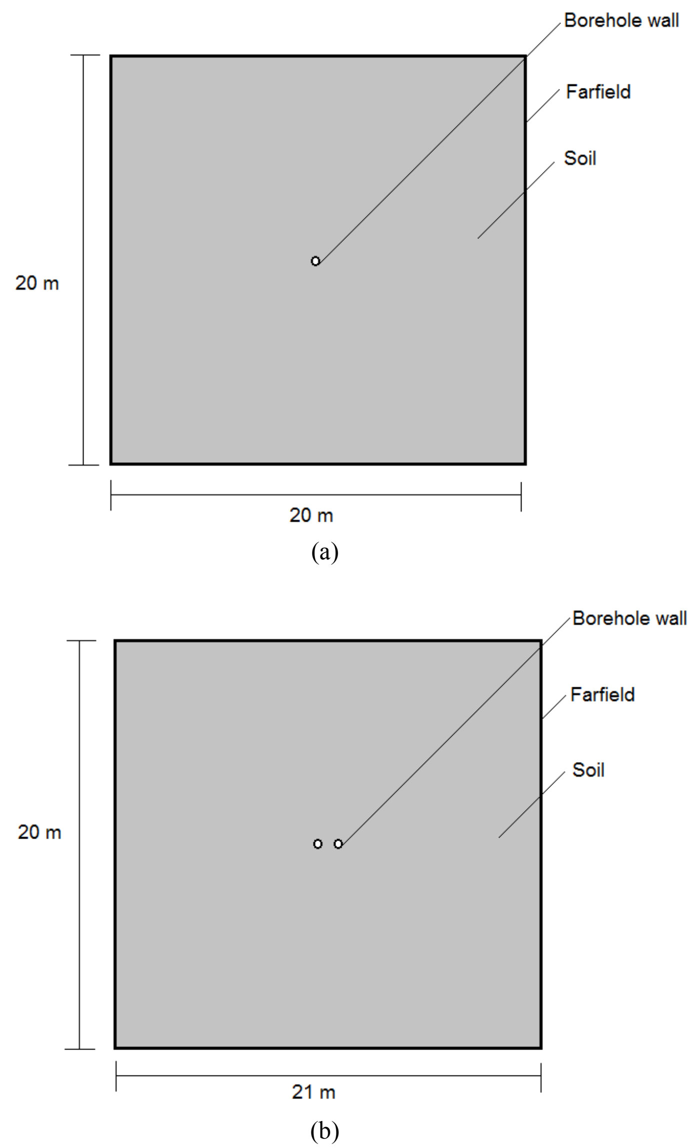

Figure B-1 Solution domain.

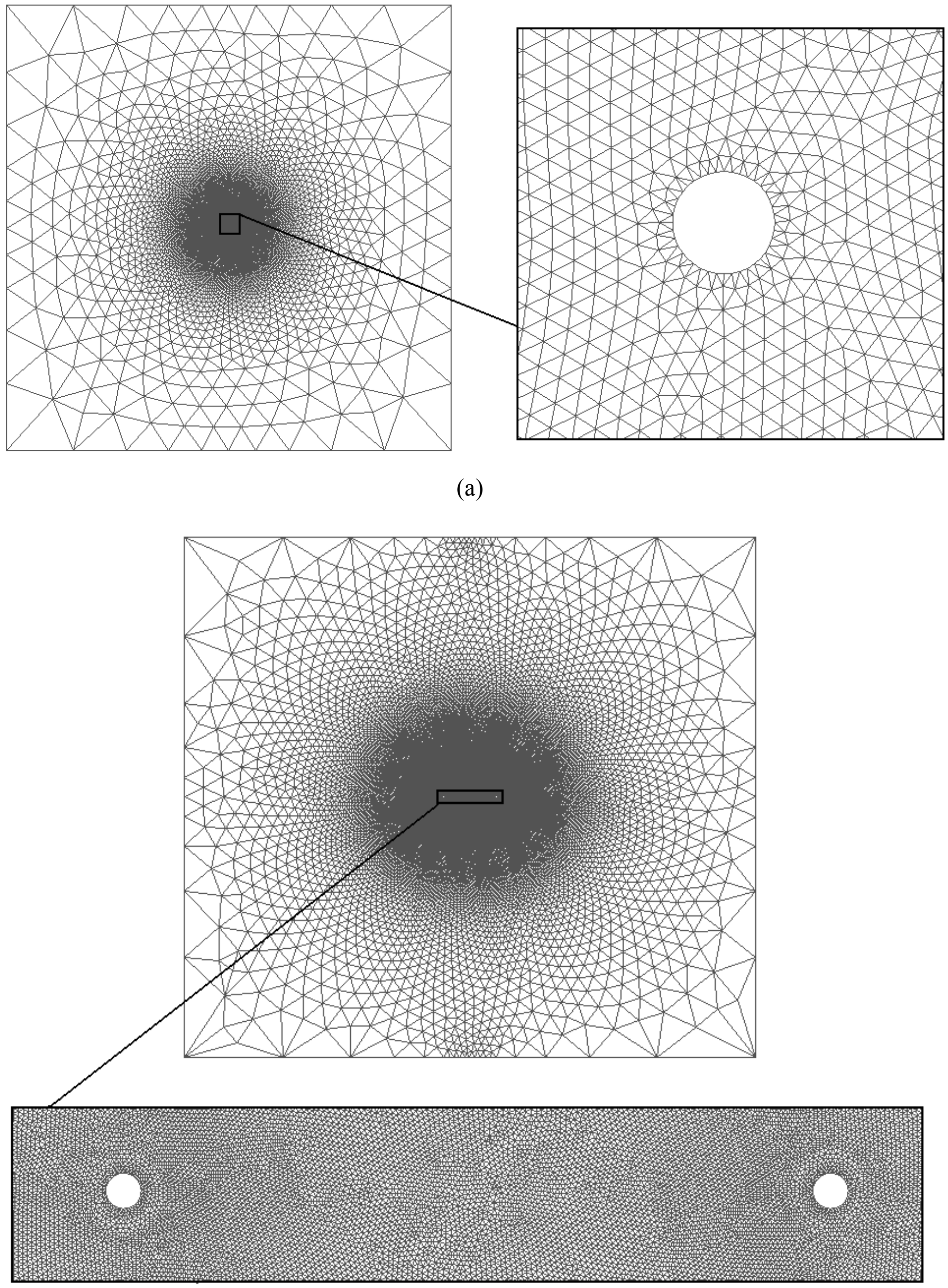

(a)

(b)

Figure B-2 Computational triangular grids used in the solution domain (a) single borehole and (b) multiple boreholes.

Table B-1 Thermal properties and geometrical characteristics of the model [Adapted from (Incropera and DeWitt, 2000; Gao et al. 2008; Hepbasli et al. 2003; Shonder and Beck 1999)].

Soil	
Undisturbed ground temperature	15 C (288 K)
Soil thermal conductivity	1 W/mK
Soil specific heat capacity	1200 J/kgK
Soil density	1381 kg/m^3
Borehole geometry	
Total borehole length, H	200 m (three-dimensional case)
Borehole radius, r_b	0.050 m
Number of Boreholes	2
Borehole distance, D_b	2 m
Heat flow rate per unit length, q'	3.14 W/m

B.2 Three-dimensional Numerical Model

The transient governing integral equations for the conservation of energy are solved for multiple boreholes in a three-dimensional domain with a control volume method in ANSYS FLUENT software. The heat transfer symmetry about the two vertical planes shown in Figure B-3 (a) is utilized and, since a geometric symmetry along the borehole length exists, it is assumed that the heat transfer along the borehole is symmetrical about a horizontal plane passing through the borehole mid-length Figure B-3 (b). Therefore, only one eighth of the borehole field is modeled and the solution domain (soil) is enclosed by the farfield, the ground surface and three symmetry planes. In Figure B-3 (b), the gray area is the solution domain, the results of which can be replicated to the other areas drawn with dashed lines due to their symmetry. Since the temperature gradient in the domain between the borehole wall and the farfield changes gradually from large to small, the size of the mesh cells is chosen based on this gradual change to reduce computer memory and computational time.

An initial temperature of 288 K, which is the undisturbed ground temperature, is assumed for the entire borefield. At the outer edge of the domain, a constant farfield temperature condition equal to the initial temperature (288 K) is applied. The conditions at the symmetry planes are set for zero heat flux. To simplify the current model, a constant heat flux of 10 W/m^2 on the borehole wall is assumed since, in order to study the thermal interaction between multiple boreholes, their inner dynamic heat exchange process can be of second priority compared to the heat dissipation in the soil surrounding them.

An adiabatic heat transfer condition for the ground surface is assumed in the three-dimensional analysis. In addition, to account for the transient term in Eq. (B-1), the time is subdivided into 4200 time steps of 3600 s which equals a time period of 6 months.

Since the purpose of this study is comparison of its results with the two dimensional model presented in the previous section, soil thermal properties and borehole geometry similar to the two-dimensional case is selected (Table B-1). In addition, the lengths of the boreholes are assumed to be 200 m [Figure B-3 (b)] and an adiabatic heat transfer condition for the ground is assumed.

This model is used in obtaining the results presented in Section 7.1.3.

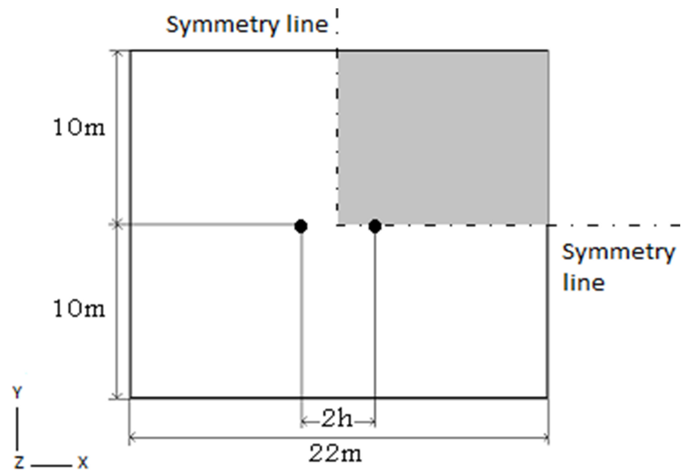

(a)

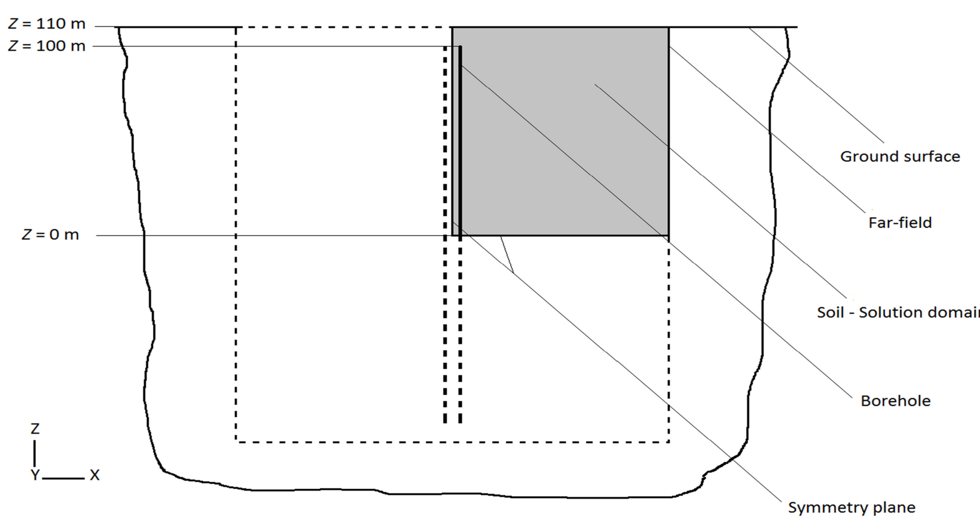

(b)

Figure B-3 Two-dimensional view of the solution domain (a) horizontal cross sections (*xy*) at the borehole mid-length (*z*=0 m) (b) vertical cross section (*xz*).

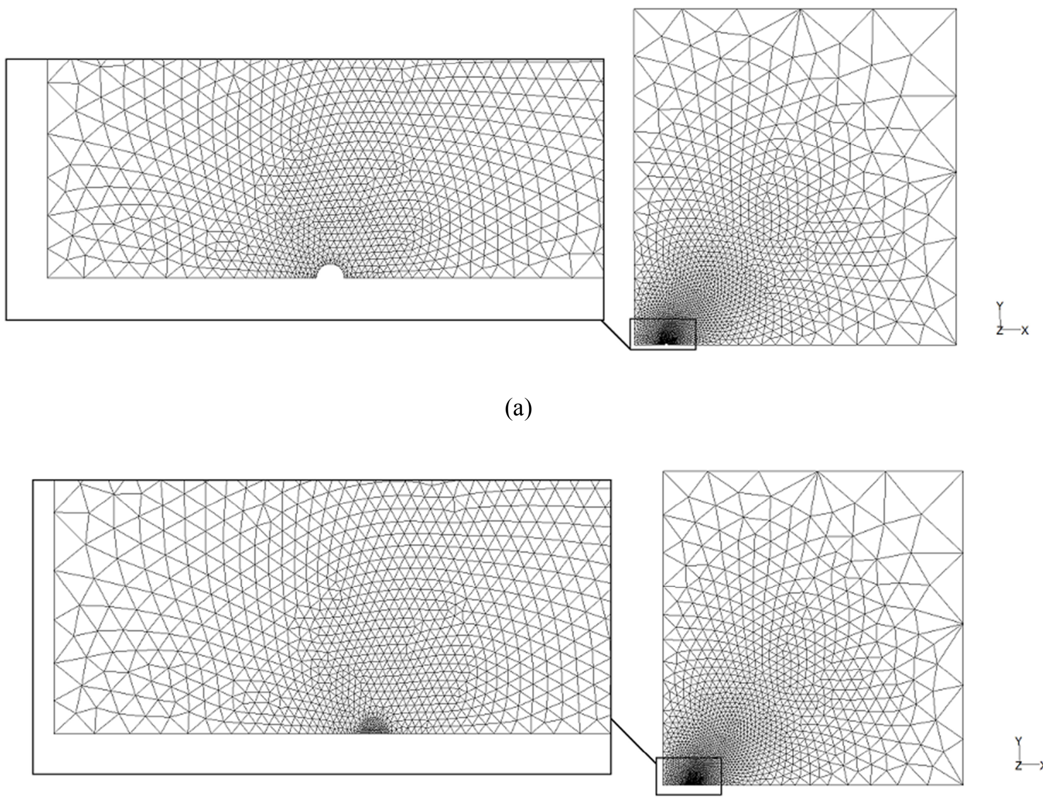

(a)

(b)

Figure B-4 Computational triangular grids used in the solution domain in *xy* cross section.

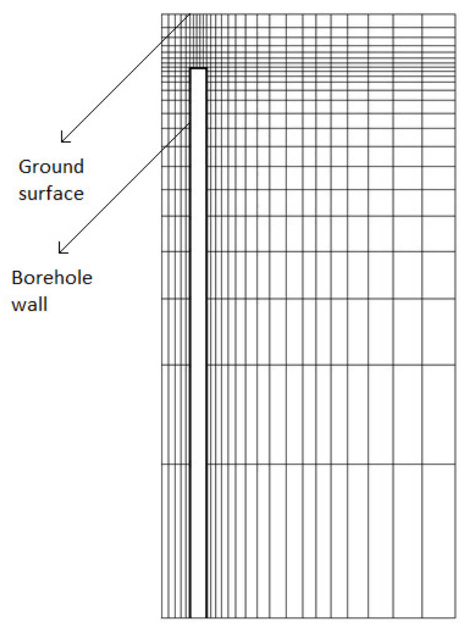

Figure B-5 Computational triangular grids used in the solution domain in *yz* cross section.

B.3 Two-dimensional Model for 16 Boreholes

A two-dimensional model of transient heat conduction in the soil around multiple ground heat exchangers is presented in this section. A domain consisting of several borehole systems, each consisting of 16 vertical boreholes is considered (Figure 7-24). The borehole systems are placed at every 100 m and the boreholes are installed at 6-meter distances.

After building the geometric model and defining the cell size and type with the GAMBIT software, the software can automatically generate a meshed model which consists of nodes and unstructured computational triangular cells, as shown in Figure B-1. The region nearest to the boreholes, where the temperature gradient is the higher, is meshed more finely to enable the temperatures to be accurately predicted. The necessary parameters including the material thermal properties as well as the boundary conditions are defined in ANSYS FLUENT. After the volume model is built in ANSYS FLUENT, the heat transfer problem can be solved numerically. In the numerical approach, the transient governing integral equations for the conservation of energy are solved with a control volume method to perform the numerical simulations of heat transfer in the borehole domain.

The heat transfer symmetry about the system shown in Figure 7-24 is utilized. Therefore, only one fourth of a borehole field is modelled and the solution domain (soil) is enclosed by the farfield and three symmetry planes. In Figure 7-24, the grey area is the solution domain, the results of which can be replicated to the other areas due to their symmetry. Here, the farfeild representing the undisturbed ground is selected far enough from the boreholes to ensure the boundary temperature is maintained consistently at the value of the farfield temperature over the concerned time, i.e., the amount of heat flux at the outer edge of the domain is zero or insignificantly small. In The reason for selection of farfield rather than another symmetry, with which thermal interaction can be examined, is to examine the migration of thermal plume to the undisturbed ground where ecosystems might be affected.

For numerical heat transfer calculation, a uniform initial temperature of 282 K (equal to the undisturbed ground temperature) is assumed to be effective over the entire borefield. At the symmetry boundaries, there is no heat flux across the symmetry plane which results in zero normal gradients of temperature at a symmetry plane. At the outer edge of the domain, a constant farfield temperature condition equal to the initial temperature is applied (282 K) to obtain the closed-form solution to the heat transfer problem. A periodic heat flux on the borehole wall is determined and used at the borehole wall (See Appendix C). In order to account for the transient term in Eq. (B-1), the time is subdivided into time steps of 3600 s.

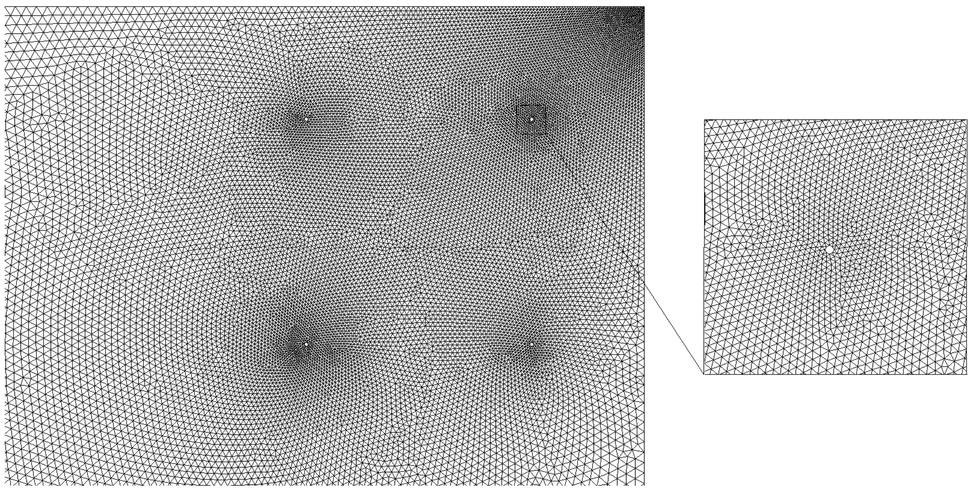

Figure B-1 Triangular mesh used for the solution domain.

In this model, the following geometrical and thermal characteristics for the borehole and the surrounding soil are assumed

Table B-2 Thermal properties and geometrical characteristics of the model [Adapted from (Incropera and DeWitt, 2000; Gao et al. 2008; Hepbasli et al. 2003; Shonder and Beck 1999)].

Soil	
Undisturbed ground temperature	9 C (282 K)
Soil thermal conductivity	1.5 W/mK
Soil specific heat capacity	1200 J/kgK
Soil density	1381 kg/m^3
Borehole geometry	
Total borehole length, H	N/A
Borehole radius, r_b	0.050 m
Number of Boreholes	16
Borehole distance, D_b	6 m
Heat flow rate per unit length, q' (W/m)	Periodic [Eq. (C-4) and (C-5)]

Appendix C Ground Heat Load Calculations Using Bin Method

In evaluating the temperature rise in the soil due to installation of ground heat exchangers, a key step is to define the heat flux from the surface of the heat exchanger to the soil. This can be very complicated due to the dynamic nature of the heat transfer from the fluid flowing in the U-tubes within the borehole to the borehole wall. For simplicity, the U-tube configuration in the borehole is not simulated in the model and the boundary condition at the borehole wall is set to the heat flux. In this section, the weather annual periodic variations with the heat flux at the wall of the heat exchanger, here, the borehole are correlated using building and weather specifications for a case study.

A building in Belleville, IL is considered. The simplified load profiles as shown in Figure C-1 are given by

Heating load: $\dot{q}_{HL} = 32.7 - 2.7T_o$ (C-1)

Cooling load: $\dot{q}_{CL} = 2.7T_o - 52.3$ (C-2)

This correlation yields $\dot{q}$ in units of kW and requires that the temperature be in units of ºC.

Note that these load profiles are assumptions for an arbitrary building. It is assumed that the building does not have any shift-breakdowns, i.e. the building is used in the same way during a 24-hour period and the internal heat gains by people, equipment, lights, etc. do not change with time during the day. In the case of an office building, for example, the building is used for only 8 hours a day resulting in a heating and cooling load profile for the 8-hour period and when the building is not occupied, due to different internal heat gains and sometimes a different thermostat temperature setting, the heating and cooling loads of the building have a different profile. Note that the balance point for this building is approximately 13ºC (55ºF) and 19ºC (67ºF) for heating and cooling modes, respectively.

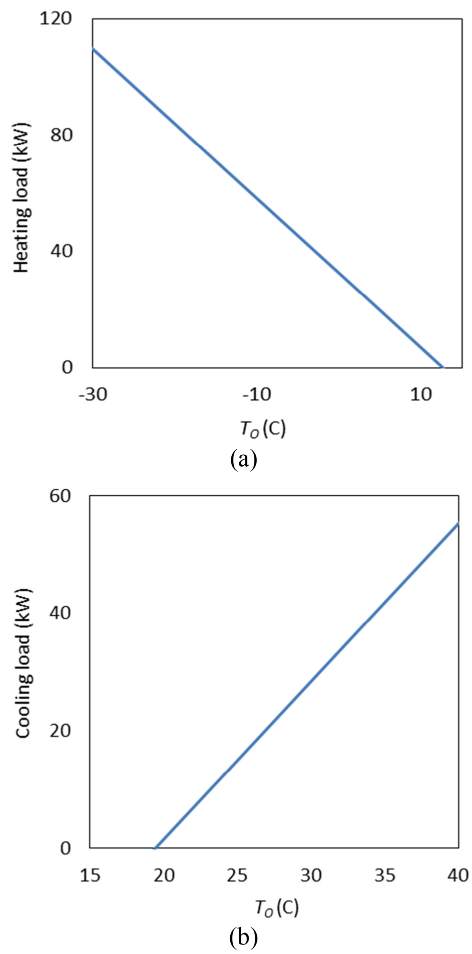

Figure C-1 Heating and cooling loads for a building in Belleville, IL. (a) Heating load profile, (b) Cooling load profile.

Heat pump efficiency varies with soil temperature and therefore bin summaries are needed in order to calculate heat pump power consumption as well as its capacity for several values of soil temperature throughout the year. Table C-1 shows an example of heat pump performance variation with soil temperature.

The numbers of hours that temperatures occur in 23 2.8-Celsius-degree (5-Fahrenheit-degree) bins for each month in Belleville, IL (Table C-2) are used as an example in order to estimate energy consumption patterns for cooling and heating equipment at different times of the year (USAF 1978). Using the load profiles [Eqs. (C-1) and (C-2)] and the heat pump performance, the bin calculation procedure is performed. Note that, the heat pump integrated capacity and the rated electric input are calculated separately for each month and vary for other months based on the average temperature of that month as seen in Figure C-2. These average temperatures are obtained with an iterative procedure assuming a transient profile for soil temperature and correcting it to the results after the first-year simulation until the assumption for the soil temperature leads to the same soil temperature in the simulation.

Table C-1 Typical heat pump heating and cooling capacities at an air flow rate of 6000 CFM (2.8 m^3/s).

Soil temperature (ºC)	Heating capacity (kW)	Total power input (kW)	Cooling capacity (kW)	Total power input (kW)
	At indoor dry bulb temperature 21ºC		At indoor dry bulb temperature 24ºC	
3	39.9	16.6	57.8	18.9
6	45.1	17.4	56.3	19.2
8	50.4	18.3	54.9	19.6
11	53.9	18.8	53.4	19.9
14	57.4	19.3	51.9	20.3
17	61.0	19.9	50.5	20.6

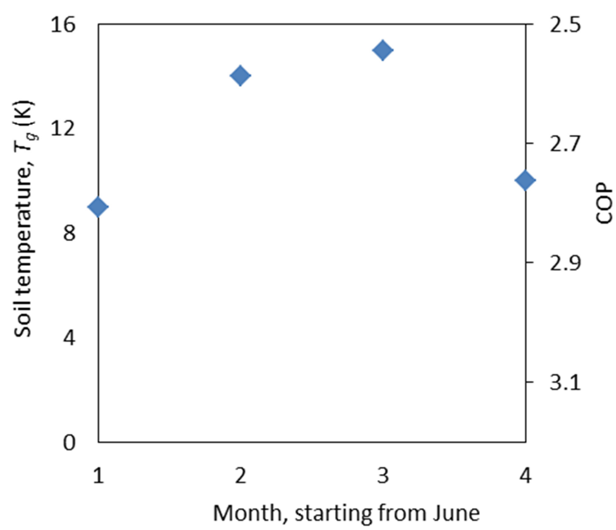

(a)

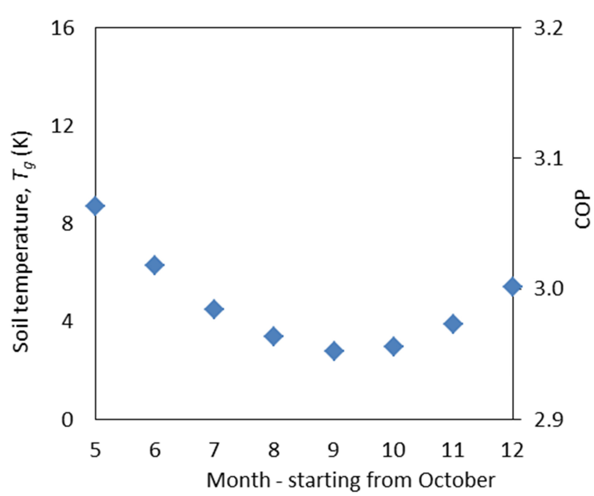

(b)

Figure C-2 Transient soil temperature in response to (a) heat injection, and (b) heat extraction.

Performing bin calculations similar to the one shown in Table C-3, the variation of heating and cooling load of the building throughout the year is determined (see Figure C-3). In a balanced system, almost all the heat that is stored in the ground during the summer, is used in the winter. It is seen in Figure C-3 that the heating and cooling loads of the building are not balanced throughout the year; there are 8 months of heating (red bars) and 4 months of cooling (blue bars). In order to balance the amount of heat that is stored in the ground, the size of the ground heat exchanger is designed based on the cooling load and supplemental heat in the form of electrical resistance is required when the heating load from the ground heat exchanger is not met.

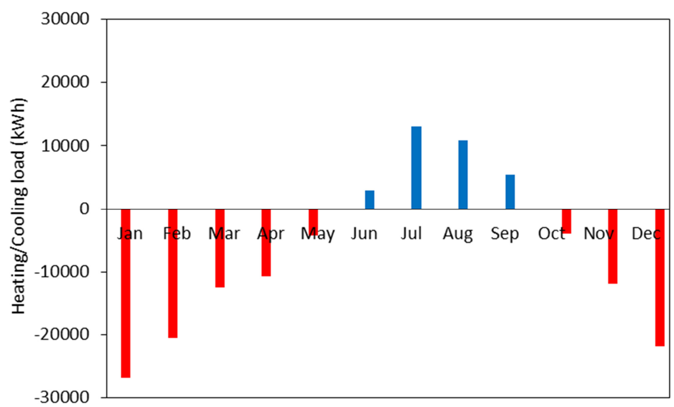

Figure C-3 Variation of heating and cooling load of the building throughout the year.

The average temperature of the ground depends on how the cycle of the heat storage removal starts the first time the system starts to operate. It would become lower or higher than the initial temperature of the ground according to the first operation time in winter or summer. Here, it is assumed that the heat is stored in the ground during the 4-month cooling season through two vertical boreholes of 200 m length. Based on the building heating and cooling load calculated form the bin data, the magnitude of the heat flux from the borehole wall is shown in Figure C-5. It is seen there that a sinusoidal function can be fit to the monthly cooling load data. Note that due to the unbalanced weather of this area, the heat that is stored in the ground in the cooling season only covers part of the total heating load in the 8-month heating season; therefore, in the heating months a curve must be chosen that results in the same amount of heat removal from the ground over its period as the heat stored in the ground in the cooling season. That is,

$$\int_{0}^{day_{sr}} q''_{storage}\, d(day) + R_s \int_{day_{sr}}^{365} q''_{removal}\, d(day) = 0 \qquad \text{(C-3)}$$

where R_s is the ratio of heat extraction to heat injection in the soil. This parameter accounts for part of the stored heat in the cooling mode that dissipates away from the borefield and cannot be extracted in heating mode. Starting from the first day of heat storage in the ground, d_{sr} is the last day of heat injection and the start of heat removal from the ground. Based on Eq. (C-3), a sinusoidal curve can be chosen that represents the heat injection or extraction profile based on the provided data from the load analysis of the building (straight lines in Figure C-4), and the other mode of operation (heat extraction or injection) can be defined based on Eq. (C-3) that results in a balanced system that collects all the heat that it injects into the ground (dotted lines in Figure C-4). Three typical heat injection and extraction profiles are shown in Figure C-4 where a naturally balanced profile (6 months heat injection and 6 months heat extraction) is compared with two systems with unbalanced heat injection and extraction needs where one mode of heat injection or extraction is balanced according to Eq. (C-3) (dotted lines).

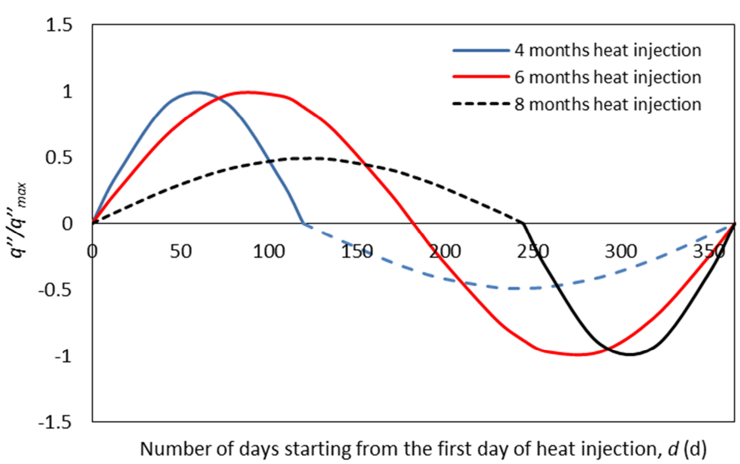

Figure C-4 Typical balanced heat injection and extraction profiles.

Table C-2 Dry-bulb temperature hours for an average year in Scott AFB, Belleville, IL; period of record = 1967 to 1996 [Adapted from USAF (1978)].

Temperature (^oC)	Jan	Feb	Mar	Apr	May	Jun	Jul	Aug	Sep	Oct	Nov	Dec
39							2	1				
36							18	12	2			
33						1	64	43	12	0		
31			0		0	5	102	83	34	4		
28			3	1	4	35	138	118	64	14	0	
25		1	7	4	22	76	163	153	94	33	3	
22	1	2	17	16	47	109	149	160	137	57	11	1
19	2	5	30	29	75	134	71	99	120	91	26	4
17	6	13	47	52	110	153	29	52	103	112	53	13
14	13	24	65	78	140	105	8	19	77	121	65	26
11	22	31	87	105	134	64	1	4	47	113	84	36
8	35	50	105	109	100	28		0	21	95	105	58
6	72	84	111	107	63	7			7	59	119	102
3	112	119	108	97	36	1			2	33	117	140
0	143	111	89	66	10				0	11	82	140
-3	102	90	50	34	3					2	35	96
-6	84	54	16	18	0						14	54
-8	64	37	5	3							5	33
-11	41	29	2	0							2	20
-14	26	15	1								0	10
-17	13	6	0									6
-19	5	1										3
-22	2	1										2
-25	1	0										1
-28	0											

Table C-3 A sample of bin energy calculation for month of July in Scott AFB, Belleville, IL.

Climate		Building		Heat pump						
Temperature (°C)	Temperature diff. T_{bin} - T_{bal} (°C)	Hours in July (hr)	Building cooling load (kW)	Heat pump integrated capacity (kW)	Cycling capacity adjustment factor	Adjusted heat pump capacity (kW)	Operating time fraction	Rated electric input (kW)	Seasonal heat pump electric consumption (kWh)	Heat exchanger heat injection (kWh)
39	17.9	2	52.3	51.9	1.00	52.0	1.00	20.3	40.6	145.2
36	15.1	18	44.8	51.9	0.97	50.1	0.89	20.3	326.9	1134.0
33	12.3	64	37.4	51.9	0.93	48.3	0.77	20.3	1006.2	3397.6
31	9.6	102	29.9	51.9	0.89	46.4	0.64	20.3	1334.6	4383.7
28	6.8	138	22.4	51.9	0.86	44.5	0.50	20.3	1411.0	4505.0
25	4.0	163	14.9	51.9	0.82	42.7	0.35	20.3	1159.8	3596.1
22	1.2	149	7.5	51.9	0.79	40.8	0.18	20.3	554.4	1667.9
								Total	5833.4	18829.5

The following heat flux profiles for heat injection and extraction are chosen for the current unbalanced system where the system injects heat into the ground for 130 days. It is seen that the amplitude of the heat extraction profile is chosen so that the system would remain balanced [Eq. (C-5)]. Substituting the number of days (d) from June (start of cooling season), this correlation yields q'' in units of kW (Figure C-5):

Heat storage: $$q''(d) = 55.9 \sin\left(\frac{d}{130}\pi\right) \tag{C-4}$$

Heat removal: $$q''(d) = -0.70 \times 53.7 \sin\left(\frac{d-130}{235}\pi\right) \tag{C-5}$$

The amplitude of the sinusoidal heat injection profile in Eq. (C-4) is chosen assuming an average heat injection of 11 W/m. Note that the ratio of heat extraction to heat injection (R_s) in the above annual profile is chosen based on an iterative procedure. At R_s=0.7, the system seems to have collected all the heat that it stored in the ground. To model the heat exchanger system and assess the effects of a periodic variation of heat flux on the borehole wall, the fitted curve for the cooling season in Figure C-5 and the curve for heat removal from the ground resulting in the same amount of heat removal from the ground [Eqs. (C-4) and (C-5)] can be used as boundary conditions on the borehole wall.

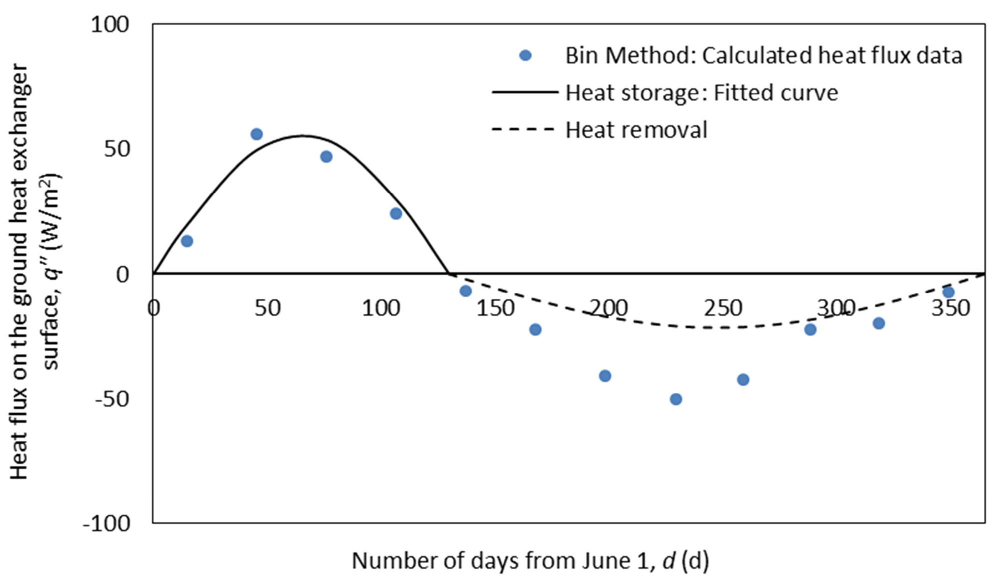

Figure C-5 Variation of heat flux on the ground heat exchanger wall.

Appendix D Source Codes Developed for Solutions

In this Section, two programming codes are presented that are developed in Fortran and C and are used in analytical and numerical solutions, respectively. The first program is written in Fortran to evaluate the integrals in the analytical solution as well as coupling the solutions for inside and outside the borehole. The second program in written in C and is hooked to ANSYS FLUENT in order to calculate the average temperature of the outlet running fluid face meshes and use it to calculate and assign a new temperature to the boundary condition at the running fluid inlet according to the ground heat load profile at every time step.

D.1 Analytical Temperature Evaluations in Fortran

```
Program Analytical

       Teta1(BB,ZZ,PP)=cosh(BB*ZZ)-(1/sqrt(1-PP**2))*(1-PP*(cosh(BB)-sqrt((1-
       PP)/(1+PP))*sinh(BB*ZZ))/(cosh(BB)+sqrt((1-
       PP)/(1+PP))*sinh(BB)))*sinh(BB*ZZ)

       Teta2(BB,ZZ,PP)=((cosh(BB)-sqrt((1-PP)/(1+PP))*sinh(BB))/(cosh(BB)+sqrt((1-
       PP)/(1+PP))*sinh(BB)))*cosh(BB*ZZ)+(1/sqrt(1-PP**2))*((cosh(BB)-sqrt((1-
       PP)/(1+PP))*sinh(BB))/(cosh(BB)+sqrt((1-PP)/(1+PP))*sinh(BB))-
       PP)*sinh(BB*ZZ)

       q(tt)=30*sin(tt*3.1415/(0.5*365*3600*24))

       devq(tt)=30*3.1415/(0.5*365*3600*24)*cos(tt*3.1415/(0.5*365*3600*24))

       real Tb,Tf1,Tf2,kb,D,rb,rp,M,H,hh,R,Rd1,Rd2,Db
       real R11,R12,R1,Beta,P,Teta1,Teta2,Zd,Hp,dHp
       real int,int1,int2
       real k,ro,c,cb,dq(100000)
       real fo,t,yr,Bc,Cc

!      Soil properties

       k=1.5
       ro=1950.
       c=1550.

!      Borehole properties

       kb=2.6
       cb=4182.
```

```
!       Geometrical characteristcs

        D=.026
        rb=.1
        rp=.016
        M=.225
        H=50.
        hh=1.
        Db=4.

!       Calculating the borehole resistances

        R11=(1/(2*3.1415*kb))*(log(rb/rp)
        ++(kb-k)/(kb+k)*log(rb**2/(rb**2-D**2)))

        R12=(1/(2*3.1415*kb))*(log(rb/(2*D))
        ++(kb-k)/(kb+k)*log(rb**2/(rb**2+D**2)))

        Beta=H/(M*cb*sqrt((R11+R12)*(R11-R12)))
        P=R12/R11
        R1=R11+R12


        R=Db/2+rb
        Zd=0.5+hh/H
        t=24*3600
        yr=30
        n=365*(24*3600/t)/12/2

!       Initial temperatures

!       dq(1)=q(900.0/2.0)
        do 555 i=1,yr*365*24*3600/t
555     dq(i)=devq((i-0.5)*t)*t

        open(1,file='Temperature.dat')

!       tarting time loop

222     Tb=282.

!       Starting inner Duhamel loop

        do 15 kk=1,n
        fo=k*kk*t/(ro*c*(H**2))

!       Reset the int value

        int=0
        Hp=0
        dHp=.0001
!       R=(.1*(j-1)+.05)/H
        Rd1=(sqrt((R-Db/2)**2))/H
        Rd2=(sqrt((R+Db/2)**2))/H

!       Integrate over Borehole I
```

```
4       int1=(dHp*dq(n-kk+1)/(4*k*3.1415))*(erfc(sqrt(Rd1**2+(Zd-Hp-
        hh/H)**2)/(2*sqrt(fo)))/sqrt(Rd1**2+(Zd-Hp-hh/H)**2)-
        (erfc(sqrt(Rd1**2+(Zd+Hp+hh/H)**2)/(2*sqrt(fo)))/sqrt(Rd1**2+(Zd+Hp+hh/H)**2
        ))

!       Integrate over Borehole II

        int2=(dHp*dq(n-kk+1)/(4*k*3.1415))*(erfc(sqrt(Rd2**2+(Zd-Hp-
        hh/H)**2)/(2*sqrt(fo)))/sqrt(Rd2**2+(Zd-Hp-hh/H)**2)-
        (erfc(sqrt(Rd2**2+(Zd+Hp+hh/H)**2)/(2*sqrt(fo)))/sqrt(Rd2**2+(Zd+Hp+hh/H)**2
        ))

!       write(*,*)int2
        int=int+int1+int2

!       Checking if the integral range has reached the end of the borehole (Hp=1)

        if(Hp-1)5,15,15
5       Hp=Hp+dHp
        goto 4

15      Tb=Tb+int

!       write(*,*)n,n*t,Tb

        Bc=Teta2(Beta,0.0,P)
        Cc=-q(n*t)*H/(M*cb)

        Tf1=Tb-Cc/(1-Bc)
        Tf2=Tb-Bc*Cc/(1-Bc)

        write(*,*)n*t,Tf1,Tf2,Tb,q(n*t)
        write(1,*)n*t,Tf1,Tf2,Tb

        if(n-yr*8760*3600/t)556,556,224
556     n=n+365*(24*3600/t)/12
        goto 222

!       End of time loop

224    end

        FUNCTION erfc(x)
        real erfc,x
C       Uses gammp,gammq
        if(x.lt.0.)then
        erfc=1.+gammp(.5,x**2)
        else
        erfc=gammq(.5,x**2)
        endif
        return
        end

        FUNCTION gammp(a,x)
        real a,gammp,x
C       Uses gcf,gser returns the incomplete gamma function P(alpha,x)
        real gammcf,gamser,gln
        if(x.lt.0..or.a.le.0.)pause 'bad arguments in gamnp'
```

```
      if(x.lt.a+1.)then
!     Use the series representation.
      call gser(gamser,a,x,gln)
      gammp=gamser
      else
!     Use the continued fraction representation
      call gcf(gammcf,a,x,gln)
      gammp=1.-gammcf
!     and take its component.
      endif
      return
      end

      FUNCTION gammq(a,x)
      real a,gammq,x
C     Uses gcf,gser
!            Returns the incomplete gamma function Q(alpha,x)=1-P(alpha,x)
      real gammcf,gamser,gln
      if(x.lt.0..or.a.le.0.)pause 'bad arguements in gamnq'
      if(x.lt.a+1.)then
!     Use the series representation
      call gser(gamser,a,x,gln)
      gammq=1.-gamser
!     and take its component
      else
!     Use the continued fraction representation.
      call gcf(gammcf,a,x,gln)
      gammq=gammcf
      endif
      return
      end

      Subroutine gcf(gammcf,a,x,gln)
      integer ITMAX
      real a,gammcf,gln,x,EPS,FPMIN
      PARAMETER(ITMAX=100,EPS=3.e-7,FPMIN=1.e-30)
C     Uses gammln
!            Returns the incomplete gamma function Q(alpha,x) evaluated by
!             its continued fraction representation as gammcf. Also returns
!              Gamma(a) as gln. Parameters: ITMAX is the maximum allowed
!              number of iterations; EPS is the relative accuracy; FPMIN
!               is a number near the smallest representable floating-point
!                number.
      integer i
      real an,b,c,d,del,h,gammln
      gln=gammln(a)
      b=x+1.-a
      c=1./FPMIN
      d=1./b
      h=d
      do i=1,ITMAX
      an=-i*(i-a)
      b=b+2.
      d=an*d+b
      if(abs(d).lt.FPMIN)d=FPMIN
      c=b+an/c
      if(abs(c).lt.FPMIN)c=FPMIN
      d=1./d
```

```
      del=d*c
      h=h*del
      if(abs(del-1.).lt.EPS)goto 1
      enddo
      pause 'a too large, ITMAX too small in gcf'
1     gammcf=exp(-x+a*log(x)-gln)*h
!     Put factors in front.
      return
      END

      Subroutine gser(gamser,a,x,gln)
      integer ITMAX
      real a,gamser,gln,x,EPS
      PARAMETER (ITMAX=100,EPS=3.e-7)
C     Uses gammln
!            Returns the incomplete gamma ffunction P(alpha,x) evaluated by
!             its series representation as gamser. Also returns
!              ln gamma(alpha) as gln.
      integer n
      real ap,del,sum,gammln
      gln=gammln(a)
      if(x.le.0.)then
      if(x.lt.0.)pause 'x < 0 in gser'
      gamser=0.
      return
      endif
      ap=a
      sum=1./a
      del=sum
      do n=1,ITMAX
      ap=ap+1.
      del=del*x/ap
      sum=sum+del
      if(abs(del).lt.abs(sum)*EPS)goto 10
      enddo
      pause 'a too large, ITMAX too small in gser'
10    gamser=sum*exp(-x+a*log(x)-gln)
      return
      End

      FUNCTION gammln(xx)
      real gammln,xx
!            Returns the value ln[Gamma(xx)] for xx > 0.
      integer j
      Double precision ser,stp,tmp,x,y,cof(6)
!            Internal arithmetic will be done in doule precision, a nicety
!             that you can omit if five-figure accuracy is good enough.
      save cof,stp
      data cof,stp/76.18009172947146d0,-86.50532032941677d0,
      , 24.01409824083091d0,-1.231739572450155d0,.1208650973866179d-2,
      , -.5395239384953d-5,2.5066282746310005d0/
      x=xx
      y=x
      tmp=x+5.5d0
      tmp=(x+0.5d0)*log(tmp)-tmp
      ser=1.000000000190015d0
      do j=1,6
      y=y+1.d0
```

```
        ser=ser+cof(j)/y
        enddo
        gammln=tmp+log(stp*ser/x)
        return
        END
```

D.2 User Defined Function in C

```
#include "udf.h"
#include <cmath>

DEFINE_ADJUST(average_exit_temp, domain)
{

  face_t f1;
  face_t f2;
  real tempa=0.0;
  real totalarea=0.0;
  real avetempa=0.0;
  real A[ND_ND];
  real tt=RP_Get_Real("flow-time");

  int ID1 = 10;  /* Zone ID for Outflow zone from Boundary Conditions panel */
  Thread *outlet_thread = Lookup_Thread(domain, ID1);

  int ID2 = 11;  /* Zone ID for Inlet zone from Boundary Conditions panel */
  Thread *inlet_thread = Lookup_Thread(domain, ID2);

  //printf("average temperature1= %e\n",avetempa);

    /* Loop over faces in a face thread to get the information stored on faces.*/
    begin_f_loop(f1,outlet_thread)
      {
      /*  F_T gets face temperature. += causes all face areas/temperatures to be
added together. */
        F_AREA(A,f1,outlet_thread);
              totalarea += NV_MAG(A);
              //printf("Total_area= %e\n",totalarea);
        tempa += NV_MAG(A)*F_T(f1,outlet_thread);
      }
    end_f_loop(f1,outlet_thread)
       //printf("average temperature2= %e\n",avetempa);
    avetempa = tempa/totalarea +
30*(sin(tt*3.1415/(0.5*365*3600*24)))*50/(0.225*4182);
       printf("average inlet temperature= %e\n",tempa/totalarea);
       printf("temp diff=
%e\n",30*sin(tt*3.1415/(0.5*365*3600*24))*50/(0.225*4182));
    printf("new average inlet temperature= %e\n",avetempa);

    begin_f_loop(f2, inlet_thread)
      {
              //printf("average temperature4= %e\n",avetempa);
        F_UDMI(f2,inlet_thread,0) = avetempa;
      }
       end_f_loop(f2,inlet_thread)
       //printf("average temperature5= %e\n",avetempa);
}
```

```
DEFINE_PROFILE(Inlettemp,t,i)
{

  real time=RP_Get_Real("flow-time");
  face_t f;

  if(time<=5.0)
  {
    printf("t1= %e\n",time);
    begin_f_loop(f, t)
      {
         F_PROFILE(f, t, i)=282.0;
      }
    end_f_loop(face, t)
  }

  else
  {

    begin_f_loop(f, t)
      {
          if(F_UDMI(f,t,0)<(310+30*50/(0.561*4182)))
          {F_PROFILE(f,t,i) = F_UDMI(f,t,0);}
          else
          {
                 //exit(0);
                 printf("break %e\n");
                 break;
          }
      }
    end_f_loop(f, t)
    printf("t2= %e\n",time);
  }
}
```

Appendix E Publications

Book Chapters

- **Koohi-Fayegh, S.**, M.A. Rosen. Thermal interaction of multiple geothermal storages for ground source heat pump systems. *Energy Storage*. Nova Science Publishers, 2011, 393-420.
- Leong W.H., V.R. Tarnawski, **S. Koohi-Fayegh**, M.A. Rosen, Ground thermal energy storage for building heating and cooling. *Energy Storage*. Nova Science Publishers, 2011, 421-440.

Journal Papers

- **Koohi-Fayegh, S.**, M.A. Rosen. An Analytical Approach to Evaluating the Effect of Thermal Interaction of Geothermal Heat Exchangers on Ground Heat Pump Efficiency. *Energy Conversion and Management*, in press.
- **Koohi-Fayegh, S.**, M.A. Rosen. A Review of the Modelling of Thermally Interacting Multiple Boreholes, *Sustainability* 2013, *5*, 2519-2536; doi:10.3390/su5062519.
- **Koohi-Fayegh, S.**, M.A. Rosen. On thermally interacting multiple boreholes with variable heating strength: Comparison between analytical and numerical approaches. *Sustainability* 2012, *4*, 1848-1866; doi:10.3390/su4081848.
- **Koohi-Fayegh, S.**, M.A. Rosen. Examination of thermal interaction of multiple geothermal storage and heat pump systems. *Applied Energy* 97, 2012, 962–969.

Journal Paper Submissions

- **Koohi-Fayegh, S.**, M.A. Rosen. Three dimensional analysis of thermal interaction of multiple vertical ground heat exchangers. *Int. J. Green Energy*, IJGE-2012-0255, April 2012.

Conferences

- **Koohi-Fayegh, S.**, M.A. Rosen. Regulating underground boundaries for geothermal energy systems: An analytical approach to evaluating the effect of thermal interaction

of geothermal heat exchangers on their sustainability, *3rd Climate Change Technology Conference* (*CCTC*), 27-29 May 2013.

- **Koohi-Fayegh, S.**, M.A. Rosen. Modelling thermally interacting multiple boreholes with variable heating strength, *Proc. 2nd World Sustainability Forum*, 1-30 Nov 2012.
- **Koohi-Fayegh, S.**, M.A. Rosen. Long-term study of thermal interaction of vertical ground heat exchangers with seasonal heat flux variation, *11th International Conference on Sustainable Technologies*, 2-5 Sep 2012, Vancouver, British Colombia.
- **Koohi-Fayegh, S.**, M.A. Rosen. Three dimensional analysis of thermal interaction of multiple vertical ground heat exchangers, *The 12th International Conference on Energy Storage (Innostock 2012)*, poster presentation.
- **Koohi-Fayegh, S.**, M.A. Rosen. Thermally interacting multiple boreholes with variable heating strength, *eSim conference*, 2-3 May 2012, Halifax, Nova Scotia.
- **Koohi-Fayegh, S.**, M.A. Rosen. A Numerical approach to assessing thermally interacting multiple boreholes with variable heating strength, *Proc. 1st World Sustainability Forum*, 1-30 Nov 2011.
- **Koohi-Fayegh, S.**, M.A. Rosen. Examination of thermal interaction of multiple geothermal storage and heat pump systems, *International Conference on Applied Energy*, Perugia, Italy, May 2011.
- **Koohi-Fayegh, S.**, M.A. Rosen. Thermal Interaction in Multiple Vertical Geothermal Heat Exchangers, *UOIT 2nd Graduate Student Conference*, University of Ontario Institute of Technology (UOIT), Oshawa, Ontario, Canada, May 2011.
- **Koohi-Fayegh, S.**, M.A. Rosen. The modelling of geothermal heat pumps with vertical ground interfaces for use in HVAC systems, *The Fifth International Green Energy Conference*, University of Waterloo, Waterloo, Ontario, Canada, June 2010.
- **Koohi-Fayegh, S.**, M.A. Rosen. A review of analytical models for vertical ground heat exchangers, *UOIT 1st Graduate Student Conference*, University of Ontario Institute of Technology (UOIT), Oshawa, Ontario, Canada, May 2010.